Pathophysiological relevance of PDE inhibition in lung fibroblasts for the treatment of pulmonary diseases

Dissertation

Zur Erlangung des akademischen Grades des
Doktors der Naturwissenschaften (Dr. rer. nat.)

der Universität Konstanz
im Fachbereich Biologie

vorgelegt von

Jens Ditmar Selige

Tag der mündlichen Prüfung: 29.03.2010

1. Referent: Herr Prof. Dr. A. Wendel
2. Referentin: Frau Priv. Doz. Dr. E. May

Das Glück, kein Reiter wird's erjagen,
es ist nicht dort und ist nicht hier.
Lern überwinden, lern entsagen,
und ungeahnt erblüht es dir.

Theodor Fontane (1819 – 1898)

Acknowledgement - Danksagung

Diese Dissertation begann im April 2007 und wurde im Januar 2010 fertiggestellt. Angefertigt wurde sie in den Laboren der Abteilung RDP/Biology 1 und 2, der präklinischen Forschung der Nycomed GmbH (Konstanz). Ohne das direkte und indirekte Zutun verschiedenster Menschen, wäre diese Arbeit entweder erst gar nicht zustande gekommen, wäre nur schwer realisierbar geworden oder hätte einfach nur halb so viel Spaß gemacht. All diesen Menschen möchte ich nun im Folgenden danken.

An erster Stelle möchte ich **Dr. Thomas Klein** danken. Als ehemaliger Leiter der Abteilung RDR/Biochemistry 3 der Gastroenterologie der Altana Pharma AG hat er 2006 die Weichen für diese Dissertation gestellt und mich ermutigt, diesen Weg zu gehen. Allerdings führten besondere Umstände, wie z.B. die Firmenübernahme durch die Nycomed GmbH mit anschließender Umstrukturierung der Forschung zu einer Richtungsänderung. Und so kommen wir zu **Dr. Armin Hatzelmann**, der mich in der Abteilung RDP/Biology 2 unter seine Fittiche nahm. Ihm danke ich für meine Aufnahme in die Abteilung und seine äußerst konstruktive Unterstützung beim Verfassen von wissenschaftlichen Publikationen. Ich fühlte mich unter seiner Leitung in sicheren Händen und als Führungsperson wird er mir stets ein Vorbild sein.

Besonderer Dank in vielerlei Hinsicht gebührt meinem Betreuer **Dr. Torsten Dunkern**. Besonders seine Ausdauer und Engagement, seine wertvollen Ratschläge und fachlichen Gespräche sowie seine Zuversicht und Vertrauen in meine Person waren wesentliche Komponenten, die zum Fortschritt und Gelingen dieser Arbeit beigetragen haben.

Zu der Kategorie „Menschen, ohne die es erst gar nicht zustande gekommen wäre“, gehört vor allem auch **Prof. Dr. Albrecht Wendel**. Ihm danke ich ganz besonders dafür, daß er in mir einen „besonders qualifizierten FH-Absolventen“ gesehen hat, mein Eignungsfeststellungsverfahren an der Universität Konstanz unterstützt hat und schließlich dafür, daß er mein Doktorvater geworden ist. Danke!

Ein großes Dankeschön geht auch an **Dr. Christian Hesslinger** und **Dr. Hermann Tenor**. Ihre Unterstützung, Gespräche, kritischen Augen, Hinweise und Anregungen waren elementar für das Gelingen dieser Dissertation.

Prof. Dr. Klaus Peter Schäfer und **Priv. Doz. Dr. Elisa May**, als Teil meines Thesis-Komitees, sowie den Professoren und Betreuern des Graduiertenkollegs IRTG 1331 danke ich für die Aufnahme ins Graduiertenkolleg, sowie für die konstruktiven Fragen,

Anregungen und die Kritik bei den jährlichen Evaluierungen. Sie waren stets motivierend und lehrreich für mich.
Prof. Dr. Marcel Leist danke ich für seine Unterstützung und die beeindruckende Zusammenarbeit im Rahmen der Organisation des „1st Insel-Symposium, 2009“. Desweiteren danke ich den beiden Koordinatorinnen, **Dr. Jutta Schlepper-Schäfer** sowie **Josepha Ittner** für die stets gute Zusammenarbeit innerhalb des IRTG 1331.

Kommen wir nun zur Rubrik „Menschen, ohne die es nur halb so viel Spaß gemacht hätte“. Allen voran danke ich hier meinen Kolleginnen und Kollegen innerhalb der Abteilung RDP/B2 für ihre Hilfsbereitschaft und das angenehme Arbeitsklima. Besonders **Sabine Drewitz** und **Betina Mueller** danke ich dafür, dem Laboralltag stets eine besondere Note gegeben zu haben. **Horst Mählmann** danke ich für seine außergewöhnliche Hilfsbereitschaft, seinen individuellen Humor sowie zahlreichen Geschichten, die so manchen Arbeitstag aufgewertet haben. **Sandra Hamm** und **Daniel Knaack** gilt mein Dank für zahlreiche erquickende Mittagspausen bzw. unvergessliche Segelabenteuer auf dem Bodensee.
Heike Goebel gehört in die Rubrik „Menschen, ohne die es nur schwer realisierbar gewesen wäre“, deswegen ein riesen Dankeschön an sie für das Durchstehen aller meiner Hochs und Tiefs. Ihr stets offenes Ohr bei allen Sorgen und Nöten, ihre Hilfsbereitschaft und Freundschaft waren die Basis meiner täglichen Motivation.
Dr. Michael Herrmann danke ich für „B.u.4“, für das Korrekturlesen sowie den ganzen Spaß, den es nie zu vergessen gilt. **Dr. Wolfgang Alexander Simon** danke ich für gemeisame gesangliche und besonders stilvolle seglerische Erlebnisse im Lacustre, die den nötigen Ausgleich zur Laborarbeit bildeten.

Den teils ehemaligen Kollegiaten des IRTG 1331, besonders **Dr. Oliver Dehus, Dr. Tobias Speicher, Dr. Andrea Kunzmann, Dr. Steffi Siegel, Dr. Christine Hoffmann, Dr. Sebastian Bunk** und natürlich **Christopher Schliehe** danke ich für eine ausgefüllte Doktorandenzeit die teils auf dem Land, teils auf dem Wasser stattfand.

Selbstverständlich danke ich zum Schluß meinen Eltern und Familie sowie meiner Freundin **Alexandra** für ihre Liebe und Unterstützung. Sie bilden stets die Grundlage für das Gelingen sämtlicher Projekte.

Danke !

Table of contents

List of abbreviations

Abbreviation	Full name	Abbreviation	Full name
18S rRNA	18S ribosomal RNA	g	Gravitational constant, 9.81 m/s^2
5'AMP	Adenosine 5' monophosphate	GAF	cGMP binding domain
5'GMP	Guanosine 5' monophosphate	GAPDH	Glycerinaldehyd-3-phosphate-dehydrogenase
AC	Adenylyl cyclase		
AKAP	A-kinase anchor protein	GPCR	G protein-coupled receptor
Akt	Protein kinase B	GTP	Guanosine 5'-triphosphate
AMV	Avian myeloblastosis virus	HARBS	High-affinity rolipram-binding site
APS	Ammonium peroxodisulfate	HCl	Hydrochloric acid
AR	Adrenergic receptor	HEPES	4-(2-Hydroxyethyl)-1-piper-azineethanesulfonic acid
ATP	Adenosine 5'-triphosphate		
bFGF	Basic fibroblast growth factor	IBMX	3-Isobutyl-1-methylxanthine
BSA	Bovine serum albumin	IPF	Idiopathic pulmonary fibrosis
CamKII	Calcium/calmodulin-dependent protein kinase II	kDa	Kilo Dalton, molecular weight
		LARBS	Low-affinity rolipram-binding site
cAMP	Adenosine 3'-5' cyclic mono-phosphate	LPS	Lipopolysaccharide
		MAPK	Mitogen-activated protein kinase
CBP	CREB-binding protein	MGB	Minor groove binder
cDNA	Copy deoxyribonucleic acid	min	Minute
cGMP	Guanosine 3'-5' cyclic monophosphate	MUC5AC	Mucin 5AC
		NF	Nucleofection
CNG	Cyclic nucleotide gated channel	NHLF	Normal human lung fibroblast
COPD	Chronic obstructive pulmonary disease	NO	Nitric oxide
		qPCR	Quantitative PCR
cpm	Counts per minute	PAGE	Polyacrylamide gel electrophoersis
CRE	cAMP response element		
CREP	CRE-binding protein	PBS	Phosphate buffered saline
DMSO	Dimethylsulfoxide	PCR	Polymerase chain reaction
DNA	Deoxyribonucleic acid	PDE	Phosphodiesterase
dNTP	2'-Deoxy-nucleoside triphosphate	PGE_2	Prostaglandin E_2
		PKA (PKC)	Protein kinase A (C)
EDTA	Ethylenediaminetetraacetic acid	REU	Relative expression unit
EGTA	Ethylene glycol-bis(2-amino-ethylether)-tetraacetic acid	RNA	Ribonucleic acid
		RNAi	RNA interference
ELISA	Enzyme-linked immunosorbent assay	RT-PCR	Reverse transcriptase – PCR
		SDS	Sodium dodecyl sulfate
Epac	Exchange protein activated by cAMP	siRNA	Small interfering RNA
		TGF	Tranforming growth factor
ERK	Extracellular signal-regulated kinase	tmAC	Transmembrane adenylyl cyclase
		TNF	Tumor necrosis factor
FAM	Reporter dye: 6-carboxy-fluorescein	Tris	2-Amino-2-(hydroxymethyl) propane-1,3-diol
FCS	Fetal calf serum	UCR	Upstream conserved region
FEV1	Forced expiratory volume in one sec	VIC	Reporter dye
		v/v	Volume by volume
FVC	Forced vital capacity	w/v	Weight by volume

All further abbreviations are explained in the text.

1. Introduction

Signal transduction is one of the principle characteristics of all organisms. The ability to recognize external signals or stimuli, to convert and to transmit them into internal signals is fundamental and of pivotal importance for either survival in a changing environment (unicellular organisms) or for cell-to-cell communication in order to coordinate the functions of the system and body (multicellular organisms). In multicellular organisms, a multitude of signals (first messengers) e.g. hormones, growth factors or neurotransmitters bind specifically to cell-surface receptors and initiate the signal transduction inside the cell. The intracellular signal transduction is processed by second messenger molecules, such as cyclic adenosine 3’, 5’- monophosphate (cAMP), which induce and regulate various cellular functions.

1.1 The pathway of the second messenger cyclic AMP

The second messenger cAMP has been extensively studied for half a century. Since its discovery in 1957 (Sutherland et al., 1958; Berthet et al., 1957), no less than five different Nobel Prizes have been awarded in this field of research and therewith underline the importance of this regulatory system (Beavo et al., 2002). Once, the classical cAMP pathway as paradigma of the second messenger concept was considered simple and straightforward, but with increasing number of investigations it has become very complex. One reason is that cAMP not only induces phosphorylation of proteins via activation of a cAMP-dependent protein kinase A (PKA) but also induces protein-protein interaction independently of any phosphorylation event (Hanoune et al., 2001). Another reason for this complexity is the extreme variety of potential regulators of cAMP such as G protein-coupled receptors (GPCR) that trigger cAMP generation (1.1.1), numerous adenylyl cyclase (AC) isoforms for the synthesis of cAMP (1.1.2), different cAMP effector mechanisms (1.1.3) and finally a multitude of enzymes having cAMP phosphodiesterase (PDE) activity to degrade cAMP (1.1.4). By these boundless possibilities, cAMP can influence a broad range of metabolic processes, including gluconeogenesis, glycogenolysis and lipogenesis, as well as secretory processes, muscle contraction, learning, ion channel conductance, pro-inflammatory cytokine production and action, differentiation, apoptosis and growth control (Houslay et al., 1997).

1.1.1 G protein-coupled receptors (GPCRs)

Extracellular signals (first messengers) are transmitted into the cell interior by means of different classes of membrane receptors. GPCRs constitute the largest and most ubiquitous family among these surface receptors (Pierce et al., 2002). More than 800 genes encoding GPCRs involved in sensory (odorants, light, etc.) and chemical stimuli (catecholamines, amino acids, peptides, and even ions) have been identified so far (Hermans, 2003; Wess, 1998). Based on their amino acid similarity, ligand structure and G-Protein coupling, GPCRs can be grouped within mammalian cells into four different classes (Foord et al., 2005). Further classifications were proposed for pheromone receptors of yeasts and nematodes (Pierce et al., 2002; Wess, 1998).

1. Class I is the largest group, and includes a multitude of GPCRs sensitive for sensory stimuli (rhodopsin, colors, odorants), glycoprotein hormones, a broad range of peptides (e.g. chemokines, opioids, neuropetides, etc.), biogenic amines (e.g. adrenaline, dopamine, acetylcholine, etc.) and diverse miscellaneous receptors that bind for example prostanoids or leukotrienes.
2. Class II comprises members of the secretin/glucagon receptors.
3. Class III includes metabotrophic glutamate receptors, calcium sensors and γ-aminobutyric acid (GABA) receptors.
4. Class IV represents a separate class of frizzled and smoothened GPCRs sensitive for “Wnt”, a small group of secreted peptides involved in oncogenesis and embryogenesis (Foord et al., 2005).

Despite enormous variations in their amino acid sequence and structural differences of their activating ligands, all GPCRs share a common three-dimensional structure of seven transmembrane helices linked by alternating intracellular (i1–i3) and extracellular (o2–o4) loops. Whereas the extracellular receptor surface, including the extracellular N-terminal domain, is known to be critically involved in ligand binding, the intracellular part of the receptor is known to be important for G-protein recognition and activation (Wess, 1998).

Beside the similar structure of GPCRs, they all operate through a similar molecular mechanism. The binding of extracellular ligands to GPCRs causes conformational changes in the receptor protein that promote the associations with distinct classes of heterotrimeric G-proteins (Wess, 1998; Dohlman et al., 1991). These G-proteins consist of α-subunits bound to $\beta\gamma$ complexes and are attached to the cytoplasmic surface of the plasma membrane. Interaction of the ligand-activated receptor with the G-protein triggers the exchange of GTP for GDP on the α-subunit and results in the dissociation of the G-protein from the receptor and the dissociation of the G-protein α-subunit from the $\beta\gamma$ complex. The released G-protein subunits, α-GTP and free $\beta\gamma$, are then able to interact with distinct effectors such as ion channels or enzymes like adenylyl cyclases. Because of the intrinsic GTPase activity of all α-subunits, α-GTP is hydrolyzed to α-GDP, which is able to bind free $\beta\gamma$ complexes with high affinity as a kind of feedback regulation (Bourne, 1997; Neer, 1995).

GPCR signalling is highly specific and complex because of the existence of numerous G-protein subunits. Up to now, at least 23 α-subunits derived from 17 different genes have been identified and are classified into four families ($G\alpha_{i/o}$, $G\alpha_s$, $G\alpha_{q/11}$, and $G\alpha_{12}$). Concerning β- and γ-subunits, at least 6 and 12 different molecular species have been described, respectively (Vanderbeld et al., 2000; Gautam et al., 1998). A large variety of intracellular and membrane effectors have been identified for G-proteins such as K^+-channels, Ca^{2+}-channels, Phospholipase C, protein kinases and adenylyl cyclases (Hermans, 2003). The latter, mostly transmembrane enzymes subdivided into numerous categories are the cAMP synthesizing enzymes.

1.1.2 Adenylyl Cyclases (ACs)

Cyclic AMP is synthesized in mammalian cells by two evolutionary related families of adenylyl cyclases, soluble adenylyl cyclases (sAC) and transmembrane adenylyl cyclases (tmAC). These two enzymes share a conserved overall architecture in their catalytic domains and a common catalytic mechanism, but they differ in their subcellular localization and response to various regulators. Both ACs catalyze the cyclization of ATP to generate cAMP and inorganic pyrophosphate (Kamenetsky et al., 2006). Up to now, at least nine closely related isoforms of tmACs (AC1-9), encoded by different genes and two different splicing variants of isoform AC8 have been discovered (view Table 1). Each tmAC isoform and variant consists of two hydrophobic domains (with six transmembrane spans) and two cytoplasmic domains resulting in a pseudosymmetrical protein. The cytoplasmic domains, which constitute the catalytic site, are subject to intracellular regulations specific for each subtype. The major regulators of tmACs are heterotrimeric G proteins, which transduce extracellular signals via GPCRs. Further important regulators of tmACs are the calcium receptor protein calmodulin, protein kinases (PKA and PKC), NO-dependent inhibition and presumably many more. Forskolin, a diterpene compound isolated from plants (*Plectranthus barbatus* or *Coleus forskohlii*) is an often experimentally used activator of tmACs (Kamenetsky et al., 2006; Hanoune et al., 2001).

	Response to cAMP signaling pathway component[a]					
AC isoform	**Gαs**	**Gαi**	**G$\beta\gamma$**	**FSK**	**Calcium**	**Protein kinases**
AC1	↑	↓ (CaM- or FSK-stimulated activities)	↓	↑	↑ (CaM) ↓ (CaM kinase IV)	↑ PKC (weak) ↓ (CaM kinase IV)
AC2	↑	→	↑ (when stimulated by Gαs)	↑		↑ (PKC)
AC3	↑	↓		↑	↑ (CaM) (in vitro) ↓ (CaM kinase II)	↑ (PKC) (weak) ↓ (CaM kinase II)
AC4	↑		↑	↑		↑(PKC)
AC5	↑	↓	↓ ($\beta 1\gamma 2$)	↑	↓ (<1 μM)	↓ (PKA) ↑ (PKCα/ζ)
AC6	↑	↓	↓ ($\beta 1\gamma 2$)	↑	↓ (<1 μM)	↓ (PKA, PKC)
AC7	↑		↑	↑		↑ (PKC)
AC8	↑	↓ (Ca^{2+} rises)		↑	↑ (CaM)	→ (PKC)
AC9	↑	↓		↑ (weak)	↓ (calcineurin)	
sAC	→	→		→		

Table 1. Regulatory properties of mammalian adenylyl cyclases (modified from Hanoune, 2001). [a] ↑= activation; ↓ = inhibition; → = neutral response. Abbreviations: CaM; Calmodulin; FSK; forskolin.

In contrast to tmACs, sACs are insensitive to forskolin and also to heterotrimeric G-protein regulation. sACs are uniquely regulated by the intracellular signaling molecules bicarbonate and calcium. Alternative splicing of the single sAC generates diverse isoforms, which are widely expressed (Sinclair et al., 2000) and are not strictly soluble proteins but mostly present at discrete subcellular localizations in a wide variety of cells (Geng et al., 2005; Jaiswal et al., 2001).

Overall, table 2 illustrates the tissue distribution of the mammalian ACs and indicates that certain isoforms are related to distinct cAMP-mediated functions, such as circadian rhythm, learning /memory, drug & ethanol dependency or cell proliferation as examples.

AC isoform	Tissue distribution[a]	Potential associated function	Human chromosome
AC1	Brain (neuron), adrenal gland (medulla)	Circadian rhythm, synaptic plasticity, learning, memory, LTP, drug dependency	7p12
AC2	Brain, skeletal muscle, lung [heart]	Synaptic plasticity, arrest of cell proliferation	5p15
AC3	Brain, olfactory epithelium, male germ cells, pancreas, BAT [uterus, heart, lung]	Odorant stimulation	2p22–24
AC4	Brain [heart, kidney, liver, lung, BAT, uterus]		14q11.2
AC5	Heart, brain [kidney, liver, lung, uterus, adrenal, BAT]		3q13.2–q21
AC6	Widespread	Cell proliferation	12q12–13
AC7	Brain, platelets, widespread	Ethanol dependency	16q12–13
AC8	Brain, lung, [testis, adrenal, uterus, heart]	Synaptic plasticity, LTP, drug dependency	8q24
AC9	Brain, skeletal muscle, widespread		16p13.3
sAC	Testis [other tissues]		1q24

Table 2. Tissue distribution of mammalian adenylyl cyclases (modified from Hanoune, 2001). [a] Underlined tissue expressed this isoform at high level; [ ] = low level of expression determined by PCR; Abbreviations: BAT; brown adipose tissue; LTP; long-term potentiation.

1.1.3 Effectors of cAMP

Today, at least three different targets of cAMP have been identified that regulate various functions in different cell types:

1. cAMP-dependent protein kinase A (PKA)
2. Cyclic-nucleotide-gated ion channels (CNG)
3. Exchange protein directly activated by cAMP (Epac) also known as cAMP-regulated guanine exchange factor (cAMP-GEF)

PKA was one of the first discovered protein kinases (Walsh et al., 1968). This enzyme is composed of two separate subunits, the catalytic (C) and regulatory (R) subunits that interact to form an inactive holoenzyme complex. Phosphorylation of the C subunit is required for the biological activity of PKA.

There are four different R subunit genes and their isoforms (RI_{α}, RI_{β}, RII_{α}, and RII_{β}), which are differentially expressed in tissues (Cheng et al., 2008; Adams et al., 1995). The subcellular distribution of PKAs is determined by a family of A-kinase anchoring proteins (Dodge et al., 2001) that link their R subunits to specific subcellular structures and ensure specificity in signal transduction by placing the kinase close to its appropriate effectors or substrates (Scott et al., 1994).

The binding of the ligand cAMP to the R subunits induces a conformational change and subsequently the dissociation of the holoenzyme into its constituent C and R subunits. The free active C subunit can then affect a multitude of diverse cellular events by phosphorylating cytoplasmic and nuclear protein substrates (Cheng et al., 2008; Taylor et al., 1990). For example, by phosphorylating the nuclear cyclic-AMP-response-element-binding-protein, the co-activator CREB-binding protein (CBP) is recruited, which has an intrinsic histone acetyltransferase activity and interacts with RNA polymerase II. This process results in an enhanced transcription of a great number of genes that carry the cAMP response element (CRE) motif in their promotor region (Zhang et al., 2006; Beavo et al., 2002).

In addition to PKA, cyclic-nucleotide-gated ion channels (CNG) are also critical effectors of cAMP signaling. These nonselective cation channels are opened by the direct binding of guanosine 3'-5' cyclic monophosphate (Marienfeld et al., 2001) and cAMP that regulate the influx of Ca^{2+} in particular, but also alkali ions like Na^{+}. CNG channels are expressed in many neurons of the mammalian brain, in the photoreceptors of the retina, in the chemosensory cells of the olfactory, vomeronasal and taste system, but also in spermatozoa, and act as molecular links between GPCR cascades and Ca^{2+}-signalling systems (Kaupp et al., 2002; Zufall et al., 1997).

Another family of recently discovered cAMP sensor proteins, named Epac becomes more and more important (Mei et al., 2002). Similar to PKA, these proteins contain a cAMP-binding domain (CBD). Epac proteins bind to cAMP and subsequently activate the Ras superfamily small GTPases Rap1 and Rap2. By discovering Epac as cAMP regulated protein, the cAMP-mediated signaling mechanism became much more complex. Several studies demonstrated that activation of Epacs is also responsible for effects that were previously thought to be controlled by PKA alone. Similar to PKA, Epac proteins mediate also many cAMP-related cellular functions such as cell adhesion, cell-cell junction, cell differentiation and proliferation. Since both, PKA and Epac are ubiquitously expressed in all tissues, an increase in intracellular cAMP levels will consequently lead to the activation of both PKA and Epac and requires therefore control mechanisms that act in a spatial, temporal or collaborative manner (Cheng et al., 2008). The underlying reasons leading to opposite or synergistic effects of PKA and Epac activation are not fully understood and are actually the objectives of various studies.

1.1.4 Cyclic nucleotide phosphodiesterases (PDEs)

By hydrolizing cyclic nucleotides, PDEs play a crucial role in the regulation of various cellular functions and cAMP-signalling in particular. Twenty-one genes with multiple promotors have been identified that encode PDE transcripts. Alternate splicing of these genes leads to the expression of over 50 distinct PDE isoforms. This diversity and the specific distribution at cellular and subcellular levels provide an effective tool to control the magnitude and duration of the cAMP signal in a spatial and temporal manner (Lugnier, 2006).

Based on sequence similarity, kinetics, modes of regulation, and pharmacological properties, the PDE superfamily is subdivided into eleven families (PDE1–PDE11, see figure 1). Their nomenclature uses arabic numbers after the PDE acronym to identify the different families. The genes and subtypes of the individual family are expressed by capital letters respectively. Additionally arabic numbers after these letters indicate the corresponding isoform (e.g. PDE4B1). Furthermore, the PDE families can be differentiated functionally by means of their relative affinities for cAMP and cGMP. Three of the eleven PDE families selectively hydrolyze cAMP (PDEs 4, 7, and 8). Another three families are selective for cGMP (PDEs 5, 6, and 9), and five families hydrolyze both cyclic nucleotides with varying efficiency (PDEs 1, 2, 3, 10, and 11) (Lugnier, 2006; Conti et al., 1999). Figure 1 illustrates that all PDEs share common structural elements like a highly conserved catalytic domain with a 20– 45% identity of about 270 amino acids. It is composed of 17 alpha helices consisting of 3 subdomains that define a deep pocket where the substrate or inhibitors can bind. Furthermore, it includes binding domains for two metal ions (Zn^{2+} and Mg^{2+}) essential for the catalysis (Conti et al., 2003).

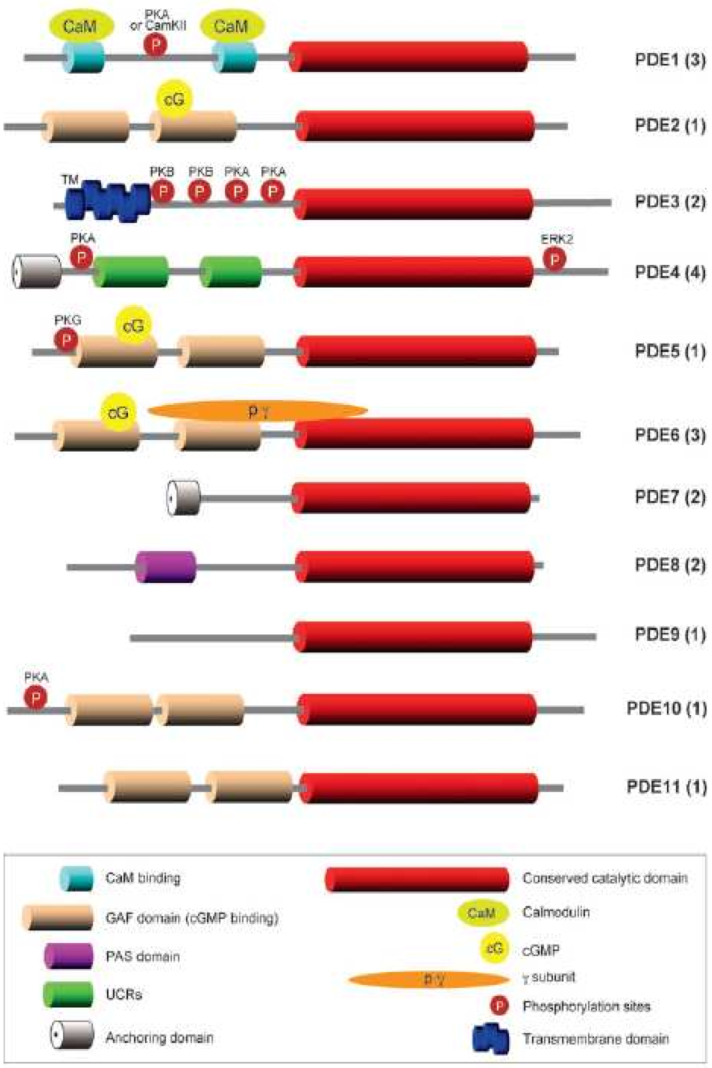

Figure 1. Schematic illustration of the structure of the 11 phosphodiesterase (PDE) families (modified from Conti & Beavo 2002). The family name is reported on the side of each structure, and the number in parenthesis denotes the number of genes composing the family. The conserved catalytic domain is represented as a red cylinder. Binding proteins are marked yellow. Phosphorylation sites are reported as a red symbol marked P. Abbreviations: CaM; calmodulin, CamKII; calmodulin-regulated kinase II, ERK2: extracellular signal-regulated kinase 2, pγ; PDE γ subunit, GAF; cGMP-activated PDEs, PAS; period aryl-hydrocarbon receptor nuclear translocator (ARNT), PKA; protein kinase A; PKB, protein kinase B; TM, transmembrane domain of PDE3, UCRs; upstream conserved regions.

The second common element is the regulatory domain located between the amino terminus and the catalytic domain, which represent diverse regulatory units among the PDE family members: Calmodulin binding sites for PDE1, allosteric cGMP binding sites, that is, GAF domains for PDE2, PDE5, PDE6, PDE10, and PDE11, phosphorylation sites of different kinases (PKA, PKB, MAPK and CamKII) for PDE1, PDE3, PDE4, PDE5 and PDE10, PAS domain for PDE8, autoinhibitory sequences for PDE1 and PDE4, a transmembrane domain for PDE3, as well as anchoring domains for PDE4 and PDE7 (Conti et al.,2007; Lugnier, 2006; Houslay et al., 1997). Each isoform of a PDE subtype is characterised by a unique N-terminal region and therewith has unique properties concerning activation, regulation and subcellular distribution. The various isoforms of PDEs represent a fine-tuned control system of distinctly compartmentalised PKA-R species that generate cAMP (figure 2). The spatial separation of the sites of synthesis, detection and degradation of cAMP leads to the establishment of spatial gradients. This compartmentalisation has functional consequences for the integration of cellular signalling responses mediated by cAMP and the means by which they are modulated through the action of other signalling systems (Houslay et al., 1997).

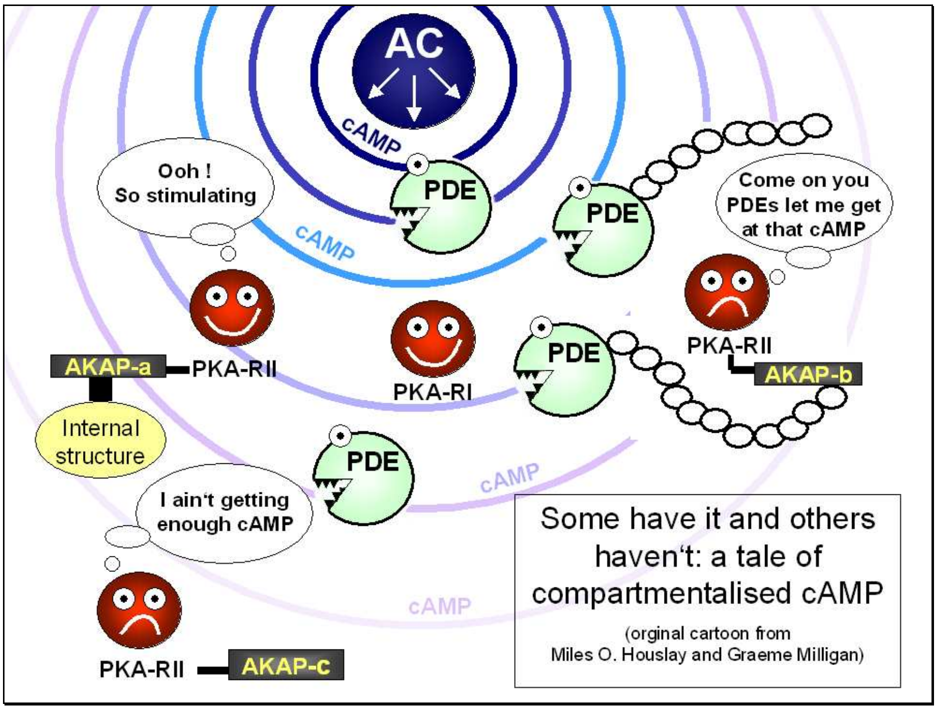

Figure 2. The tale of compartmentalised cAMP (modified from Houslay and Milligan 1997). The cAMP produced by AC at the plasma membrane diffuses into the cytosol where both anchored (chains) and free, cytosolic PDE activities allow gradients of different cAMP concentrations to be established (blue). Anchored PDEs can also create localised cAMP gradients. Changes in cAMP concentrations in specific intracellular compartments (blue shades) can be sampled and monitored by anchored PKA-RII isoforms. By contrast to this, PKA-RI isoforms can sample cAMP levels throughout the cell cytosol. The pattern of PKA-RII activation in a cell will depend upon (1) the site of cAMP production, (2) the rate of cAMP hydrolysis by soluble PDEs, (3) the activity of anchored PDEs and the specific location of the anchored PKA-RII.

1.2 Phosphodiesterase 4 (PDE4)

In 1980 there was one of the first biochemical characterizations of a PDE enzyme, proteolysed from liver membranes that demonstrated to be cAMP-specific and cGMP-insensitive (Marchmont et al., 1980). Few years later, PDE4 enzymes were first recognized (Reeves et al., 1987) as a distinct family, originally called “PDE-IV”, based upon their unique sensitivity to inhibition by Rolipram (Wachtel, 1982), which is now considered as the archetype of a PDE4 selective inhibitor. The first molecular cloning of PDE4 enzymes became possible by the identification of the *dunce* gene in the fruitfly *Drosophila melanogaster* genome (Qiu et al., 1991). Disruption of this gene led to learning and memory defects. This *dunce* PDE was then used to isolate rat PDE4 forms (Davis et al., 1989) and a following study demonstrated the presence of four PDE4 genes in rat (Swinnen et al., 1989). A few years later, theses genes were also identified in man encoding four subfamilies PDE4A, PDE4B, PDE4C and PDE4D (Bolger et al., 1993).

Since that time the PDE4 family has been target for the development of selective inhibitory drugs that provide therapeutical potential for the treatment of inflammatory diseases, such as asthma, chronic obstructive pulmonary disease and psoriasis, as well as depression and might serve as cognitive enhancers (Houslay et al., 2005).

1.2.1 Structural and functional properties of the PDE4 family

The PDE4 family, which exclusively hydrolyzes cAMP is the largest PDE family and is constituted by 4 genes that form the subtypes PDE4A, PDE4B, PDE4C and PDE4D. Multiple transcriptional start sites as well as alternative mRNA splicing enable these genes to encode at least 35 different PDE4 proteins (Lugnier, 2006). The high homology of PDE4 exonic sequences and the range of isoforms among different species suggests that there has been a strong selective pressure during evolution to protect them from mutation and divergence and underline their role as important key players (Houslay et al., 2003).

Due to a highly conserved catalytic domain, all PDE4 isoforms have similar kinetic properties and ion requirements and are all inhibited by rolipram. This similar structure of the catalytic domain has been resolved at the atomic level for PDE4B (Xu et al., 2000) and PDE4D (Huai et al., 2004).

This domain is composed of 17 α helices connected by loops, with helices 6–13 containing residues critical for substrate binding and coordination of two metal ions involved in catalysis. Helices 1–7, 8–11, and 12–16 are clustered in subdomains allowing different conformational states of the catalytic center (Conti et al., 2003; Xu et al., 2000). PDE4 enzymes as metallohydrolases adapt their conformation of the catalytic domain depending on metal ion binding (cofactors) and thereby change their substrate or inhibitor affinity (Liu et al., 2001). Overall, the catalytic domain of PDE4 is composed of three important domains; First, a bivalent metal binding pocket (Zn^{2+}, Mg^{2+}) that forms a complex with the phosphate moiety of cAMP. Further, a pocket containing glutamine, which forms hydrogen bonds with the nucleotide moiety of cyclic AMP, and finally a solvent pocket (Houslay et al., 2003; Xu et al., 2000).

Although, the spatial relationship between the catalytic domain and the surrounding domains is still unknown, it is widely accepted that domains at the amino and carboxyl termini of the PDE4 protein exert important functions concerning conformation and regulation of the catalytic core (Conti et al., 2003). PDE4 specific sites for this interaction are two regions named upstream conserved regions 1 and 2 (Beard et al., 2000), highly conserved and arranged on the amino-terminal side of the catalytic domain (Bolger et al., 1993). Depending on the presence of UCR1 and UCR2, PDE4 isoforms can be subdivided into three groups, the long, the short and the super short forms (Houslay et al., 2005). The long isoforms have both UCRs, whereas the short forms lack UCR1. The super-short forms not only lack UCR1, additionally the UCR2 is truncated (figure 3).

This UCR1/UCR2 module functions as a regulatory domain that controls the conformation of the catalytic domain. Moreover Conti and coworker have shown that the UCR1-UCR2 domain has a major role in the quaternary structure of PDE4. Splicing variants containing both modules behave as dimers, whereas variants with one of the two UCRs missing behave as monomers. This dimerization is most likely critical for transmitting the conformational changes at the amino terminus to changes in conformation of the catalytic domain (Conti et al., 2003; Richter et al., 2002). Kinetic and inhibitor binding analyses with the longform PDE4A4 demonstrated that two conformational states of the enzyme coexist. Rolipram binds to the catalytic sites of both conformers, but with substantially different affinities (K_d ~ 2 nM versus K_d ~ 100 nM). These two sites are named low-affinity rolipram binding site (LARBS) and the high-affinity rolipram binding site (HARBS) (Zhao et al., 2003; Jacobitz et al., 1996). Although the catalytic activity is rather enhanced with N-terminal deletion as in short and super

short forms of PDE4, the potency of rolipram is reduced 10- to 30-fold. In contrast, this deletion has no effect on the affinity (Gresch et al., 2004) of cyclic AMP or the K_d of a structurally distinct PDE4-selective inhibitor like piclamilast (Jacobitz et al., 1996).
Finally, there is the carboxy-terminal region that is unique to each of the four PDE4 subtypes and whose role is still not clear (Houslay et al., 2003).

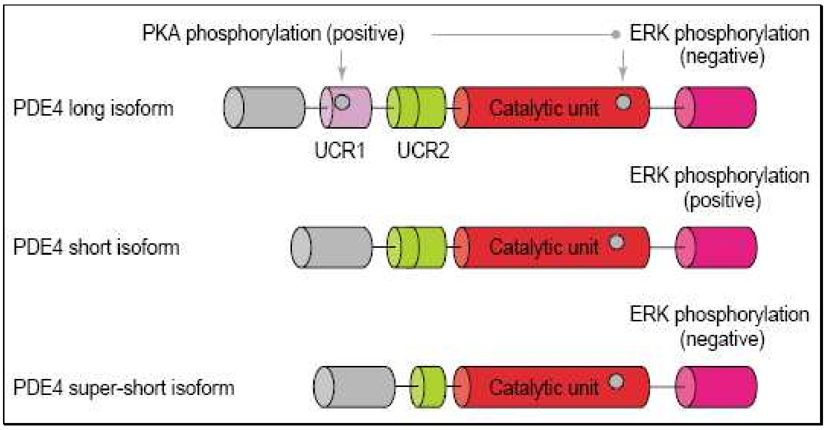

Figure 3. PDE4 subdivided isoforms (modified from Houslay, 2005). Their unique N-terminal region defines the three different groups of PDE4 isoforms. Indicated are; the regulatory UCR1 and UCR2 regions, the catalytic unit and sites for phosphorylation by PKA (Beard et al., 2000) and ERK (on the catalytic unit). The isoform-specific N-terminal region is shown in grey and the subfamily-specific C-terminal region is shown in pink.

1.2.2 Regulation of PDE4 and its role in cAMP-signaling

PDE4s are considered to be important cAMP homeostatic regulators, because they participate in feedback regulations involved in cell desensitization, adaptation, signaling cross talk, and cAMP signal compartmentalization (Conti et al., 2003).
As indicated in the previous chapter (figure 3), the UCR1/UCR2-module plays a key role in regulating the activity of PDE4s. The UCR1 of PDE4 longforms can be phosphorylated and thus activated by PKA. This activation is achieved by disrupting an H-bond interaction between UCR1 and UCR2 through a conformational change (Beard et al., 2000). Furthermore, PKA phosphorylation increases also the affinity for Mg^{2+} and therefore enhances the catalysis of cAMP. These events represent an important feedback mechanism for cAMP signaling by increasing the cellular capacity for cAMP degradation (Sette et al., 1996).
Another regulatory intervention allows the phosphorylation by ERK. With the exception of PDE4A, all remaining isoforms can be phosphorylated by ERK at the catalytic unit and

provide an isoform-dependent regulation of either activation or inhibition (Baillie et al., 2000). The functional outcome of ERK phosphorylation depends on the interplay with the available UCR unit(s) of the individual PDE4 isoform. On the one hand, inhibition is seen in PDE4 longforms, where UCR1 and UCR2 form a regulatory modul that inhibit the catalytic unit. The consequence is an increase of cAMP levels that could potentially activate PKA, which alters the regulatory modul by phosphorylating UCR1 and finally overcome the inhibitory ERK signal as feedback mechanism.

On the other hand, PDE4 short forms with an intact UCR2 unit show the opposite. ERK phosphorylation leads to an augmentation of their catalytic activity (Baillie et al., 2000). On the contrary the activity of PDE4 super short forms, with their truncated version of UCR2, are inhibited after phosphorylation by ERK, and in contrast to the long forms, the lack of UCR1 prevent a feedback regulation by PKA (Houslay et al., 2000).

The PDE4 activity and the regulation of the cAMP signaling respectively are complemented by a supplemental diversification of the spatial occurrence of PDE4 isoforms in the cell. Therefore, the unique N-terminal region does not only regulate the catalytic activity of PDE4 isoforms, but is also involved in intracellular targeting. A study on PDE4A1 (Bruno et al., 2009) showed, that the simple deletion of the N-terminal region converted an entirely membrane-associated enzyme into a cytosolic one without changing the catalytic activity (Shakur et al., 1993). This targeting is due to a unique N-terminal domain named TAPAS-1 that binds to lipids in the membrane bilayer (Baillie et al., 2002). Such lipid interaction as intracellular targeting represents an exception, since the spatial distribution of the residual PDE4 isoforms is based on protein-protein interaction (Houslay et al., 2005). Table 3 shows the group of PDE4 protein binding partners that have been identified so far.

These are mostly signaling scaffold proteins, such as β-arrestin, AKAPs, RACK1 and myomegalin. Their interaction with different isoforms of PDE4 localized to specific sites of cAMP activity, such as GPCRs or the following effectors, such as PKA and Epac, provide the basis for a fine-tuned and compartmentalized cAMP signaling network (Baillie et al., 2005; Baillie et al., 2003; Dodge et al., 2001; Verde et al., 2001; Yarwood et al., 1999). Several fluorescence-resonance-energy-transfer (FRET)-based approaches have been used to visualize cAMP dynamics and the activation of its effectors in a spatiotemporal manner (Conti et al., 2007; DiPilato et al., 2004; Zaccolo et al., 2002; Zhang et al., 2001).

PDE4 interacting proteins

Interacting protein	PDE4 isoform	Comments on interaction
SH3-domain-containing proteins	PDE4A4, PDE4A5, PDE4D4	Shows specificity for SH3 domain (e.g SRC family tyrosyl kinases). All human PDE4A species interact weakly with SH3 domains via LR2 region.
RACK1	PDE4D5	Binds to region in unique N-terminal region.
Myomegalin	PDE4D3	Shown for PDE4D3. Interacts with UCR2, implying all isoforms can bind.
β-arrestin	PDE4D5; all PDE4	Conserved interaction site within catalytic unit allows all PDE4s to interact. PDE4D5 has additional interaction site within its unique N-terminal region.
XAP2 (AIP, ARA9)	PDE4A4, PDE4A5	Binds to unique N-terminal region of indicated PDE4A isoforms and also binds to a site in UCR2.
mAKAP	PDE4D3	Involves unique N-terminal region. PKA phosphorylation of Ser13 in N-terminus of PDE4D3 enhances interaction.
AKAP450	PDE4D3	Involves unique N-terminal region.
ERK	All	Interacts with docking and specificity sites in the catalytic unit that straddle the phosphorylation site for ERK found in PDE4B, PDE4C, PDE4D but not PDE4A isoforms.

Table 3. PDE4 interacting proteins (modified from Houslay, 2005)

1.2.3 Functional impact of PDE4 subtypes

Knowledge about the functional impact of PDE4 subtypes derived from studies of either cell-based investigations of small-interfering RNA (siRNA)-mediated knockdown of specific PDE4 subtypes or by the knockout of distinct PDE4 subtype genes in mice. These studies increased evidence, that distinct PDE4 subtypes have unique non-redundant functions in various cells. Anti-inflammatory effects in different celltypes are accredited to the unique function of subtype PDE4B. In murine macrophages, it was shown that PDE4B exclusively and not PDE4A or PDE4D regulates the LPS-induced TNF-α release (Jin et al., 2005; Jin et al., 2002). Furthermore, subtype PDE4B was found to be the predominant subtype in human neutrophils and in unstimulated or LPS-stimulated monocytes (Wang et al., 1999). In this context, ablation of PDE4B and PDE4D but not PDE4A has further profound effects on neutrophils functions such as reduced chemotaxis and a decreased expression of adhesions molecules on the surface of these cells (Ariga et al., 2004).

In human T-lymphocytes it was shown that subtype PDE4D plays the predominant role in the regulation of various T-cell functions like IL-2, IL-5 and IFN-γ secretion or proliferation (Peter et al., 2007). Studies on PDE4D-knockout mice demonstrated its essential role in cAMP homeostasis and cholinergic stimulation of the airways, and in the development of airway-hyperreactivity. Furthermore, these knockout phenotypes also indicated the central role of PDE4D in balancing relaxant and contracting cues in airway smooth muscles (Mehats et al., 2003; Hansen et al., 2000). PDE4D but not PDE4A or PDE4B plays also a critical role in β_2-adrenoceptor-dependent cAMP signaling, as a study on mouse embryonic fibroblasts deficient in these genes has been demonstrated (Bruss et al., 2008). Moreover, PDE4D seems also to be responsible for the known central-nervous-system-related and cardiac-related side effects of PDE4 selective inhibitors (Lehnart et al., 2005; Robichaud et al., 2002).

Although, there are results from PDE4D-deficient mice, indicating that this subtype is required not only for the regulation of fertility but also growth (Jin et al., 1999), cellular mechanisms of it remain unknown. Despite the knowledge that PDE4 inhibitors affect a number of cellular functions, the involvement of distinct PDE4 subtypes in processes like growth or proliferation is not completely understood.

1.2.4 Inhibitors of PDE4

In the middle of the 19th century, there was the first report from Henry Salter that coffee might have benefical effects on asthma attacks (Salter, 1859). Some years later, a degradation product of caffeine namely theophylline was isolated (Kossel, 1889; Kossel, 1888). The mode of action of theophylline could at least in parts be elucidated after the discovery of PDE. It was shown, that theophylline inhibits PDEs unspecifically with a K_i of 100 µM (Butcher et al., 1962). The achieved increase of cAMP leads to bronchodilation (Rabe et al., 1998) and reduces the activation of a wide range of inflammatory and lung resident cells (Torphy, 1998).

But theophylline also exhibits a PDE-independent mode of action as the activation of histone deacetylase (HDAC) activity, which decreases inflammatory gene expression (Ito et al., 2002). However, cAMP-hydrolyzing PDEs and especially PDE4, which is present in various inflammatory cells, was identified as an interesting target to develop anti-inflammatory drugs. The antidepressant compound Rolipram was the first potent cAMP-PDE inhibitor, highly selective for PDE4 (Schwabe et al., 1976). Thereupon, many pharmaceutical companies started to develop rolipram analogues for inflammatory diseases like asthma, COPD or psoriasis. One of these developments, resulted in piclamilast also known as RP73401 from Sanofi-Aventis, formerly Rhône-Poulenc Rorer (Raeburn et al., 1994). But piclamilast and the most rolipram analogues, failed in clinical trials, due to their adverse events. These side effects, in humans namely diarrhoea, headache, nausea and emesis, narrow the therapeutic window for PDE4 administration (Dastidar et al., 2007; Rabe et al., 2005). Major efforts have been directed to design compounds with a potentially more advantageous therapeutic window, for example, by trying to achieve isotype selectivity (PDE4B > PDE4D) or decreased affinity for the high-affinity rolipram binding site, which is thought to be associated with the emetogenic potential of these compounds (Pages et al., 2009).

Table 4 shows the current status of oral PDE4 inhibitors in clinical development. The compound roflumilast, structurally similar to piclamilast (see figure 4), developed and registrated as Daxas® by Nycomed, formerly “Altana Pharma” (Hatzelmann et al., 2001) is one of the most potent oral PDE4 inhibitors. Several recently finished clinical phase III studies including over 1500 patients with Chronic Obstructive Pulmonary Disease (COPD), attested its efficacy. The increased Forced Expiratory Volume per second (FEV_1) as important paramenter of lung function, a significant reduction of the rate of exacerbations compared to placebo and tolerable adverse effects are essential outcomes of these studies (Rabe etal., 2005; Calverley et al., 2009). The submission of a Marketing Authorisation Application (MAA) to the European Medicines Agency (EMEA) and the American Food and Drug Administration for Daxas as a once-daily oral treatment for patients with COPD associated with chronic bronchitis is imminent (Pages et al., 2009). Further PDE4 inhibitors in clinical trials for the treatment of asthma, COPD or psoriasis (see table 4), are Oglemilast (Glenmark/Forest/Teijin), OX914 (Orexo), Apremilast (Celgene), MEM-1414 (Memory Pharmaceutical), GRC-4037 (Glenmark) and ELB353 (Biotie) (Pages et al., 2009).

Drug	Company	Status
Roflumilast	Nycomed	Pre-registration
Oglemilast	Glenmark/Forest/ Teijin	Phase II: COPD and asthma
OX914/IPL-455,903	Orexo AB	Phase II: COPD and asthma
Apremilast/CC-10004	Celgene	Phase II: Psoriasis
MEM-1414	Memory Pharmaceuticals	Phase II: Asthma
GRC-4039	Glenmark	Phase I: Rheumatoid arthritis
ELB353	Biotie	Phase I: Asthma and COPD

Table 4. Development of current PDE4 inhibitor (modified from Pages et al., 2009)

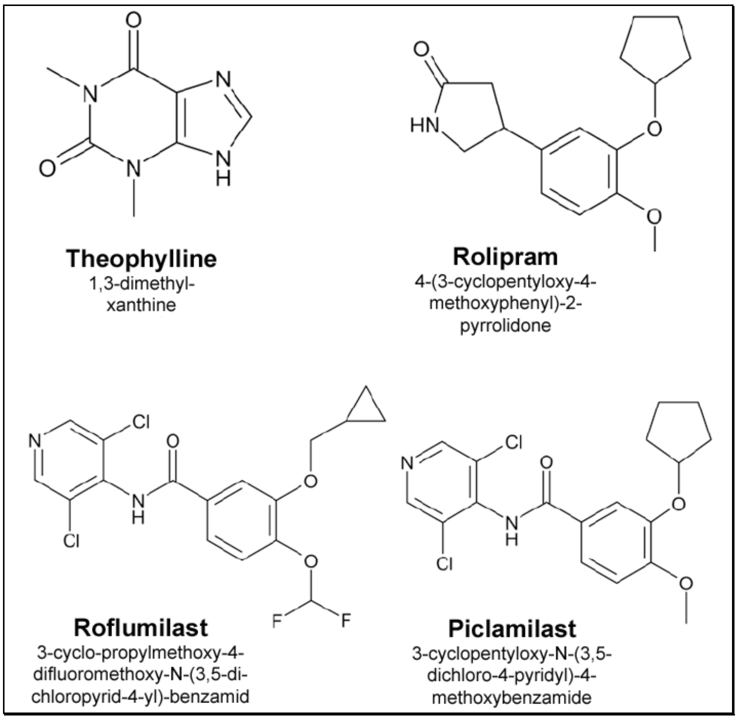

Figure 4. Chemical structures of a representative set of PDE4 inhibitors
(modified from Houslay et al., 2005)

1.2.5 Distribution of PDE4 and the biological effect of its inhibition

PDE4 is omnipresent and regulates in a broad range of different cells the signalling of cAMP and therewith its inhibition influences many cellular functions. Under various pathophysiological conditions PDE4 inhibition might offer a therapeutic benefit, which has been demonstrated in numerous in vitro and in vivo studies. Due to the fact that PDE4 subtypes are widely spread in neurons and glia cells (Conti et al., 2007), PDE4 inhibitors were initially considered as therapeutic agents for CNS-related disease, such as depression (Wachtel, 1983) or schizophrenia (Kanes et al., 2007; Maxwell et al., 2004). Further CNS related indications such as Alzheimer disease (Gong et al., 2004) or Rubinstein-Taybi syndrome (Bourtchouladze et al., 2003) are based on the improved long-term potentiation (LTP) of the memory and contextual learning after PDE4 treatment. In addition, Rolipram was suggested as useful therapy after spinal cord injury, since PDE4 inhibition promotes axonal regeneration and functional recovery (Nikulina et al., 2004). In islets of Langerhans, PDE4 inhibition leads to an enhanced glucose-dependent insulin secretion (GDIS) that might be beneficial in type 2 Diabetes (Waddleton et al., 2008). Moreover, inhibition of PDE4 in chondrocytes (Tenor et al., 2002) showed protective effects versus nitric oxide- (NO) induced cartilage degradation relevant in osteoarthritis. Furthermore, osteoporosis might also be a useful indication for PDE4 inhibitors, since PDE4 is a key regulator of TRANCE expression in osteoblasts, which in turn controls osteoclast formation (Takami et al., 2005).

The list of cellular examples is endless. Wherever cAMP plays a crucial role in biological functions, there is a justified supposition that PDE4 enzymes are involved. In general, increasing levels of cAMP decrease the activity of nearly all immunomodulatory and inflammatory cells (Hatzelmann et al., 2001) and selective PDE4 inhibitors effect this increase (Essayan, 1999; Torphy, 1998).

Therefore, PDE4 inhibitors have been proposed as a therapeutic approach for a variety of inflammatory diseases such as psoriasis and atopic dermatits (Nazarian et al., 2009). However, the predominant proportion of studies deals with benefical effects of PDE4 inhibition in respiratory diseases with an inflammatory component such as asthma (Lu et al., 2009), COPD or lung fibrosis. Table 5 lists pathophysiologically relevant cells, notes the presence of PDE4 subtypes in these cells and specifies the biological consequences of PDE4 inhibition.

Cell type	PDE4 Subtype [a]	Biological consequence of PDE4 inhibition	Reference
T lymphocytes CD4 CD8	B>A	Inhibition of proliferation and cytokine release	(Gantner *et al.*, 1997b; Hatzelmann and Schudt, 2001; Smith *et al.*, 2003; Peter *et al.*, 2007)
B cells	B, D>A	Increased proliferation	(Gantner *et al.*, 1998; Smith *et al.*, 2003)
Eosinophils	A, D>B	Inhibition of superoxide anion generation; delayed apoptosis	(Hatzelmann and Schudt, 2001; Smith *et al.*, 2003; Parkkonen *et al.*, 2007)
Neutrophils	A, D>B	Inhibition of superoxide anion and neutrophil elastase release	(Hatzelmann and Schudt, 2001; Smith *et al.*, 2003; Jones *et al.*, 2005)
Monocyte	B >A, D	Inhibition of TNF-α release	(Hatzelmann and Schudt, 2001; Smith *et al.*, 2003; Heystek *et al.*, 2003; Jones *et al.*, 2005)
Macrophages	A, B, D	Inhibition of TNF-α release[b]	(Gantner *et al.*, 1997a; Hatzelmann and Schudt, 2001; Smith *et al.*, 2003; Barber *et al.*, 2004)
DCs	A>B, D	Inhibition of TNF-α release	(Hatzelmann and Schudt, 2001; Heystek *et al.*, 2003)
Mast cells		Little if any mast cell stabilization	(Weston *et al.*, 1997; Shichijo *et al.*, 1998)
Airway epithelial cells		Increased production of PGE_2; inhibition of IL-6 production	(Fuhrmann *et al.*, 1999; Haddad *et al.*, 2002)
		Inhibition of EGF-induced MUC5AC mRNA and protein expression	(Mata *et al.*, 2005)
Endothelial cells		Inhibition of adhesion molecule expression	(Jones *et al.*, 2005; Sanz *et al.*, 2007)
Lung Fibroblasts	A, B >D	Inhibition of fibroblast chemotaxis; inhibition of pro-MMP1, 2 release; inhibition of TGF-ß -induced myofibrobalst conversion;	(Kohyama *et al.*, 2002; Smith *et al.*, 2003; Martin-Chouly *et al.*, 2004; Dunkern *et al.*, 2007)
		inhibition of bFGF- and IL-1β-induced proliferation	(Selige *et al.*, 2010)
Sensory nerves[c]	D	Inhibition of neuropeptide release	(Spina *et al.*, 1995)

Table 5. PDE distribution within human cells interesting to be targeted for the treatment of pulmonary diseases such as asthma, COPD or lung fibrosis (modified from Spina, 2008)

In this regard, lung fibroblasts are of special interest. Under healthy conditions, lung fibroblasts are involved in wound healing. In a pathological situation, these cells become key players in pulmonary diseases since the chronical inflammatory environment leads to an overactivation of fibroblasts and might worsen the course of disease (Togo et al., 2008; Agostini et al., 2006; Jeffery, 2001). By elevating cAMP, PDE4 inhibitors might mediate two distinct effects on fibroblasts. On the one hand, inflammation is attenuated and the reduced release of cytokines such as IL-1β (Chung, 2006) and growth factors from e.g. epithelial cell (Nakamura et al., 1995), T lymphocytes (Gantner et al., 1998) or monocytes (Hatzelmann et al., 2001) act on fibroblast functions (Gamble et al., 2003). On the other hand, PDE4 inhibition directly prevents lung fibroblast functions such as proliferation and conversion into myofibroblasts (Dunkern et al., 2007).

1.3 Lung fibroblasts in pulmonary diseases

Figure 5. Phase contrast microscopy picture of normal human lung fibroblasts.

Lung fibroblasts (figure 5) are ubiquitous mesenchymal cells, found in the normal adult lung in the adventitia of vascular structures and airways. These cells have a spindle-shaped morphology and express interstitial collagens (Goldring et al., 1988). Lung fibroblasts play an important role in wound healing, tissues injury, and repair/remodeling/fibrosis (Phan, 2008). The exact source of lung fibroblasts in particular under pathophysiological conditions is not assured, since resident lung fibroblasts are enforced by the recruitment of circulating fibrocytes derived from mesenchymal progenitor cells of the bone marrow (Moeller et al., 2009).

Fibrotic alterations in the lung architecture are a pathological feature of chronic pulmonary diseases like asthma (Bergeron et al., 2009), idiopathic pulmonary fibrosis (Gross et al., 2001) or chronic obstructive pulmonary disease (Hogg et al., 2008). Wound healing and scarring are essential physiological mechanisms to maintain tissue integrity and function. However, they can exaggerate to a fibrotic condition especially under repeated exposure to various insults such as virus/bacterial infections, chemicals, radiation or allergens, which at the end can impair the function of the afflicted organs. Peribronchiolar wall fibrosis is described in COPD patients (Spurzem et al., 2005) and a fibrotic thickening of the basal membrane has also been observed in asthmatic patients. For asthma and COPD the impact of these fibrotic processes, which are most likely driven by repeated inflammation-repair cycles (Barnes, 2003; Jeffery, 2001), is not totally clear. However, in IPF the massive subpleural honeycombing parenchymal fibrosis and the fibrotic vascular remodeling are the major causes for reducing lung FVC, leading to a poor prognosis of this disease (Gross et al., 2001). Thus, the 5-year mortality in IPF is higher than in many cancer types (American Thoracic Society, 2000). Although, in contrast to IPF, fibrosis is not the dominant aspect in asthma and COPD, it is assumed that progression of such structural changes have a strong impact on the long-term outcome of these diseases (Chapman, 2004). Depending on the different stages of fibrosis progression, lung fibroblasts modulate their activities in a cytokine-dependent manner from migration to proliferation and finally to differentiaton into myofibroblasts, which is triggered by TGF-β. Myofibroblasts are characterized by the expression of alpha-smooth muscle actin (α-SMA), collagen and a high level of cytokine production. Therefore, the TGF-β induced myofibroblast conversion is expected to have a key role in inflammation, connective tissue deposition, and lung function, respectively (Togo et al., 2009; Dunkern et al., 2007).

Activation of lung fibroblasts or recruited fibrocytes (Andersson-Sjoland et al., 2008) in IPF is driven by a myriad of growth factors, cytokines and chemokines, such as TGF-β, PDGF, basic FGF (bFGF) and IL-1β from various cellular sources (Agostini et al., 2006).

1.3.1 Interleukin-1β (IL-1β), basic Fibroblast Growth Factor (bFGF) and Transforming Growth Factor- β (TGF-β) are relevant for fibroblast functions in pulmonary diseases.

TGF-β regulates cell growth and differentiation as well as production of extracellular matrix proteins. Elevated production of TGF-β has been associated with chronic inflammatory and fibrotic diseases such as IPF or COPD. Epithelial cells and intra-alveolar macrophages are the major source of TGF-β that induces the conversion of fibroblasts to contractile myofibroblasts (de Boer et al., 1998; Khalil et al., 1991). In addition, TGF-β causes an immediate release of extracellular bFGF from primary pulmonary fibroblasts and thus affects their proliferative behavior (Khalil et al., 2005).

Basic FGF (Kranenburg et al., 2005b) is also a critical growth factor in fibrosis. As a potent elicitor of lung fibroblast proliferation, bFGF has been proposed to induce fibrogenic, proliferative effects on lung fibroblasts in IPF, as demonstrated by histological investigations in lung tissue from patients with IPF (Inoue et al., 2002). In COPD an up-regulation of bFGF-receptors has been described in bronchial airway walls (Kranenburg et al., 2005b). Strikingly, by using explanted rat lung slices and primary pulmonary fibroblasts a recent study demonstrated that TGF-β unfolds its proliferative activity on fibroblasts by stimulating their bFGF release that acts in an autocrine fashion (Khalil et al., 2005). Besides this activity, bFGF is supposed to contribute to vascularization of the lung parenchyma representing another disease mechanism in IPF (Strieter, 2005).

IL-1β is expressed in alveolar macrophages of IPF patients with a constitutive interstitial inflammation (Zhang et al., 1993). Overexpression of IL-1β in airway epithelium induces, yet an IL-1 receptor antagonist inhibits lung fibrosis in animal models (Lappalainen et al., 2005; Kolb et al., 2001; Piguet et al., 1993). Lower concentrations of IL-1β have been described to exert modest proliferative effects on cells such as human lung fibroblasts, aside from inducing the release of PDGF and collagen I (Raines et al., 1989; Goldring et al., 1988). Higher concentrations of IL-1ß however, have been reported to cause anti-proliferative effects, for example in endothelial cells (Cozzolino et al., 1990) and in cardiac fibroblasts (Palmer et al., 1995).

Mechanistic interactions between bFGF and IL-1β on proliferation of rat aortic smooth muscle cells (Bourcier et al., 1995) and on COX-2 expression in human osteosarcoma cells have been reported (Laulederkind et al., 2000). The crucial regulatory role of the COX-2 (Rodriguez-Barbero et al., 2006), its product PGE_2 and the subsequently generated cAMP via activation of prostanoid receptors EP_2 and EP_4 has been reported in various studies (Huang et al., 2007; Vancheri et al., 2000; Diaz et al., 1998). Previously, it was shown that cAMP and thus PDE4 inhibitors prevent a number of fibroblast functions.

1.4 PDE4 inhibition and cAMP-increase in lung fibroblasts has benefical effects in pulmonary diseases

As already detailed in chapter 1.2.5, by elevating cAMP, PDE4 inhibitors mediate a lot of cellular functions in various cells and also lung fibroblasts, which are major key players in pulmonary diseases. Because PDE4 enzymes degrade cAMP, its inhibition gets relevant for cellular processes controlled/triggered by mediators that activate ACs and subsequently generate cAMP. In this context, prostaglandine E_2 (PGE_2) as mediator, plays a key role in modulating inflammation and tissue repair (Vancheri et al., 2004). PGE_2 is formed from arachidonic acid and a product of the cyclooxygenase pathway. There are four different prostanoid receptors (GPCRs) sensitive for PGE_2 (EP_{1-4}, Sugimoto et al., 2007). In lung fibroblasts, EP_2 and EP_4 are predominant expressed and both, via G_s-signaling increase by cAMP in these cells (Haag et al., 2008). In the lung, PGE_2 is the major prostanoid synthesized by lung fibroblasts but also by neighboring alveolar epithelial cells (Huang et al., 2007). By elevating cAMP, PGE_2 influences a range of fibroblast functions. Figure 6 depicts the interplay of lung fibroblasts, inflammatory cells and epithelial cells as well as the role of PGE_2 and cAMP elevation within pathophysiologic conditions.

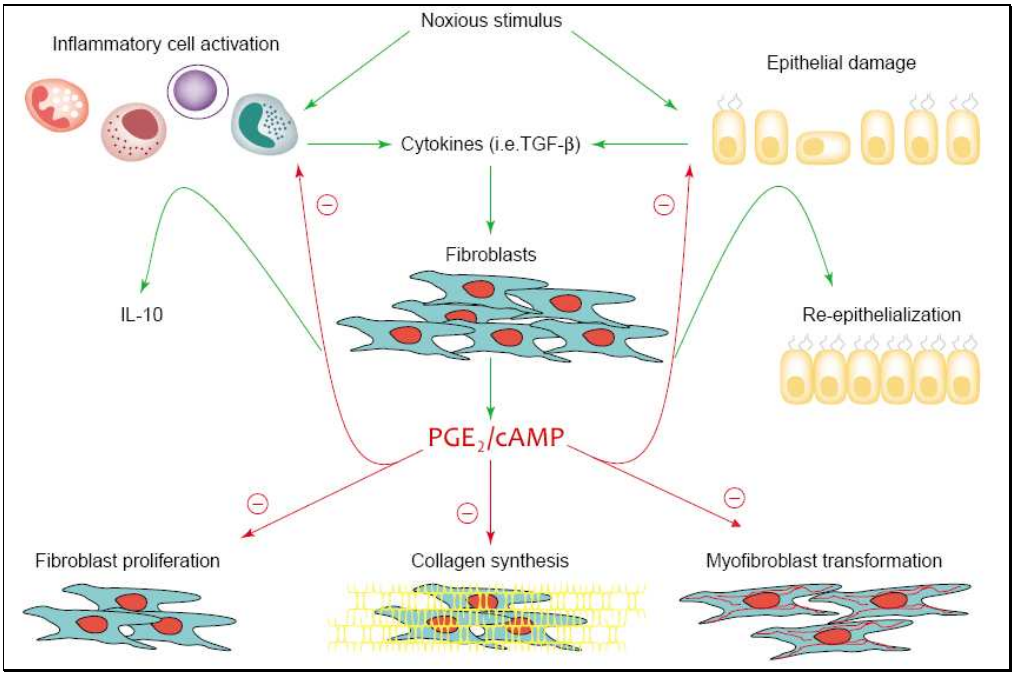

Figure 6. The role of PGE_2 in inflammation and tissue repair (modified from Vancheri et al., 2004). A noxious stimulus causes damage and the activation of airway and/or alveolar epithelial, as well as inflammatory cells. This stimulates the production of several cytokines that affect a wide range of fibroblast functions including the release of great amounts of PGE_2 that increases cAMP. These, in turn, exert a negative feedback on cytokine production and, in an autocrine manner, down-regulate fibroblast metabolic functions including proliferation, collagen synthesis and transition to myofibroblasts. PGE_2 strongly stimulates the production of the anti-inflammatory interleukin-10 (IL-10), and also promotes epithelial growth. Green and red arrows indicate stimulatory and inhibitory actions respectively.

Cytoprotective effects of PGE_2/cAMP have been demonstrated in a study of cigarette smoke extract (CSE)-induced apoptosis in human lung fibroblasts. The anti-apoptotic effect was mediated via EP_2 receptor activation. The PKA inhibitor KT-5720 abolished the PGE_2-mediated protection and confirmed the role of cAMP in this model (Sugiura et al., 2007). By contrast, another study has described an opposite effect of PGE_2 on lung fibroblasts. Under normal cell culture conditions, PGE_2 has increased apoptosis in a concentration-dependent manner. The exact reasons for these inconsistent findings are unknown, but it seems that expressed cytokines have a strong influence on the nature of PGE_2 action (Huang et al., 2009).

Furthermore, several studies demonstrated that PGE_2 inhibits a range of profibrotic responses such as fibronectin-induced chemotaxis, fibroblast-driven collagen-gel contraction (Kohyama et al., 2001), myofibroblast conversion (Dunkern et al., 2007), proliferation (Fine et al., 1987) and formation of extracellular matrix (Liu et al., 2004). In addition, it was demonstrated that the antiproliferative effect in lung fibroblasts is mediated via EP_2 activation. The associated increase of cAMP affected not the PKA pathway since the PKA selective agonist 6-Bnz-cAMP was not effective. Altough the PKA inhibitor Rp-8-Br-cAMP inhibited EP_2-induced phosphorylation of CREB, the anti-proliferative effect was not affected. Finally, the siRNA-mediated knockdown of Epac1 showed a clear attenuation of the inhibitory potency of EP_2 receptor activation and therewith confirmed its involvement (Haag et al., 2008). However, since cAMP is the mediator of PGE_2-induced action, also PDE4 inhibitors were tested for efficacy in some studies and showed similar effects. Roflumilast and rolipram for example, inhibited fibroblast-mediated contraction of three-dimensional collagen gels and fibroblast chemotaxis towards fibronectin (Togo et al., 2009; Kohyama et al., 2004). Furthermore, PDE4 inhibitors have shown to inhibit the release of matrix metalloproteinases and therewith to inhibit tumor necrosis factor-α (TNF-α)-induced degradation of collagen gels (Martin-Chouly et al., 2004; Kohyama et al., 2002b). Another example is a study using the PDE4 specific inhibitor piclamilast, which demonstrated to enhance PGE_2-mediated inhibition of TGF-β induced myofibroblast conversion. All of these studies with PDE4 inhibitors have in common that they need a minimum of basal cAMP generation by the cells to accomplish measurable effects (Togo et al., 2009). Interestingly, lung fibroblasts derived from fibrotic lung tissue exhibit different functional features compared to those from healthy donors. Fibrotic fibroblasts produce less PGE_2 and consequently show a reduced ability to downregulate the production of TNF-α by lipopolysaccharide (Jin et al., 2002)- activated monocytes. One of the reasons is that fibrotic fibroblasts express less COX-2, due to reduction of TNF-α receptors (Vancheri et al., 2000). Under such fibrotic conditions the treatment with PDE4 inhibitors may have the potential to support PGE_2-mediated functions and to reconstitute homeostasis within the interplay of cells involved in PGE_2-signaling.

1.5 Aims of the study

The second messenger cAMP has been recognized as critical regulator of lung fibroblast functions that might be relevant in pulmonary diseases related to fibrosis. By hydrolyzing cAMP, isoforms of the PDE4 family are capable to regulate intracellular levels of cAMP and thus modulate signaling evoked by numerous mediators such as growth factors or inflammatory cytokines. The PDE4 family comprises four distinct genes/subtypes, which encode for multiple splice variants that are widely expressed and set up a complex regulatory repertoire. The different functions of single PDE4 subtypes in human lung fibroblasts are unclear. Due to the lack of PDE4 subtype-specific inhibitors, the functions of PDE4 subtypes cannot be investigated pharmacologically. Thus, a mRNA knockdown method would be a feasible tool to study the functional role of PDE4 subtypes in human primary lung fibroblasts.

The intention of the present study was to demonstrate that distinct PDE4 subtypes participate in distinct fibroblast-relevant functions such as proliferation and myofibroblast differentiation. For this purpose, the following approaches were performed:

(1) Analysis of cytokine induced proliferation in NHLF and to determine the efficacy of PDE4 inhibitors in this context.
(2) Validation of a PDE4 subtype-specific siRNA-mediated knockdown technique and to examine the impact of PDE4 subtype on cell functions such as proliferation and TGF-β induced myofibroblast conversion in NHLF.

A better understanding of the function of individual PDE4 subtypes may help to explain the biological role of the plethora of PDE4 family members. Furthermore, detailed information about functionally relevant PDE4 subtypes may help to define the rationale for the development of PDE4 inhibitors that have an improved therapeutic profile.

2. Material and Methods

2.1 Materials

The selective PDE3 inhibitor motapizone (Borbe et al., 1986) was a generous gift from Sanofi-Aventis (formerly Rhône-Poulenc Rorer, Cologne, Germany). The PDE2 inhibitor 9-(6-phenyl-2-oxohex-3-yl)-2-(3,4-dimethoxybenzyl)purin-6-one; example 100 from US patent 5861396 (Bayer AG)). The selective PDE4 inhibitor piclamilast RP73401 (Benzamide, 3-cyclopentyloxy-4-methoxy-N-3,5-dichloro-4-pyridyl (Raeburn, 1994 189 /id), Roflumilast N-oxide (Hatzelmann et al., 2001) and the PDE5 inhibitor sildenafil were synthesized at the chemical facilities of Nycomed GmbH (Konstanz, Germany). Dilutions were prepared from a 10 µM stock in 100% DMSO. A final DMSO concentration of 0.1% was identical in all incubations and did not interfere with the addressed fibroblast functions. Neither PDE4 inhibitors nor the solvent affected viability of the lung fibroblasts. Human recombinant TGF-β1 and human recombinant IL-1β were purchased from R&D Systems GmbH (Minneapolis, USA). Human recombinant basic FGF (Bosse et al., 2008) was obtained from Sigma Aldrich (Saint Louis, Missouri, USA). All the rest of materials are mentioned in the subsequent passages.

2.1.1 Cell culture

Normal human lung fibroblasts (NHFL, Cambrex Bio Science, Wakersville, MD, USA) were cultured in Fibroblast Basal Medium plus FGM SingleQuots® (both Lonza, Wakersville, MD, USA) in tissue culture flasks at 37℃ in an atmosphere containing 5% CO_2 up to the eighth passage. Cell count and mortality of NHLF was determined by either trypan blue (0.4%, Sigma Aldrich, Saint Louis, Missouri, USA) staining and using a hemacytometer or usage of the Vi-Cell™ (Beckman Counter, Krefeld, Germany).

2.1.2 Data analysis and software

Data are presented as means ± SD. For statistical analysis, one-way ANOVA (GraphPad Prism 5.0; GraphPad Prism Software Inc, San Diego, CA, USA) was used. The grubbs test (95% confidence) was used to identify and remove outliers in the sample datasets. Densitometric analysis of blots was performed with the Advanced

Image Data Analyzer (AIDA 3.22; Raytest). The primer and probe sets for quantitative PCR analysis were designed using Primer Express 2.0 (Applied Biosystems).

2.2 Methods

2.2.1 Treatment of human lung fibroblasts with TGF-β

5 x 10^4 NHLF cells were plated into 6-well cell culture plates and incubated for 24h at 37℃. Thereafter, cells were washed with PBS, original medium was replaced with medium containing no fetal calf serum and cells were cultured for further 24h until treatment with TGF-β1 (R&D Systems, Inc., Minneapolis, USA). In the case of PDE4 inhibitor treatment, the inhibitors were applied 30min before TGF-β1 treatment. 48h after TGF-β1 treatment cells were lysed (view 2.8 *Cell lysis*) and stored at –80℃.

2.2.2 RNA samples

RNA samples from primary human lung fibroblasts were prepared according to the instructions of the manufacturer using the High Pure RNA isolation kit (Roche Applied Science, Mannheim Germany). RNA concentrations were quantified with the Nanodrop ND-1000 spectrophotometer (PEQLAB Biotechnologie GmbH, Erlangen, Germany) and samples stored at -80℃ thereafter.

2.2.3 cDNA synthesis

One microgram RNA was reverse-transcribed using random hexanucleotide primers (Roche Applied Science), dNTPs (PCR 3 Mix, Larova, Teltow, Germany) and avian myeloblastosis virus (AMV) reverse transcriptase (Roche Diagnostics GmbH, Penzberg, Germany) at 42℃ for 1h. cDNAs were diluted in 1 mM Tris, 0.1 mM EDTA pH 8.0 to a final concentration of 2 ng/ml and stored at -20℃ until further use.

2.2.4 Quantitative real time PCR

All primers and 6-carboxyfluorescein (FAM)- or VIC-labeled probes were obtained from Applied Biosystems (Darmstadt, Germany). TaqMan® gene expression assay HS00153133_m1 was used for specific detection of prostaglandin-endoperoxide synthase 2 and used the intron-exon boundary 5-7. For normalization we used primers and VIC-labeled probes for detection of 18S ribosomal RNA. The following endogenous

18S rRNA control primers and probe were used: sense 5'-CGGCTACCACATCCAAGGAA-3', antisense 5'-GCTGGAATTACCGCGGCT-3', probe 5'-VIC-TGCTGGCACCAGACTTGCCCTC-TAMRA-3'.

For analyzing the gene expression of PDE4, designed primer and probe sets as follows were used: PDE4A (NM_006202) sense, 5'-GTGGCTCCGGATGAGTTCTC-3', antisense, 5'-GGGCTGCTGTGGCTTACAG-3', probe 5'-FAM-CCGGGAGGAATTCGTGGT-minor groove binder-3' (MGB); PDE4B (NM_002600) sense, 5'-AGCAGCACAAAGACGCTTTGT-3', antisense, 5'-TCAGTCTCTCCCAGGGAATCTC-3', probe 5'-FAM-TGATTGATCCAGAAAAC-MGB-3'; PDE4C (NM_000923) sense, 5'-ACTCTGGAGGAGGCAGAGGAA-3', antisense, 5'-AGGCAACTCCAAGGCCTCTT-3', probe 5'-FAM-AAGAGACAGCTTTAGCC-MGB-3'; PDE4D (NM_006203) sense, 5'-GGCAGGGTCAAACTGAGAAATT-3', antisense 5'-TGACTGCCACTGTCCTTTTCC-3', probe 5'-FAM-TAGAGGAAGATGGTGAGTCAG-MGB-3'. The PDE4 subtype primer/probe sets have been designed to bind at the 3' end of the open reading frame of each subtype, at positions where individual splice variants of one subtype are identical.

For analyzing the gene expression of cyclin D1, cyclin E1, CDK6 and CDK2, the following TaqMan® gene expression assays from Applied Biosystems (Darmstadt, Germany) were used: Hs00277039_m1, Hs00233356_m1, Hs01026372_m1 and Hs00608082_m1.

TaqMan PCRs were run on ABI 7900 HT Sequence Detection Systems (Applied Biosystems). Each PCR reaction was performed in a total volume of 25 µl in 96-well plates, containing 2.5 µl cDNA (5 ng), 12.5 µl qPCR Mastermix Plus (Eurogentec, Seraing, Belgium), 1.25 µl of the primer/probe set, and nuclease-free water. 18S rRNA primers and probe were used at a concentration of 50 nM each. All PCRs were performed in triplicate for each sample. Relative expression units (REUs) were calculated from $\Delta Ct = Ct_{FAM} - Ct_{VIC}$ according to the equation REU = $2^{(-\Delta Ct)} \times 10^7$. This REU unit describes the expression of a target RNA relative to the 18S rRNA internal standard of the respective sample (Herrmann et al., 2007).

By using plasmid DNA with PDE4 subtype-specific sequence inserts (PDE4 subtypes A4, A10, B1, B2, C1 and D4 and D5) the specificity of the used PDE4 subtype specific primer / probe sets was verified and similar amplification efficacy was shown.

2.2.5 Measurements of phosphodiesterase isoenzyme activities and preparation of cellular extracts

Cells (1-3 × 10^6) were washed twice in phosphate buffered saline (PBS) and resuspended in 1 ml homogenization buffer (137 mM NaCl, 2.7 mM KCl, 8.1 mM Na_2HPO_4, 1.5 mM KH_2PO_4, 10 mM HEPES, 1 mM EGTA, 1 mM $MgCl_2$, 1 mM β-mercaptoethanol, 5 mM pepstatin A, 10 mM leupeptin, 50 mM phenylmethyl-sulfonyl fluoride, 10 mM soybean trypsin inhibitor, 2 mM benzamidine, pH 8.2). Thereafter, cells were disrupted by sonification and PDE activity was assessed as described by Thompson and Appleman (Thompson et al., 1979) with some modifications (Bauer et al., 1980). The assay mixture (final volume 200 µl) contained: Tris–HCl 30 mM; pH 7.4, $MgCl_2$ 5 mM, 0.5 µM of either cyclic AMP or cyclic GMP as substrate including [^{3}H]cAMP or [^{3}H]cGMP, 0.1 mM EGTA, PDE isoenzyme-specific activators and inhibitors as described and cellular lysates. Reactions were performed for 30min at 37℃ in 96-well plates and terminated by adding 50 µl 0.2 M HCl per well. Assays were left on ice for 10min and then 25 µg 5′-nucleotidase (Crotalus atrox) was added. Following incubation for 10min at 37℃ assay mixtures were loaded onto Q AE-Sephadex A25 columns and subsequently eluted with 30 mM ammonium formiate (pH 6.0). Thereafter radioactivity in the eluate was measured. Results were corrected for blank values (measured in the presence of denatured protein) that were below 2% of total radioactivity. Cyclic AMP degradation did not exceed 25% of the amount of substrate added. The final DMSO concentration was 0.3% (v/v) in all assays. Selective inhibitors and activators of PDE isoenzymes were used to determine activities of PDE families as described previously (Rabe et al., 1993) with modifications. Briefly, PDE4 was calculated as the difference of PDE activities at 0.5 µM cyclic AMP in the presence and absence of 1 µM piclamilast. The difference between piclamilast-inhibited cyclic AMP hydrolysis in the presence and absence of 10 µM motapizone was defined as PDE3. The fraction of cyclic GMP (0.5 µM) hydrolysis in the presence of 10 µM motapizone that was inhibited by 100 nM sildenafil reflected PDE5. At the concentrations used in the assay piclamilast (1 µM), motapizone (10 µM) and sildenafil (100 nM) completely blocked PDE4, PDE3 and PDE5 activities without interfering with activities from other PDE families.

PDE1 was defined as the increment of cyclic AMP hydrolysis (in the presence of 1 µM piclamilast and 10 µM motapizone) or cyclic GMP hydrolysis induced by 1 mM Ca^{2+} and 100 nM calmodulin. The increase of cyclic AMP (0.5 µM) degrading activity (in the presence of 1 mM piclamilast and 10 mM motapizone) induced by 5 µM cyclic GMP represented PDE2. The PDE2 inhibitor (100 nM) completely inhibited this cyclic GMP-induced activity increment further verifying that this activity is PDE2.

2.2.6 Measurements of PDE4 activities and preparation of cellular extracts

Cells (1-3 × 10^6) were washed twice in phosphate buffered saline (PBS) and resuspended in 1 ml homogenization buffer (137 mM NaCl, 2.7 mM KCl, 8.1 mM Na_2HPO_4, 1.5 mM KH_2PO_4, 10 mM HEPES, 1 mM EGTA, 1 mM $MgCl_2$, 1 mM β-mercaptoethanol, 5 mM pepstatin A, 10 mM leupeptin, 50 mM phenylmethyl-sulfonyl fluoride, 10 mM soybean trypsin inhibitor, 2 mM benzamidine, pH 8.2). Thereafter, cells were disrupted by sonification and PDE activity was assessed as described by Thompson and Appleman (Thompson et al., 1979) with some modifications (Bauer et al., 1980). The assay mixture (final volume 200 µl) contained: Tris–HCl 30 mM; pH 7.4, $MgCl_2$ 5 mM, 0.5 µM of cyclic AMP as substrate including [^{3}H]cAMP, 0.1 mM EGTA. Reactions were performed for 30min at 37℃ in 96-we ll plates and terminated by adding 50 µl 0.2 M HCl per well. Assays were left on ice for 10min and then 25 µg 5′-nucleotidase (Crotalus atrox) was added. Following incubation for 10min at 37℃ assay mixtures were loaded onto QAE-Sephadex A25 columns and subsequently eluted with 30 mM ammonium formiate (pH 6.0). Thereafter radioactivity in the eluate was measured. Results were corrected for blank values (measured in the presence of denatured protein) that were below 2% of total radioactivity. Cyclic AMP degradation did not exceed 25% of the amount of substrate added. The final DMSO concentration was 0.3% (v/v) in all assays. Piclamilast (RP730401) was used to determine the activity of PDE4 in NHLF after knockdown of PDE4 subtypes A, B and D. The difference of PDE4 activities was calculated in the presence and absence of 1 µM piclamilast. At this concentration PDE4 is completely blocked without interfering with activities from other PDE families.

2.2.7 Cell lysis

For protein expression analysis, cells were lysed using the following buffer; Mixture: 50mM Hepes, pH 7.5, 150 mM NaCl, 1.5 mM $MgCl_2$, 10% glycine, 1% Triton X-100, 0.5% Desoxycholat, 0.2% SDS, 1mM EGTA (ethylene glycol tetraacetic acid), 100 mM NaF, 10 mM $Na_4P_2O_7$. Before usage, 1 mM Na-Vanadat, 1mM PMSF (phenylmethyl-sulfonylfluorid) and 50U/ml Benzonase (Merck KGaA, Darmstadt, Germany) was added to the buffer. Phosphatase Inhibitor Cocktail tablet (Complete Mini from Roche Molecular Biochemicals) in 10 ml buffer was added to minimize protein degradation.

Lysis procedure: cells were washed twice in PBS, trypsinated and centrifuged at 500 *x* g for 10 min. Afterwards the cell pellet was resuspended in 150 µl lysis buffer and stored at -80℃ for further use. Protein concentration was de termined by proceeding the manual of the BCA Protein Assay (Pierce Biotechnology, Rockford, Illinois, USA). Photometric measurements were performed with the microplate reader Sunrise from Tecan Group Ltd. (Männedorf, Switzerland).

2.2.8 Western Blot

Proteins (6 µg for detection of α-SMA , ~80 µg for the detection of PDE4 subtypes and COX-2) of the samples were separated on a 10% SDS polyacrylamide gel. Thereafter, proteins were blotted onto a nitrocellulose transfer membrane (Protran nitrocellulose transfer membrane, Schleicher & Schuell Bioscience GmbH, Dassel, Germany) for 2–3h. Membranes were blocked for 2h in 5% (w/v) milk powder in PBS containing 0.1% Tween 20 (PBT), incubated for 4h with the primary rabbit monoclonal antibody detecting either PDE 4 subtype A or B, which were generously provided by Prof. Conti (Stanford University School of Medicine, Stanford, USA). The antibodies were diluted of 1:1000 in 5% (w/v) milk powder in PBT. For detection of α-smooth muscle actin, we used mouse monoclonal anti-αSMA (Sigma Aldrich, Saint louis, Missouri, USA) in dilution of 1:2000 (5% (w/v) milk powder in PBT). For detection of COX-2, we used mouse monoclonal anti-COX-2 (Cayman Chemicals, Ann Arbor, USA) in a dilution of 1:1000 (5% (w/v) milk powder in PBT). After incubation with primary antibodies blots were washed three times in PBT, and incubated for 2 h with a horseradish peroxidase-coupled secondary antibody (diluted 1:10000 in 5% (w/v) milk powder in PBT, Jackson ImmunoResearch, Inc., USA). After final washing with PBT (3 times for 10min each) blots were developed by using a chemiluminescence detection system (Lumi Light Plus, Roche GmbH, Mannheim, Germany) and a luminescent image analyzer. To control homogenous protein loading, blots were additionally hybridized with a primary mouse monoclonal anti-GAPDH antibody (diluted 1:2000 in 5% (w/v) milk powder in PBT, Calbiochem®, Darmstadt, Germany).

The AIDA image analyzer software was used to perform the densitometric analyses of the blots. Each signal was normalized to the overall signal of the corresponding blot. Results are expressed as arbitrary units related and normalized to the signal of GAPDH.

2.2.9 cAMP and PGE_2 ELISA measurements

$5x10^5$ human lung fibroblasts were seeded in 6-well plates and starved the day after for 24h. Thereafter, the cells were treated with bFGF (Sigma-Aldrich, Missouri, USA) and IL-1ß (R&D Systems, Inc., Minneapolis, USA) as indicated for additional 24h at 37℃.

For detection of PGE_2, 1 ml medium was removed and stored at -80℃ until measurement with a PGE_2 ELISA (Assay Designs, Ann Harbor, USA) according to the manufacturers instructions.

Alternatively, for cAMP measurements treated adding HCl to a final concentration of 0.3 M lysed cells and were stored at -20℃. For measure ment, thawed samples were diluted 1:2 (v/v) in 0.1 M HCl. cAMP was quantified by competitive ELISA as instructed by the manufacturer (Assay Designs, Ann Harbor, USA).

2.2.10 (^{3}H)thymidine incorporation and flow cytometric cell cycle analysis

2 x 10^4 NHLF cells were plated into 24-well or 10^5 cells into 6-well cell culture plates precoated with 30 µg/ml collagen (INAMED Biomaterials, Fremont, CA), 10 µg/ml fibronectin (from human plasma, Sigma-Aldrich, Missouri USA), 10 µg/ml bovine serum albumin (Sigma-Aldrich, St Louis, USA) and incubated for 24h by 37℃. Thereafter, cells were starved for 24h in serum-free Fibroblast Basal Medium. Following the preincubation with piclamilast (1 µM), motapizone (1 µM) and IL-1β (10-100 pg/ml) (R&D Systems, Wiesbaden, Germany) fibroblasts were stimulated with 10 ng/ml bFGF. For flow cytometric cell cycle analysis, the cells were trypsinated, washed twice in PBS, resuspended in 500 µl PBS, treated with RNase (10 µg/ml, RNase A, VWR International GmbH, Darmstadt, Germany) and propidium iodide (50 µg/ml, Sigma Aldrich, St. Louis, USA) was added. Thereafter, samples were analyzed on a FACSCalibur (BD Bioscience, Heidelberg, Germany).

For DNA synthesis measurement (methyl-^{3}H)thymidine (1 µCi/well) was added to the cells for the last 6 hours of the incubation period. Thereafter, culture supernatants were removed, adherent cells were washed twice in PBS and exposed to ice-cold 10% (w/v) trichloroacetic acid (TCA) for 30min. Thereafter, TCA was removed and the fixed cells dissolved in 0.2 N NaOH for 16h. DNA-incorporated radioactivity in the lysates was counted and expressed as cpm per well (LS6500, Beckman Counter, Krefeld, Germany).

2.2.11 RNA interference of PDE4 subtypes with siRNA

Synthetic siRNA oligonucleotides (Stealth RNAi) specific for regions of the mRNAs of PDE4 subtype A, B and D were designed and synthesized by Invitrogen (Paisley, UK) or in case of “On-Target plus Duplex siRNAs” by Dharmacon (Lafayette, CO, USA). The silencing effects of several siRNA oligonucleotides were screened and tested initially for their ability to silence the different subtypes of PDE4 expression. The most active of these oligonucleotides for PDE4A (On-Target plus Duplex J-007647_14: target sequence: 5’ to 3’: CAG GAG UCG UUG GAA GUU A), subtype PDE4B (Stealth RNAi: HSS107718: 5’ to 3’: UUA GAA GCC AUC UCA CUG ACA GAC C) and subtype PDE4D (On-Target plus Duplex J-004757_17: target sequence: 5’ to 3’: GAG UUC UUC UUC UUG AUA A) blocked the expression in a range of about 70% - 90% (determined after qPCR, related to the corresponding control). NHLF were transfected with siRNA oligonucleotides by either Electroporation/Nucleofection (NF) (Amaxa Nucleofector™, Koeln, Germany) or Lipofection (Lipofectamine™ RNAiMAX, Invitrogen, Karlsruhe, Germany).

NF of NHLF was carried out using the nucleofector kit for primary mammalian fibroblasts (Amaxa, Koeln, Germany) according to the instructions of the manufacturer. Different siRNA concentrations were tested (0.03 µM – 2 µM).

To test the transfection efficiency, different concentrations of FITC-labeled non-targeting siRNA (siGLO Green, Dharmacon, Lafayette, CO, USA) and different NF-programs were tested and the cells were analyzed by fluorescence microscopy. The NF-program U-23 performed the best results. Immediately after electroporation, the samples were removed from the cuvette with 1 ml prewarmed medium and transferred to 6-well plates (Corning Costar, Corning, USA) containing 1 ml of prewarmed medium. For electroporation controls, only 1x siRNA buffer, but no siRNA was added to the cell suspension prior transfection. For untreated controls, cells were resuspended in nucleofection solution, but no electroporation was carried out.

Lipofection of NHLF was carried out using Lipofectamine™ RNAiMAX according to the instructions of the manufacturer for reverse transfection. Different siRNA concentrations were tested (0.015 nM - 150 nM). For lipofection controls, cells were treated with RNAiMAX without siRNA. As siRNA negative control Silencer® Select Negative Control

#1 siRNA (Ambion / Applied Biosystems, Darmstadt, Germany) was used in a concentration of 5 nM. In order to confirm the achieved mRNA knockdown and siRNA specificity, gene expression assays (RT-PCR), as described in the parts “RNA samples”, “cDNA-synthesis” and “Quantitative real time PCR” were performed. Alternative, the TaqMan® Gene Expression Cells-to-C_T™ Kit (Ambion, Austin, USA) to validate the mRNA knockdown in parallel to the functional investigations was used.

3. Results

3.1 Cytokine-dependent effects in primary human lung fibroblasts related to cyclic AMP signaling and phosphodiesterase 4 inhibition

3.1.1 Biphasic effects of IL-1β on proliferation – Interaction with bFGF and the role of cAMP

In a first series of experiments the combined effects of IL-1β and bFGF on primary human lung fibroblast proliferation was investigated. For this purpose, cells were starved overnight in serum free medium, stimulated subsequently for 24h with IL-1β and bFGF at varying concentrations, and assessed for proliferation as measured by (^{3}H)thymidine incorporation (Fig. 7A and B).

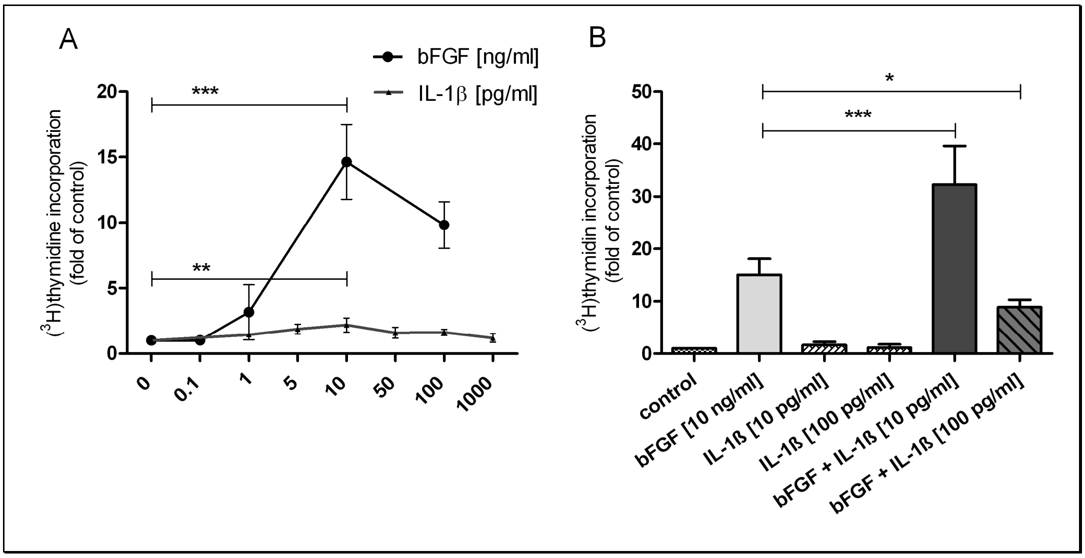

Figure 7. Effects of IL-1β and bFGF on proliferation of NHLF. A: NHLF were starved for 24h and subsequently treated for 24h with IL-1β or bFGF at different concentrations. Data are expressed as fold of control of (^{3}H)thymidine incorporation (mean ± SD; n = 3), ** p ≤ 0.01, ***p ≤ 0.001. **B:** Proliferation of 24h starved NHLF induced by subsequent combined treatment with bFGF or / and IL-1β for 24h. A synergistic mitogenic effect at a concentration of bFGF at 10 ng/ml and IL-1β at 10 pg/ml is observed, whereas a significant decrease of proliferation is measured when using a co-treatment with IL-1β at 100 pg/ml. Data are expressed as fold of control of (3H)thymidine incorporation (mean ± SD; n = 5-8), * p ≤ 0.05, *** p ≤ 0.001.

As expected, bFGF strongly induced proliferation of lung fibroblast in a concentration-dependent manner and at 10 ng/ml induced maximum proliferation of 14.6 ± 2.8 -fold of control (figure 7A; n = 3, mean ± SD). In contrast, treatment with IL-1β up to concentrations of 10 pg/ml only slightly increased proliferation (maximum: 2.2 -fold), whereas higher concentrations appeared even to decrease DNA synthesis. This observation suggests that at higher concentrations of the cytokine mechanisms opposing the mitogenic effects of IL-1ß may evolve.

Co-incubation of NHLF with IL-1β (10 pg/ml) and bFGF (10 ng/ml) overadditively augmented proliferation of NHLF (figure. 7B). Under these conditions, (^{3}H)thymidine incorporation was approximately doubled compared to bFGF alone. In contrast, at the higher IL-1β concentration of 100 pg/ml the cytokine reduced bFGF-induced (^{3}H)thymidine incorporation by approximately 41% . This inhibitory effect of higher concentrations of IL-1β on bFGF-induced lung fibroblast proliferation corroborates findings observed with IL-1β treatment alone.

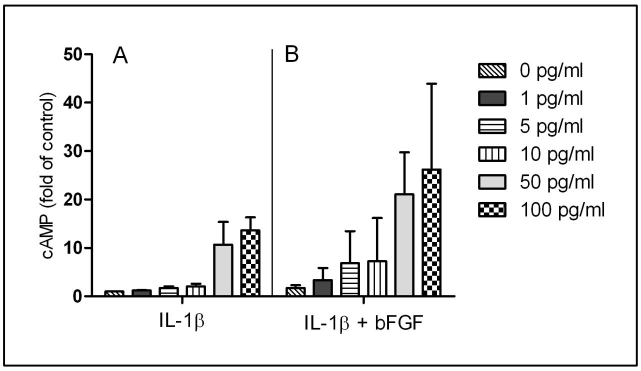

Figure 8. Influence of treatment with IL-1β and bFGF on cellular cAMP. NHLF were starved for 24h and subsequently treated for 24h with (**A**) IL-1β alone or combined with (**B**) bFGF [10ng/ml]. Data are expressed as fold of control (mean ± SD; n = 3).

The second messenger cAMP has repeatedly been described to mediate antiproliferative effects in lung fibroblasts (Haag et al., 2008). Whereas bFGF treatment (24h with 10 ng/ml) alone did not influence intracellular cAMP concentrations in lung fibroblasts, IL-1β treatment at concentrations of up to 10 pg/ml resulted in a modest yet concentration-dependent increase in cAMP (figure 8A). At IL-1β concentrations higher than 10 pg/ml a substantial increase in cAMP of up to tenfold (for 50 pg/ml IL-1β) compared to untreated controls was measured. In the additional presence of bFGF (10 ng/ml), while the concentration-dependent increase of cAMP by IL-1β followed a comparable pattern, absolute cAMP levels in the lung fibroblasts were approximately doubled (figure 8B). The higher IL-1β concentration shown to augment cAMP was also found to reduce bFGF-induced fibroblasts proliferation.

3.1.2 bFGF increases the IL-1β induced COX-2 expression in NHLF

The mechanism behind the observed pattern of cAMP following IL-1β in presence or absence of bFGF was explored. As expected, incubation of NHLF for 24h with IL-1β concentration-dependently increased COX-2 expression (figure 9A, B and C). Thus, IL-1β at the concentration of 10, 50 or 100 pg/ml induced COX-2 protein expression to 0.2 ± 0.1 %, 11.5 ± 5.2 % and 14.1 ± 4.4 % of total arbitrary units (related to GAPDH, serving as the house-keeping protein) (figure 9A and B, n = 3, mean ± SD). COX-2 expression was already detectable 1h after adding IL-1β to the cells (data not shown). Surprisingly, co-treatment with 10 ng/ml bFGF, which by itself had no effect, significantly potentiated COX-2 expression by approximately threefold compared to IL-1β alone. Supportive evidence for this finding is obtained from COX-2 mRNA expression analyses (figure 9C). By analogy to COX-2 protein expression, bFGF potentiated accumulation of COX-2 transcripts following IL-1ß irrespective of the selected cytokine concentration. Addition of bFGF at 10 ng/ml to IL-1β at 10 pg/ml, 50 pg/ml and 100 pg/ml increased the expression of COX-2 mRNA by approximately 3.0 -fold, 5.7 -fold and 2.4 -fold compared to the corresponding IL-1β concentration alone. bFGF alone did not increase accumulation of COX-2 transcripts. The potentiating effect of bFGF on IL-1β–induced COX-2 protein is predominantly due to enhanced transcription, although any post-translational regulation cannot be ruled out.

3.1.3 bFGF potentiates IL-1β induced formation of PGE_2 in NHLF

In order to analyze whether the changes in COX-2 expression translate into corresponding changes of PGE_2 release, this prostanoid was measured in conditioned medium following incubation of NHLF over 24h with IL-1β in the presence or absence of bFGF. IL-1β at concentrations of 10, 50 or 100 pg/ml increased accumulation of PGE_2 in the conditioned medium of NHLF to 0.2 ± 0.1 ng/ml, 5.7 ± 0.8 ng/ml and 6.6 ± 0.5 ng/ml; (figure 9D; n = 3, means ± SD).

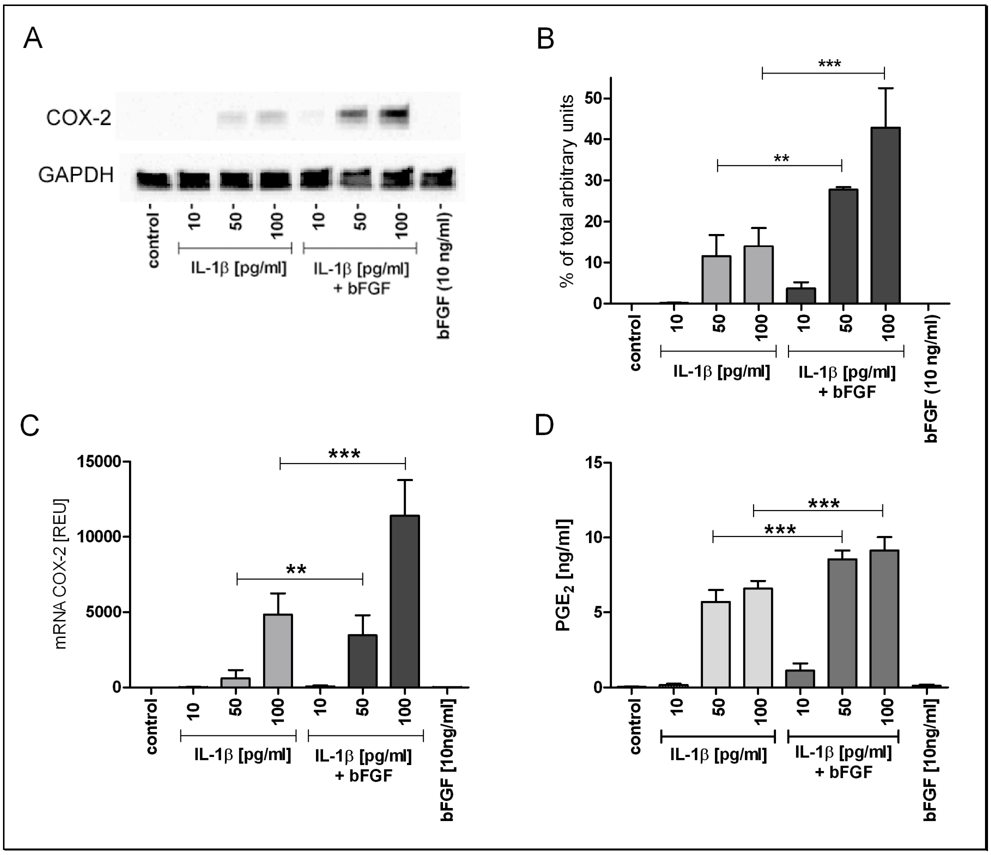

Figure 9. Influence of treatment with IL-1β and bFGF on COX-2 expression and subsequent PGE_2 generation in NHLF.A: COX-2 protein expression of starved (24h) NHLF after treatment (24h) with bFGF (10 ng/ml) and / or IL-1β at different concentrations. The Western blot shown is a representative out of three independent experiments. **B:** Densitometric quantification of Western blots shows that bFGF significantly potentiated the IL-1β–induced COX-2 expression. Data are expressed as percent of total arbitrary units (mean ± SD; n = 3), **p ≤ 0.01, ***p ≤ 0.001. **C:** COX-2 gene expression of NHLF (same experimental setting as A). BFGF significantly potentiated IL-1β–induced COX-2 gene expression. Data are expressed as relative expression units (mean ± SD; n = 3), **p ≤ 0.01, ***p ≤ 0.001. **D**: Prostaglandin E_2 synthesis from NHLF (same experimental setting as A). BFGF significantly potentiated IL-1β -induced PGE_2 expression. Data show PGE_2 concentrations (mean ± SD; n = 3), ***p ≤ 0.001.

Control cells did not produce any detectable basal PGE_2. The distinct rise in accumulated PGE_2, when elevating IL-1β from 10 to 50 pg/ml, is in agreement with the COX-2 expression and cAMP levels. The additional presence of bFGF further increased IL-1β-induced PGE_2 accumulation to 1.1 ± 0.5 ng/ml of PGE_2 at 10pg/ml; 8.6 ± 0.6 ng/ml at 50 pg/ml and 9.2 ± 0.9 ng/ml at 100pg/ml IL-1ß. These findings are in line with the results obtained for cAMP levels and COX-2 expression. bFGF treatment alone did not result in detectable PGE_2 accumulation.

3.1.4 The PDE4 inhibitors elevate cAMP levels and inhibit the bFGF- and IL-1β-induced cell proliferation in NHLF

In order to identify the cyclic nucleotide hydrolyzing phosphodiesterase isoenzymes in NHLF, PDE activities by using isoenzyme-specific inhibitors and activators was measured by the lab of Dr. Hermann Tenor. As shown in figure 10A cGMP hydrolysis substantially exceeds cAMP hydrolysis. The main cGMP-hydrolyzing PDE activities in these cells are PDE5 and PDE1, while cAMP hydrolysis is attributed to PDE1, PDE4 and to a minor extent to PDE3.

PDE4 subtype gene expression in NHLF were analysed by RT-PCR. Under basal, unstimulated conditions PDE4A revealed as the major PDE4 subtype expressed followed by PDE4B. mRNA transcripts of the PDE4 subtypes C and D were very low and close to the limit of detection (figure 10B).

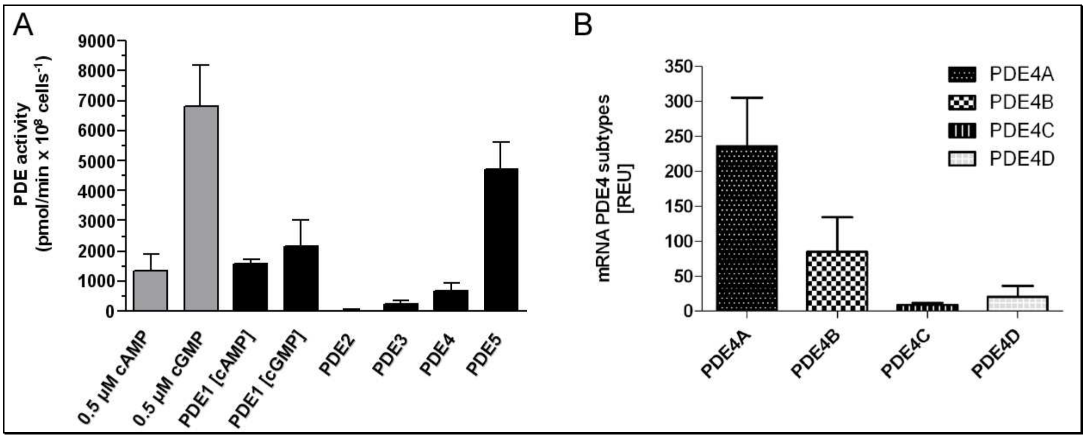

Figure 10. Activity of PDE isoenzymes and PDE4 subtype gene expression in NHLF. A: (kindly provided by Dr. H. Tenor) PDE isoenzyme activities. NHLF were analyzed for total cAMP, cGMP, PDE1 (Marienfeld et al., 2001), PDE2, PDE3, PDE4 and PDE5 activities. Data are given as pmol/min x 10^8 cells^{-1} (mean ± SD; n = 3). **B:** PDE4 subtype gene expression of unstimulated NHLF. Data are expressed as relative mRNA expression units (mean ± SD; n = 9).

The assumption that the inhibition of bFGF-induced proliferation at high IL-1β concentrations is attributed to increased cAMP levels and because PDE4 is expressed in NHLF led to the analysis of the effects of the selective PDE4 inhibitors piclamilast and roflumilast N-oxide on proliferation under various conditions (figure 11).

Piclamilast reduced the bFGF and IL-1β induced (^{3}H)thymidine incorporation in a concentration-dependent manner (figure 11A). When IL-1β was absent or present only at a low concentration (10 pg/ml), piclamilast afforded more than 20% inhibition of bFGF-induced (^{3}H)thymidine incorporation in NHLF. When IL-1β was present at a high concentration of 50 pg/ml, which substantially increased COX-2, PGE_2 and cAMP, piclamilast resulted in a maximum of approximately 60% inhibition of bFGF-induced DNA synthesis. The inhibitory effect of the PDE4 inhibitor piclamilast on (^{3}H)thymidine incorporation was reversible as proven by means of wash-out experiments (as shown in 3.1.5). Similar results were obtained from the lab of Dr. Hermann Tenor, using the PDE4 inhibitor roflumilast N-oxide (figure 11B), which also inhibited (^{3}H)thymidine incorporation in NHLF in a IL-1β dependent manner to a maximum of approx. 60%. Interestingly, the inhibitory effect was fully abolished by simultaneous treatment with the COX-1/2 inhibitor indometacin (figure 11C). This supports the hypothesis that the IL-1β induced PGE_2 formation and subsequent cAMP generation provides the basis for the anti-proliferative efficacy of PDE4 inhibition.

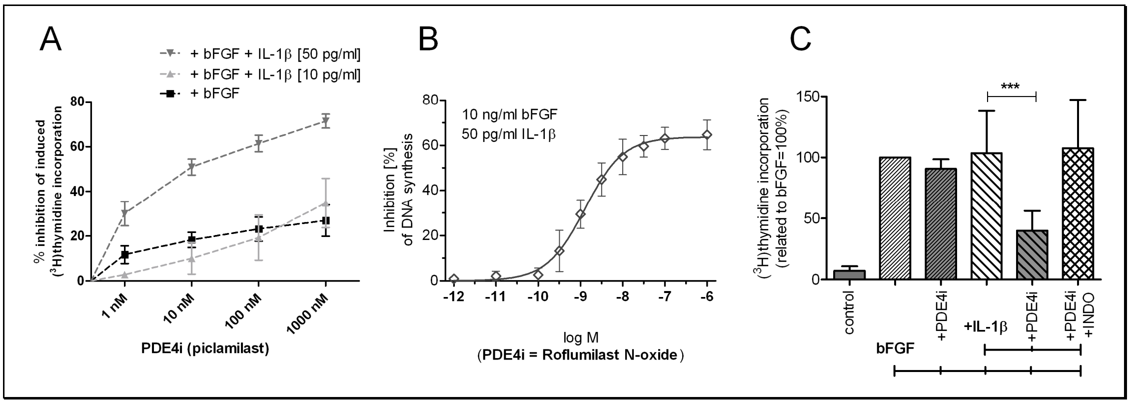

Figure 11. PDE4 inhibitors inhibit the IL-1β- and bFGF- induced proliferation in a IL-1β/COX-2 dependent manner. A: Concentration-response-relationship of the PDE4 inhibitor piclamilast. NHLF were starved for 24h, subsequently treated with piclamilast at 1µM and stimulated over 24h with bFGF alone or in combination with IL-1β. Data are expressed as percent inhibition of induced (^{3}H)thymidine incorporation (mean ± SD; n = 3). **B:** (kindly provided by Dr. H. Tenor) Concentration-response-relationship of the PDE4 inhibitor roflumilast N-oxide. NHLF were starved for 48h, subsequently treated with the PDE4i (1µM), and then stimulated over 24h with bFGF and IL-1β. Data are expressed as percent inhibition of induced (^{3}H)thymidine incorporation (mean ± SD; n = 7), * $p \leq 0.05$. **C:** (kindly provided by Dr. H. Tenor) NHLF were starved for 48h and subsequently stimulated with bFGF (10ng/ml). Starved NHLF were pre-treated with either the PDE4 inhibitor roflumilast N-oxide (1µM) and/or indomethacin (INDO, 10µM) and subsequently stimulated with bFGF (10ng/ml) and IL-1β (50 pg/ml). The COX-inhibitor INDO reversed the proliferation reducing effect of the PDE4 inhibitor under conditions of IL-1β co-treatment. Data are expressed as percent related to bFGF treated cells (mean ± SD; n = 9), *** $p \leq 0.001$.

In addition to PDE4 also a minor PDE3 activity was detected in NHLF, and therefore potential effects of a selective PDE3 inhibitor motapizone were explored. Both in the presence and absence of IL-1β the PDE3 inhibitor alone did not affect bFGF-induced DNA synthesis in NHLF. On the other hand, in the presence of IL-1β (but not in its absence) motapizone further accentuated the reduction of bFGF-induced (^{3}H)thymidine incorporation by the PDE4 inhibitor piclamilast (figure 12).

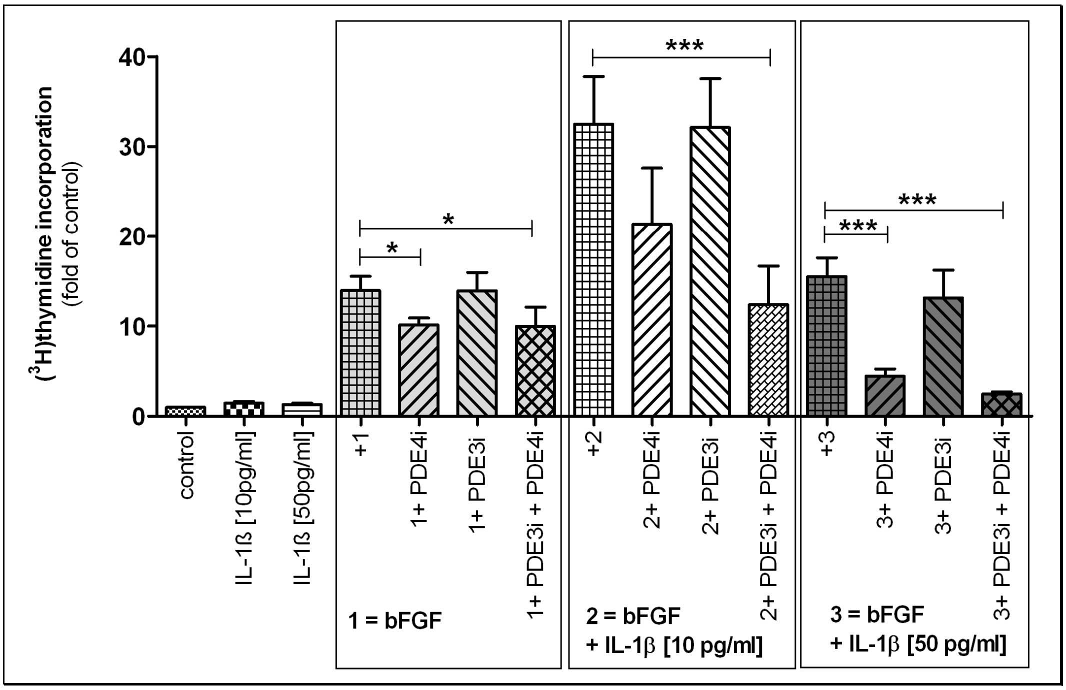

Figure 12. The PDE4 but not PDE3 inhibitor reduces proliferation of NHLF induced by bFGF plus/minus IL-1β. NHLF were starved for 24h and subsequently stimulated with bFGF (10ng/ml) alone (1) or together with IL-1β at 10 pg/ml (2) or 50 pg/ml (3). Under these conditions the PDE4i piclamilast (1µM) reduced proliferation significantly. Treatment with the PDE3 inhibitor motapizone (1µM) alone showed no reducing effect but may have some additional effects on top of the PDE4 inhibitor. Data are expressed as fold of control of (^{3}H)thymidine incorporation (mean ± SD; n = 3), * $p \leq 0.05$, *** $p \leq 0.001$.

3.1.5 High levels of cAMP block NHLF in the G1 phase of their cell cycle

In order to extend the findings obtained by measurements of (^{3}H)thymidine incorporation, flow cytometric cell cycle analysis of NHFL under various conditions were performed. As illustrated in figure 13, starving of NHLF for 24h arrested most of the cells in G1 phase (91.2 ± 1.8%, n = 6, means ± SD).

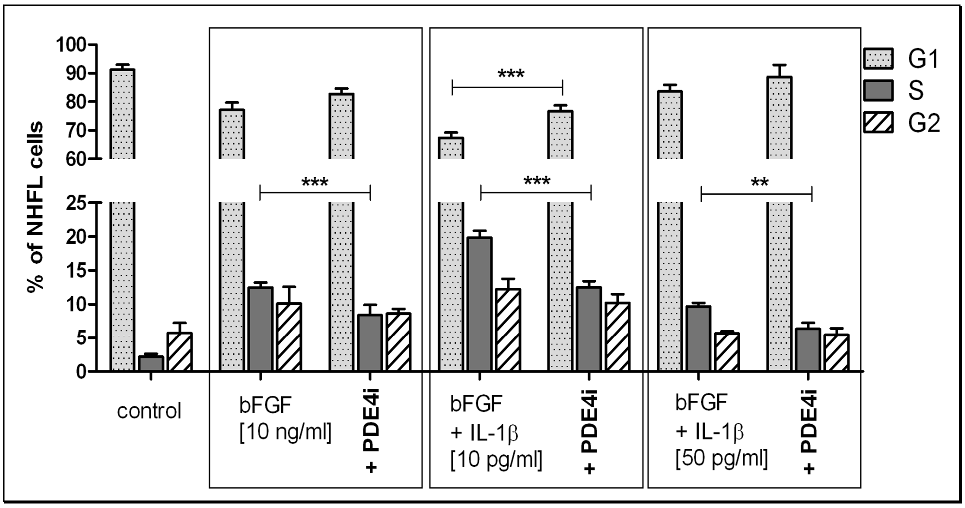

Figure 13. PDE4 inhibition provokes G1-block in NHLF. Flow cytometric cell cycle analyses from 24h starved NHLF (control) after induction of proliferation with either bFGF (10 ng/ml) alone or in combination with IL-1β at 10 pg/ml or 50 pg/ml are shown. PDE4 inhibition (piclamilast, 1µM) provokes a G1-block, which is most pronounced at a concentration of IL-1β at 50 pg/ml. Data are expressed as percent of total cells number (mean ± SD; n = 3-6), ** p ≤ 0.01, *** p ≤ 0.001.

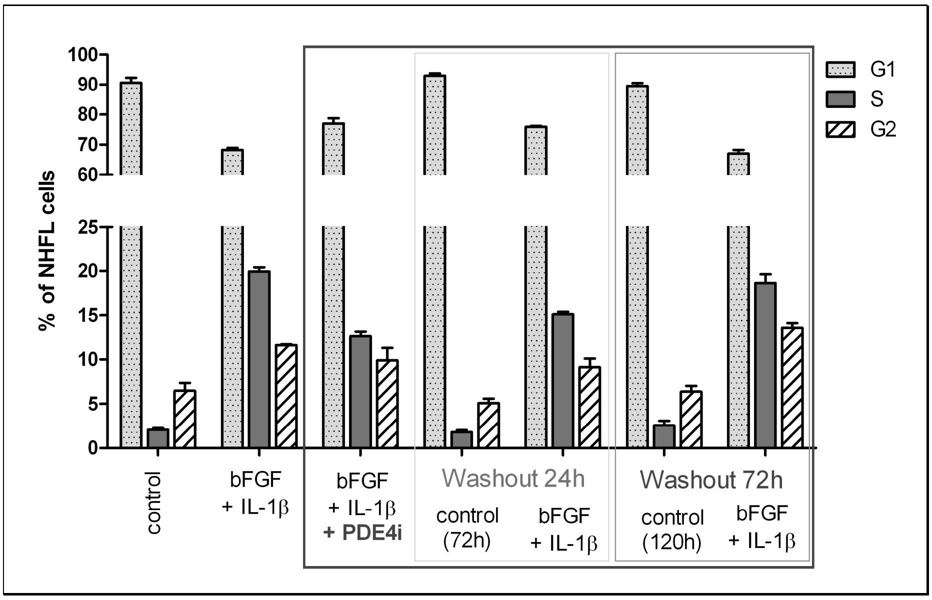

Figure 14. The effect of the PDE4 inhibitor piclamilast is reversible. Proliferation was induced with bFGF (10ng/ml) and IL-1β (10pg/ml). After inhibiton with the PDE4 inhibitor piclamilast, medium was replaced and NHLF were cultered either 24h or further 72h in normal growth medium until these cells were again starved (24h) and stimulated (24h). Data are expressed as percent of total cells number (mean ± SD; n = 3-5)

As expected from the measurements of DNA synthesis, co-incubation of starved cells with bFGF at 10 ng/ml and IL-1β at 10 pg/ml induced proliferation most efficiently resulting in an increase of the proportion of S-phase cells to 19.9 ± 1.0%, compared to bFGF alone with 12.5 ± 0.8% and 2.2 ± 0.5% for controls. Inhibition of PDE4 reduced the bFGF- induced increase of the proportion of NHLF in the S-phase by arresting cells in G1. This effect of the PDE4 inhibitor was observed following incubation with bFGF on its own and was found accentuated with increasing concentrations of IL-1β. Figure 14 depicts that the inhibitory effect of the PDE4 inhibitor piclamilast on (^{3}H)thymidine incorporation was reversible, apparent after 72h as proven by means of wash-out experiments.

Gene expression analyses showed significant down-regulation of the G1/S phase transition controlling Cyclins D1 and E1 as well as the cyclin-dependent kinases 6 and 2 under conditions of PDE4 inhibition (figure 15A-D), which is in line with investigations of other groups (Lee et al., 2003; Musa et al., 1999; L'Allemain et al., 1997). Taken together, results of the flow cytometric cell cycle analysis corroborate findings from measurements of [^{3}H]thymidine incorporation.

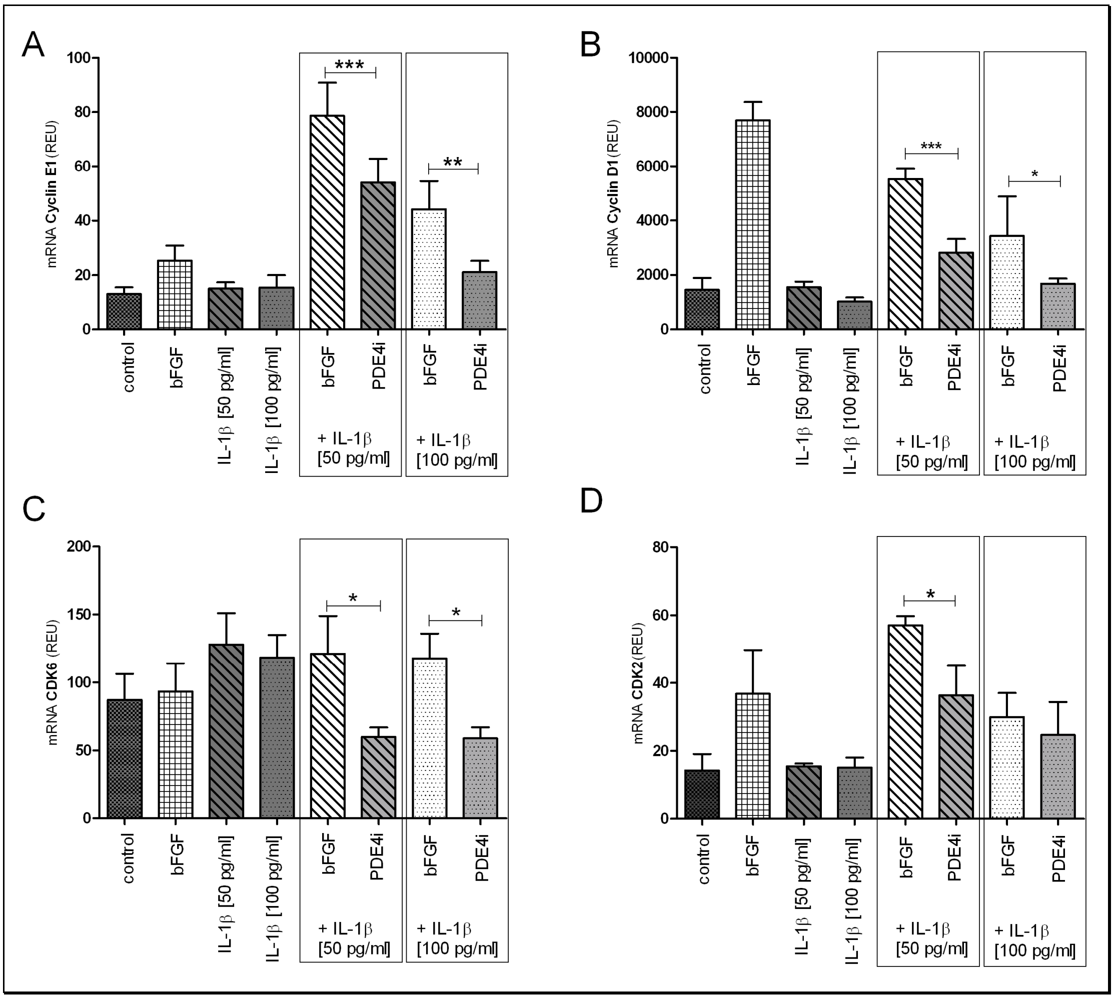

Figure 15. Gene expression of G1/S-transition regulating cyclins and cyclin-dependent kinases is downregulated by means of PDE4 inhibition in NHLF. RT-PCR gene expression analyses from 24h starved NHLF (control) after induction of proliferation with either bFGF (10 ng/ml) alone or in combination with IL-1β at 50 pg/ml or 100 pg/ml. Additionally, treatment with the PDE4 inhibitor piclamilast (1µM) reduced gene expression of cyclin E1 (**A**), cyclin D1 (**B**), CDK6 (**C**) and CDK2 (**D**) significant. Data are expressed as Relative Expression Units (mean ± SD; n = 3-4), *p ≤ 0.05, **p ≤ 0.01, ***p ≤ 0.001.

3.2 Functional impact of PDE4 subtypes in primary human lung fibroblasts

3.2.1 Gene expression of PDE4 subtypes in NHLF

The hypothesis that individual PDE4 subtypes exert distinct cellular functions in primary human lung fibroblasts was tested. For this purpose, first the expression profile of PDE4 subtypes was elucidated in human primary lung fibroblasts (as already seen in figure 10B). All used primer/probe sets for detection of each of the four PDE4 subtypes were designed and validated in our group (Peter et al., 2007). By using plasmid DNA with PDE4 subtype specific sequence inserts, it was proven that all primer/probe sets result in similar amplification rates in a standardized qPCR. Therefore, it can be assumed that the determined level of PDE4 subtypes expression obtained by the qPCR investigations can be directly compared to each other.

Under basal, unstimulated conditions PDE4A revealed as the major PDE4 subtype expressed followed by PDE4B in NHLF. mRNA transcript expression of the PDE4 subtypes C and D was very low and close to the limit of detection (figure 16).

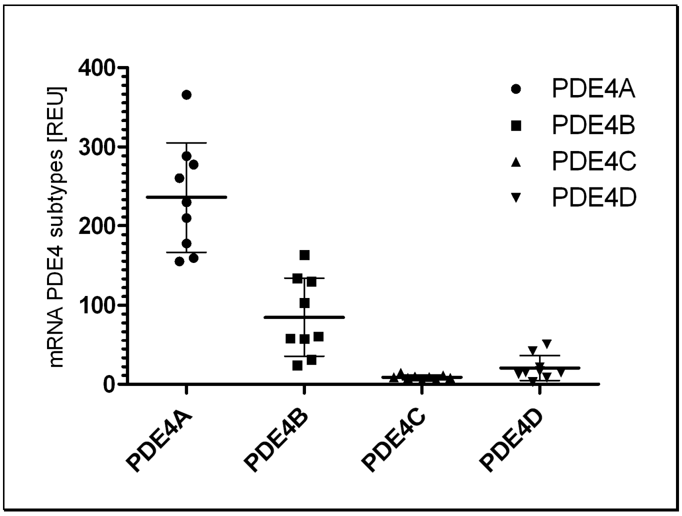

Figure 16. PDE4 subtype gene expression of unstimulated NHLF. Data are expressed as relative mRNA expression units (REU, mean ± SD; n = 9).

Treatments to induce proliferation in NHLF (bFGF and co-treatment with IL-1β; ≤ 10 pg/ml) mediated no changes in mRNA expression of the PDE4 subtypes. In contrast, treatment with IL-1β at a concentration of 50 pg/ml increased gene expression of PDE4B and PDE4D but did not affected PDE4A and PDE4C mRNA (figure 17 A-D).

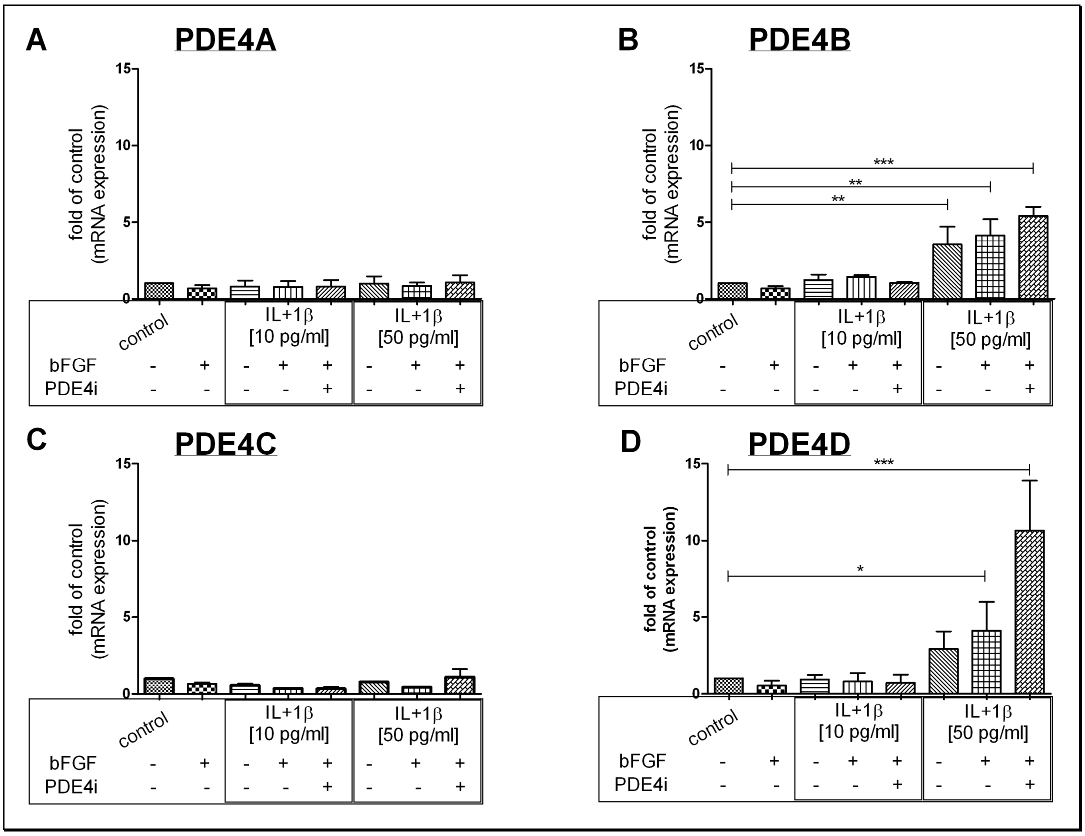

Figure 17. **Gene expression of PDE4A (A), PDE4B (B), PDE4C (C) and PDE4D (D) 24h after stimulation with bFGF (10ng/ml) ± IL-1β in NHLF.** Data are expressed as fold of control calculated on relative mRNA expression units (mean ± SD; n = 3), *p < 0.05, **p < 0.01, ***p < 0.001.

To elucidate the question whether specific subtypes of PDE4 control specific functions of lung fibroblasts, we tested different siRNA approaches to selectively knockdown the different PDE4 subtypes. To transfect primary human lung fibroblasts with siRNAs, we compared the Amaxa Nucleofetion (NF) technique (Gresch et al., 2004) with a liposome mediated transfection (Felgner et al., 1987).

3.2.2 Transfection of NHLF by means of Amaxa Nucleofection (NF)

The most efficient NF-program was identified by transfecting NHLF with FITC-labeled nontargeting siRNA and visual inspection by means of fluorescence microscopy. Thereafter from an arbitrarily assortiment of commercially available siRNAs, specific for each PDE4 subtype, individual siRNAs that were most effective in downregulating the respective mRNA (data not shown) were identified. Different siRNA concentrations were tested to determine the optimal concentration needed for mRNA knockdown (figure 18).

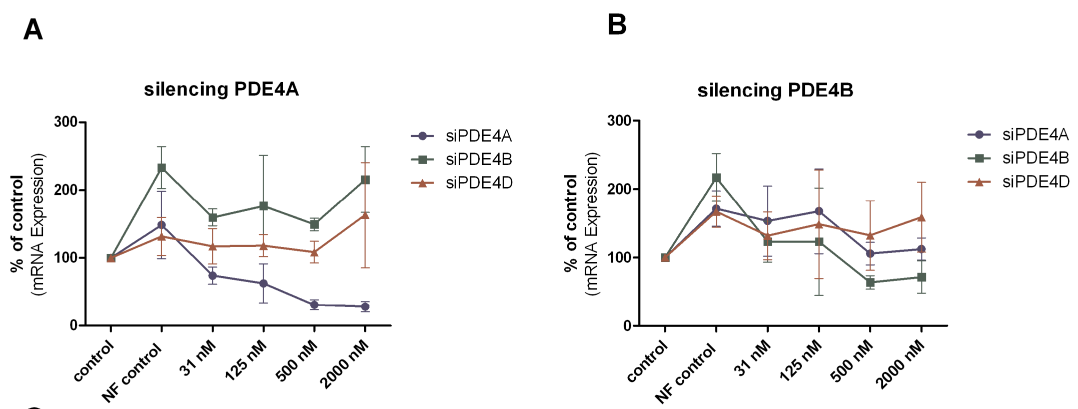

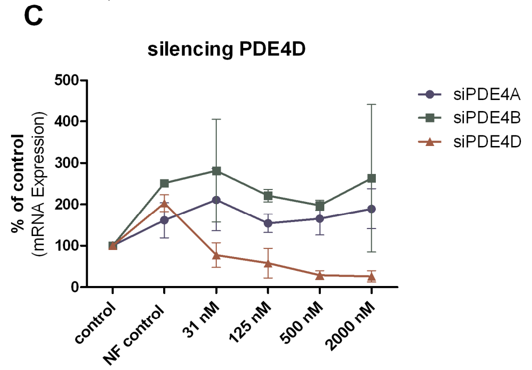

Figure 18. Gene expression of PDE4A, B and D after nucleofection (NF) with different concentrations of PDE4A (A), PDE4B (B) and PDE4D (D) specific siRNAs. Data (mean ± SD; n = 3) are shown as percent of control (absence of siRNA and reagent and non-electroporated). NF control (absence of siRNA and reagent but electroporated).

Maximal mRNA knockdown was achieved in a concentration range from 0.5 µM to 2 µM siRNA for each PDE4 subtype. Each of the selected siRNA induced a strong knockdown of the corresponding mRNA and none of the subtype specific siRNAs down-regulated the highly homologous mRNAs of the other PDE4 subtypes (figure 18). In the case of the subtype PDE4A specific siRNA, a significant downregulation with all of the used siRNA concentrations compared to the NF-control was achieved. According to the 1way Anova, this was significant with $p \leq 0.05$ for the concentrations 31nM and 125nM, and for the concentrations 0.5 µM and 2 µM with $p \leq 0.001$. However the knockdown was less pronounced by comparison to non-treated controls. Thus, compared to non-treated NHLF (control), the knockdown became only significant at the higher siRNA concentrations of 0.5 µM and 2 µM ($n = 3$, $p \leq 0.05$, 1way Anova). This is due to the fact that the nucleofection procedure by itself induced the up-regulation of various PDE4 subtypes and therefore pronounced the effect of siRNA-mediated knockdown.

Next, the question was adressed, whether the transfection of cells with PDE4A specific siRNA influences the gene expression of the subtypes PDE4B and PDE4D (figure 18A). It turned out that nucleofection with different concentrations of PDE4A specific siRNA reduced PDE4A mRNA but did not affect the mRNA expression of PDE4B and D, at least at the investigated time point of 24h after electroporation.
The treatment with siRNAs versus subtype PDE4B also induced a significant concentration-dependent knockdown of the respective mRNA in comparison to electroporated control cells at a concentration of 0.5 µM and 2 µM (figure 18B, $p \leq 0.01$). In this case gene expression of subtypes PDE4A and PDE4D was also unaffected.
Since PDE4C mRNA expression in either unstimulated or stimulated NHLF was at the limit of detection by qPCR (C_T value of approx. 37) and also knockdown experiments with siRNA (data not shown) did not lead to any measurable knockdown, the subtype was therefore considered as not expressed. Accordingly, PDE4C was not considered anymore in further experiments.
The PDE4D-siRNA mediated knockdown of subtype PDE4D was significantly achieved concentration dependently in a range from 31nM to 2µM in comparison to NF-control (figure 18C, $p \leq 0.001$) as well as in a range from 0.5 µM to 2 µM to non-transfected cells ($p \leq 0.01$). The gene expression of subtypes PDE4A and PDE4B was slightly increased after PDE4D-siRNA treatment (PDE4B more then PDE4A) but was not significant affected compared to non-transfected control cells.
Since the nucleofection method bears several disadvantages such as e.g. induction of genes of interest or experimental handling liposome mediated transfection was investigated as an alternative method.

3.2.3 Liposome mediated transfection of NHLF and comparison to NF

PDE4-siRNA transfection with Oligofectamine™ and Lipofectamine™ 2000 (Invitrogen) of primary human lung fibroblasts did not mediate mRNA downregulation of the PDE4 subtypes (data not shown).

However, the usage of Lipofectamine™ *RNAiMAX* as reagent for transfection led to an efficient knockdown of PDE4 subtype mRNAs (about 60% - 90%, as seen in figure 19/20). Different siRNA concentrations for knocking down PDEA, B and D were tested. A mRNA knockdown of all PDE4 subtypes was achieved already at the low siRNA concentration of 0.15 nM, which is much more effective than using nucleofection. Maximal effects of knockdown were reached at siRNA concentration of 1.5 nM for PDE4A and 150 nM for PDE4B and D. The selected siRNAs demonstrated high specificity for all tested PDE4 subtypes, as each one affected only the corresponding target and did not decrease the mRNA expression of the other PDE4 subtypes (figure 19).

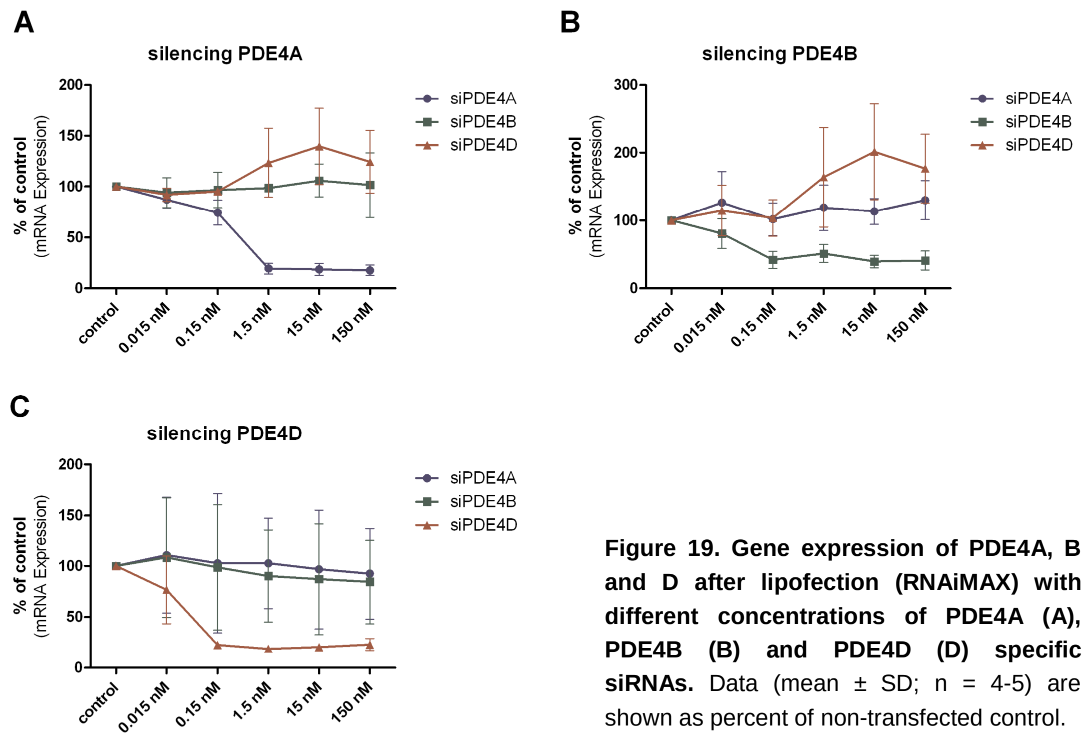

Figure 19. Gene expression of PDE4A, B and D after lipofection (RNAiMAX) with different concentrations of PDE4A (A), PDE4B (B) and PDE4D (D) specific siRNAs. Data (mean ± SD; n = 4-5) are shown as percent of non-transfected control.

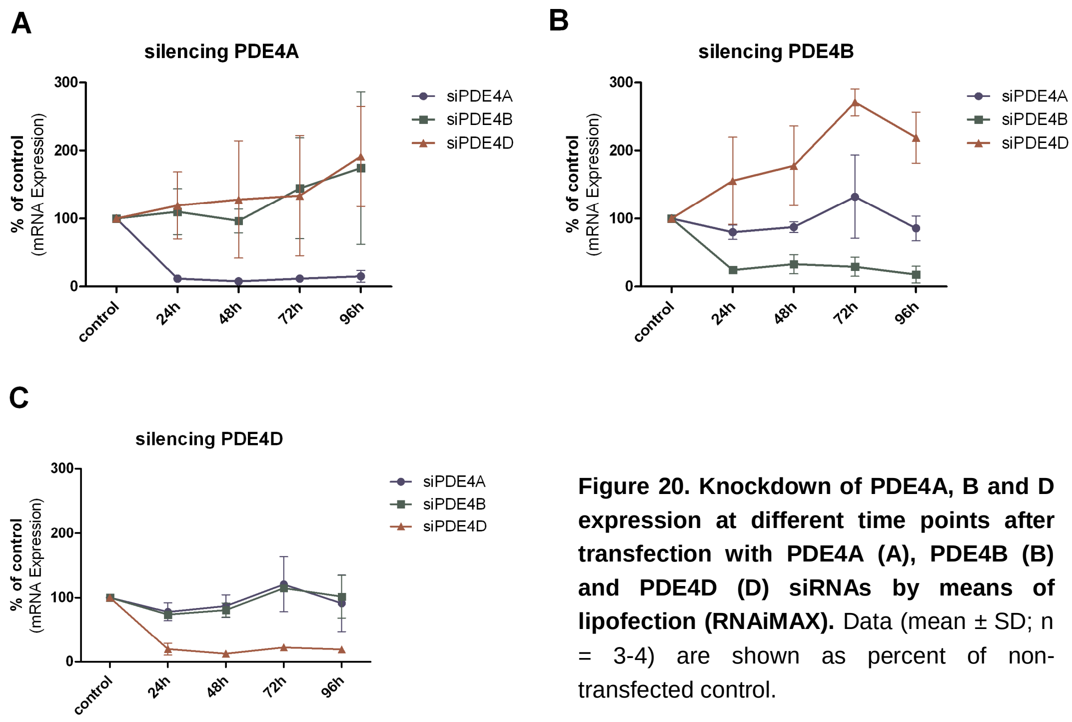

Figure 20. Knockdown of PDE4A, B and D expression at different time points after transfection with PDE4A (A), PDE4B (B) and PDE4D (D) siRNAs by means of lipofection (RNAiMAX). Data (mean ± SD; n = 3-4) are shown as percent of non-transfected control.

Further, the stability of these knockdowns up to 96h was investigated (figure 20). A consistent siRNA concentration of 5nM for all subytpes was chosen for the transfection, in order to ensure a maximal downregulation of mRNAs but also not to be in the plateau phase of efficacy, which might bear a higher risk of potential off-target effects by the siRNAs.

Summarized, all achieved knockdowns reached a significant mRNA knockdown after 24h and were very stable over the investigated time periods. Moreover, the specificity of each mRNA knockdown over time was verified by gene expression analysis of the remaining PDE4 subtypes. However it is notable that the downregulation of the subtype PDE4B induced PDE4D gene expression, which became significant 72h and 96h after transfection ($p \leq 0.01$ and $p \leq 0.05$, respectively).

Lipofection (*RNAiMAX*) without siRNA did not induce the gene expression of the different PDE4 subtypes (figure 21A), whereas the NF method statistically significant did for PDE4A and B (2way Anova; $p \leq 0.01$ and $p \leq 0.001$, respectively).

Since there was also a clear induction of mortality (figure 21B) by NF in comparison to non-treated control cells but not by transfection with Lipofectamine^{TM} *RNAiMAX,* the last method was considered as the best choice for further functional experiments described in the following chapters.

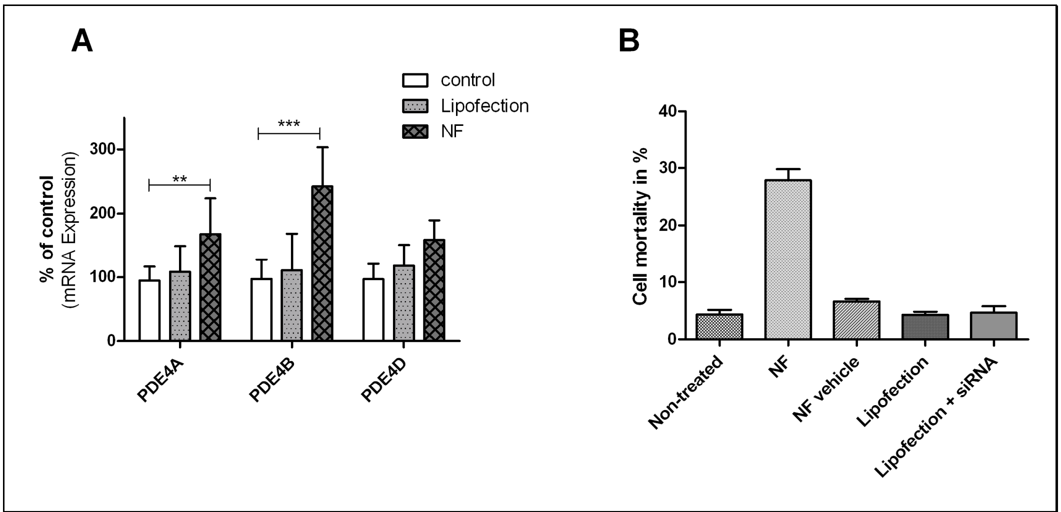

Figure 21. Comparison of Nucleofection (NF) and Lipofection. A: Gene expression of PDE4A, B and D is increased by the NF but not Lipofection procedure (in absence of siRNAs) in NHLF. Data are expressed as percent of non-treated cells (mean ± SD; n = 6); $^{**}p < 0.01$, $^{***}p < 0.001$. **B:** Cell mortality of NHLF was enumerated directly after NF or in the case of Lipofection 24h after treatment. Data are expressed as percent of total enumerated cells. „Non-treated" cells and „Lipofection + siRNA": n = 8 (mean ± SD); „NF", "NF vehicle" and „Lipofection": n = 2 (mean ± range).

3.2.4 Validation of siRNA-mediated PDE4 subtype knockdown by means of protein expression and PDE4 activity analysis in NHLF

The efficacy of the liposome mediated siRNA transfection was further investigated on the PDE4 subtype protein expression level up to 96h after transfection.The knockdown became visible for the subtypes PDE4A and PDE4B as shown in by western blotting and the respective densitometric quantifications (figure 22A, B). The pan-PDE4A specific antibody detected a broad band, which reflected the expression of PDE4A isoform 5 in NHFL. However, the signal intensity of these bands decreased strongly already 24h after siRNA transfection. The pan-PDE4B specific antibody detected two different isoforms of PDE4B in NHFL. A strong signal corresponding to the longform PDE4B1 (107 kDa) and a weaker signal reflecting isoform PDE4B2 (65-67 kDa) was measured. The densitometric quantification of these signals demonstrated the time-dependent down regulation of both PDE4B isoforms starting latest 48h after siRNA transfection. Although we tested different antibodies targeting subtype PDE4D, we were not able to illustrate the knockdown of PDE4D on protein expression in NHLF after siRNA transfection.

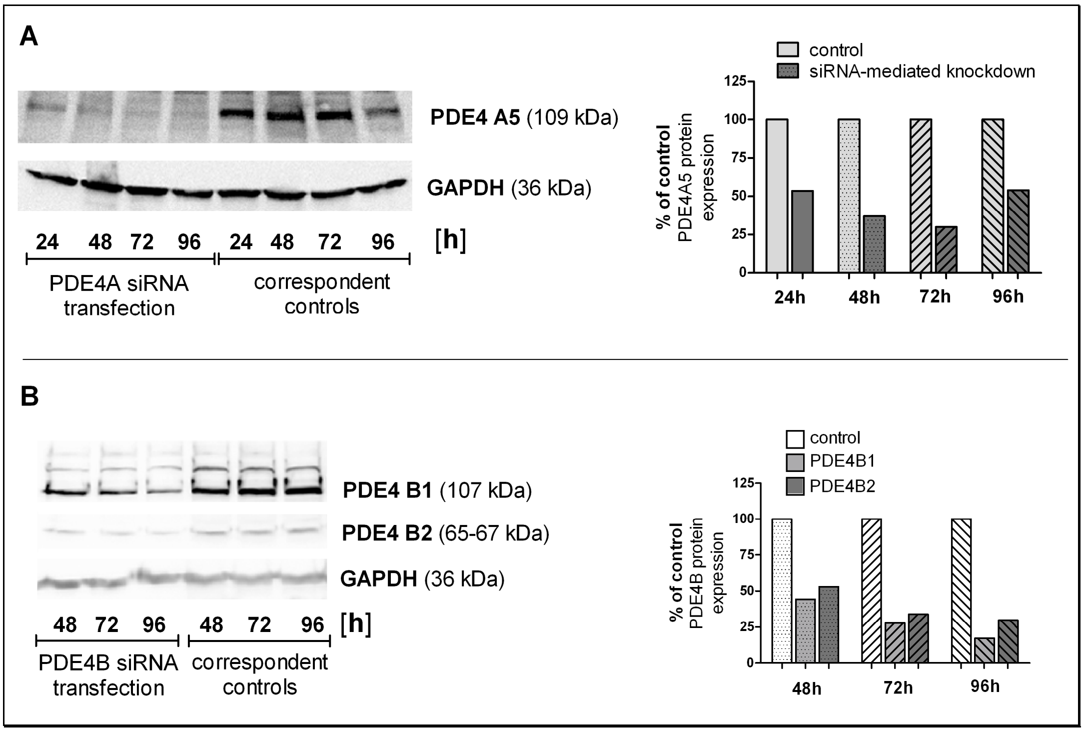

Figure 22. PDE4A5 (A) and PDE4B1/2 (B) protein expression in NHLF and densitometric quantification 24-96 hours after siRNA mediated knockdown (lipofection with RNAiMAX). Quantification data are expressed as percent of the correspondent controls. Two PDE4 longforms, PDE4A5 (109 kDa) and PDE4B1 (107 kDa) as well as the shortform PDE4B2 (65-67 kDa) were identified and downregulated after subtype specific siRNA transfection.

Next it was investigated, whether the PDE4 subtype-specific mRNA knockdown also translates into a reduction of PDE4 related cAMP hydrolysis activity besides protein reduction. Therefore PDE4 enzyme-activity assays were performed using lysates of siRNA transfected NHLF (figure 23). Transfection of NHFL with PDE4A siRNA reduced overall PDE4 activity after 72h (-19.7 ± 1.4 %) and became significant compared to vehicle control after 96h (-24.6 ± 3,0 %, *p ≤ 0.05). Twenty-four hours after knockdown of PDE4B, a marginal reduction of total PDE4 activity (-12.0 ± 4.1 %) was achieved, which increased with time and became significant compared to vehicle control 72h (-51.3 ± 9.1 %, **p ≤ 0.01) and 96h (-53.5 ± 3.8 %, ***p ≤ 0.001) after siRNA lipofection.

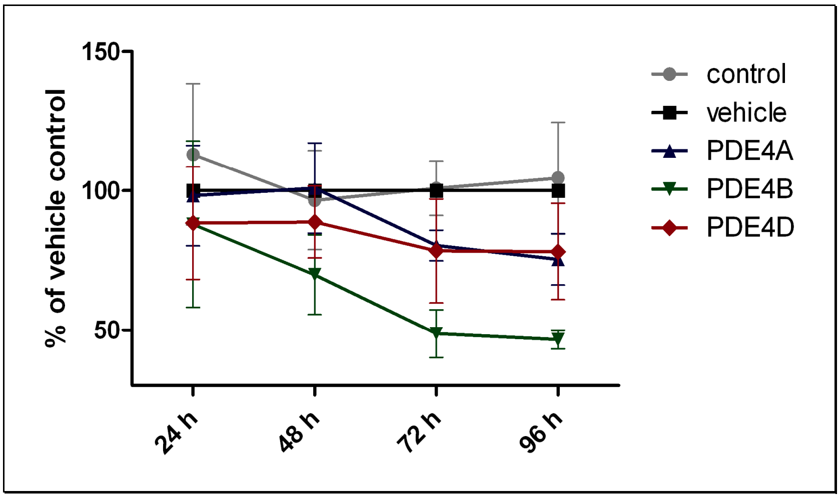

Figure 23. Total PDE4 activity is time-dependent downregulated after siRNA-liposome (RNAiMAX)-mediated knockdown in NHLF. Transfection with different PDE4 subtype-specific siRNA´s induced a downregulation in PDE4 activity, which was most prominent in the case of PDE4B. Data are expressed as percent of non-tranfected control at the individual time points (mean ± SD; n = 5).

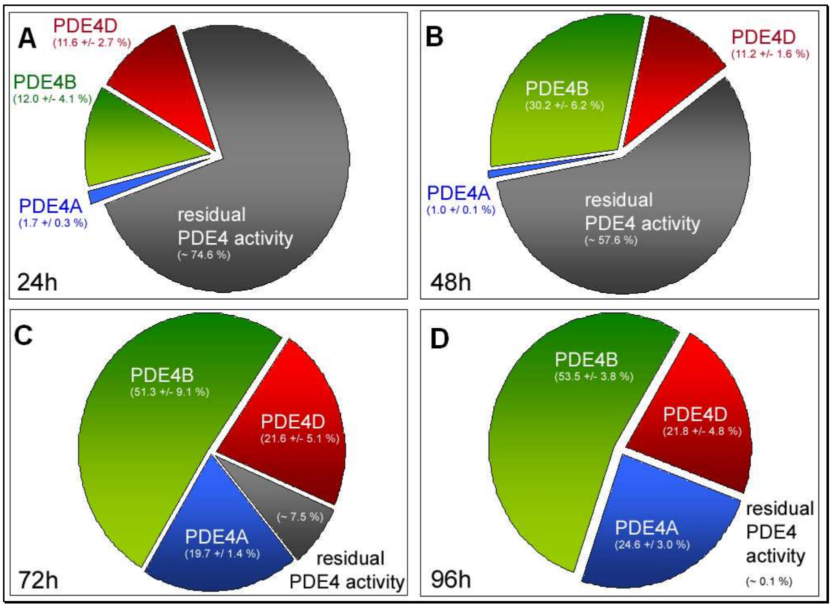

Figure 24. Pie chart of PDE4 activity in NHLF (as seen in figure 23). A-D present the timepoints (24-96h) after siRNA-liposome (RNAiMAX)-mediated knockdown of PDE4A (blue) PDE4B (green) and PDE4D (red). The grey proportion illustrates the residual PDE4 activity. The sum in PDE4 subtype specific activity decrease results in approximately 100% of the total PDE4 activity and thus indicates that the subtype PDE4C is absent under the investigated conditions in NHFL.

For knockdown of subtype PDE4D a reduction of total PDE4 activity got obvious after 72h (-11.6 ± 2,7 %) and increased up to 96h further on (-21.8 ± 4.8 %). Figure 24 visualizes the different proportions of PDE4 subtype activities after the corresponding mRNA knockdown.

In contrast to the activity of PDE4B and PDE4D, it became obvious that the PDE4A activity (blue) did almost not decrease within the first 48h. It needed more than 48h until the knockdown of PDE4A mRNA reduce overall PDE4 activity. Overall, at the timepoint of 96h, the sum of all PDE4 subtype specific reductions of activities reached nearly 100% of total PDE4 activity. This design approach does not consider the variation within these experiments. Nevertheless, it provides further evidence that under the investigated conditions the subtype PDE4C does not play a role in NHLF.

3.2.5 Effect of PDE4 subtype knockdown on cytokine induced proliferation in NHLF

As seen in chapter 3.1.4, specific inibititors of PDE4 reduced cytokine-induced proliferation significantly by elevating levels of cAMP. Moreover, the previous part of this study characterized the cytokine-induced proliferation of NHLF. The growth factor bFGF induced proliferation, which could be maximized by the treatment with IL-1β at a concentration of 10 pg/ml.

To determine which individual PDE4 subtype mediates the proliferation reducing effect of the panPDE4 inhibitor, NHLF were transfected with the PDE4 subtype-specific siRNAs by means of Lipofection as mentioned in chapter 3.2.3. The cells were reverse transfected and rested 24h in normal growth medium. After an additionally starvation period of 24h, the cells were stimulated to proliferate with bFGF (10 ng/ml) alone or in combination with IL-1β (10 pg/ml) for 24h. Thereafter proliferation was measured by means of (^{3}H)thymidine incorporation.

Figure 25A and B shows (^{3}H)thymidine incorporation induced by bFGF plus/minus IL-1β in the presence or absence of PDE4 subtype specific siRNA-mediated knockdown after 72h. (^{3}H)thymidine incorporation is calculated as percent of non-transfected cells. In more detail, each data point (stimulated value) was related and normalized to the corresponding control (starved situation) as fold of control. By these means, the extent of stimulation can be compared of each experiment in relation to non-transfected cells.

The lipofection agent (si_vehicle) itself had a slight inhibitory effect on bFGF stimulated proliferation, which became significant under conditions of bFGF plus IL-1β induced proliferation as shown in figure 25B (n = 12, p ≤ 0.05).

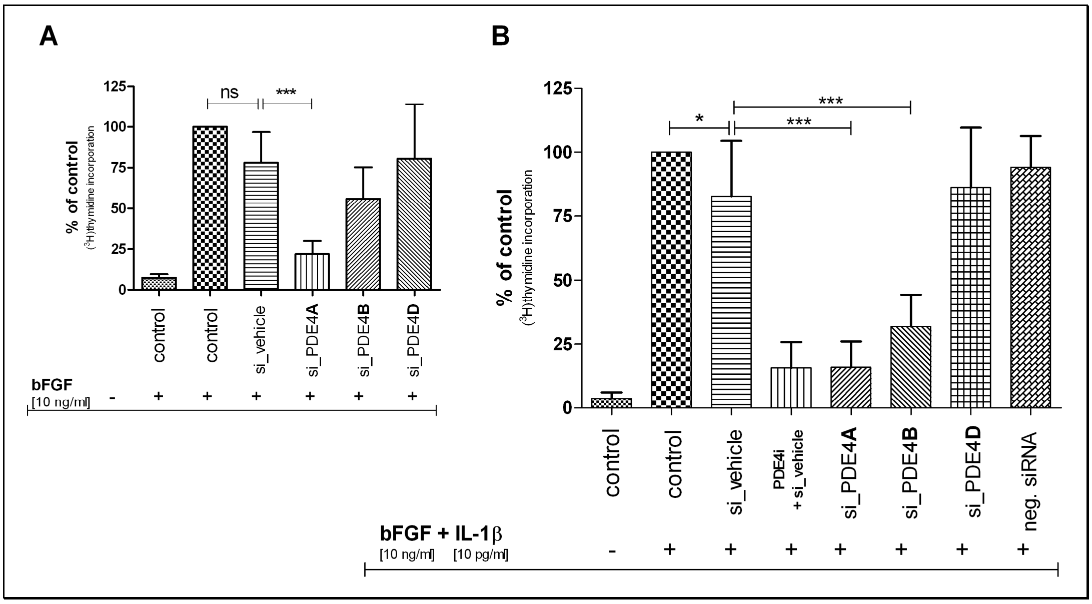

Figure 25. Knockdown of PDE4 subtype A and B reduces cytokine-induced proliferation in NHLF. A: (^{3}H)thymidine incorporation as a marker for proliferation was induced by bFGF (10 ng/ml) and inhibited after siRNA-liposome (RNAiMAX)-mediated knockdown of PDE4A. Knockdown of PDE4B and PDE4D showed no effect compared to the control. Proliferation data are expressed as percent of fold of control (mean ± SD; n = 5-8) **B:** (^{3}H)thymidine incorporation was induced in NHLF (n = 12) by bFGF (10 ng/ml) plus IL-1β (10 pg/ml) and inhibited after siRNA-liposome (RNAiMAX)-mediated knockdown of PDE4A (n = 11) and PDE4B (n = 8). The liposome (RNAiMAX) reagent itself had a significant inhibitory effect on proliferation (n = 9). The knockdown of PDE4A reached the maximum antiproliferative effect obtained by treatment with the panPDE4 inhibitor (n = 3) piclamilast (1µM) in this setup. The knockdown of PDE4D (n = 12), as well as the transfection with a scrambled siRNA as neg. control (n = 4) had no effect on proliferation compared to the vehicle control. Data are expressed as percent of fold of control (mean ± SD), *p < 0.05, ***p < 0.001.

All statistical calculations compared the PDE4 subtype specific siRNA treatments with the vehicle control. Twenty-four hours after stimulation with bFGF, transfection with the siRNA targeting PDE4A resulted in a significant reduction of (^{3}H)thymidine incorporation (Fig. 25A; p ≤ 0.001). This effect is also observed when the cells were stimulated with bFGF plus IL-1β (figure 25B; p ≤ 0.001). Therewith, the PDE4A mRNA knockdown reached the same maximum efficacy as the treatment with the panPDE4 inhibitor piclamilast that was used as positive control in this experiment. Transfection with the siRNA targeting PDE4B did not significantly effect bFGF-induced proliferation. However under conditions of co-treatment with IL-1β, which leads to maximum proliferation, the subtype specific PDE4B siRNA significantly inhibited proliferation and seems therefore to be involved in controling this process in NHLF (figure 25B; $p \leq 0.001$). Transfections with the siRNA targeting PDE4D showed no effects on the extent of cytokine-induced proliferation. Thus PDE4D seems not to be involved in bFGF/IL-1β induced signaling pathways leading to proliferation. Moreover, in this experiment PDE4D siRNA can also be considered as high-homology siRNA negative control in addition to the used scrambled siRNA, which does not target any eucaryotic genes, as shown in figure 25B.

3.2.6 The effect of PDE4 subtype knockdown on TGF-β induced lung fibroblast to myofibroblast conversion

Lung fibroblast to myofibroblast differentiation has been published to be blocked by treatment with PDE4 specific inhibitors (Dunkern et al., 2007). To ascertain which individual PDE4 subtype is involved within this effect, we transfected NHLFs with subtype-specific siRNAs and subsequently after a 48h starvation period, stimulated them with TGF-β (0.5 ng/ml) for another period of 48h. Because myofibroblasts express alpha-smooth muscle actin (α-SMA) and lung fibroblast not, this marker was used to measure the extent of myofibroblast differentiation. α-SMA signals were detected by Western blot analyses and quantified after densitometric quantification. To equalize the different exposure times of the Western blots, each quantified α-SMA signal in figure 26B was indicated as percent of total signal intensity. Furthermore, each signal was related to the corresponding endogenous control GAPDH, in order to normalize the protein content on the blots.

As shown in figure 26A untreated NHFL did not express detectable levels α-SMA. However, 48h after stimulating NHLF with TGF-β, α-SMA was strongly induced. There was no significant reduction of TGF-β induced α-SMA protein expression observed by silencing PDE4A subtype mRNA.

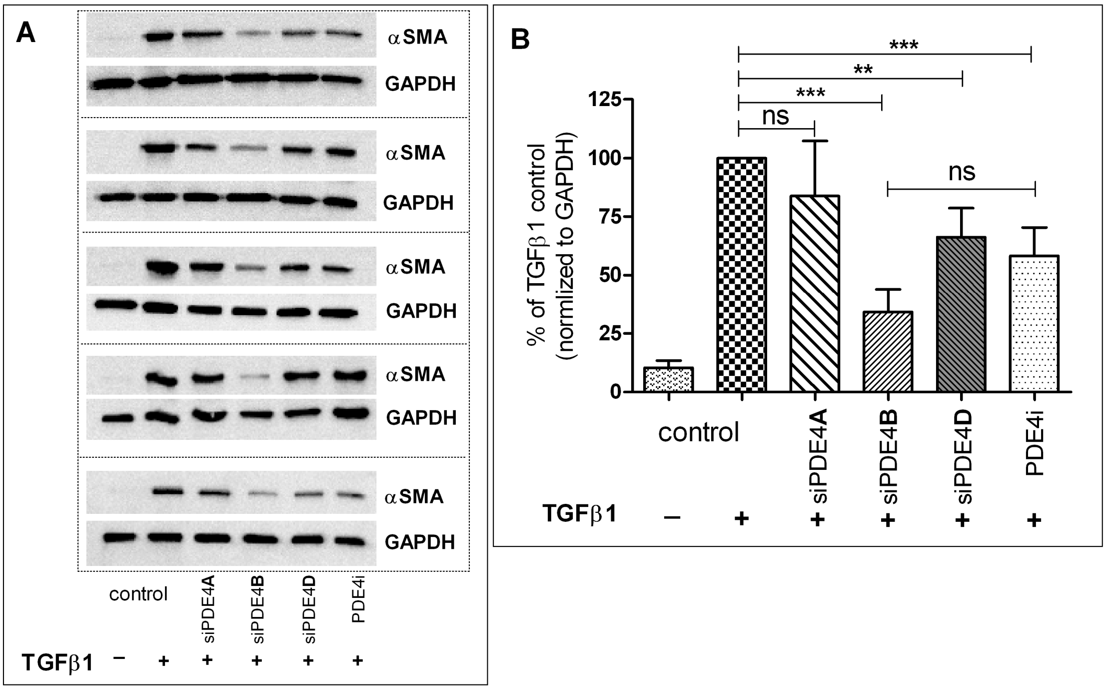

Figure 26. Knockdown of PDE4 subtypes inhibits TGF-β-induced myofibroblast differentiation of NHLF. A: α-SMA protein expression after stimulation with TGF-β1 (0.5 ng/ml) in normal (control) and siRNA-lipofected NHLF to knockdown PDE4A, B and D was detected by Western blot. Additionally, GAPDH protein expression as an endogenous control was measured. **B**: Densitometric quantification of the Western blots showed that the knockdown of PDE4B and D as well as the PDE inhibitor piclamilast (1µM) inhibited α-SMA expression as a marker of myofibroblast differentiation. The knockdown of PDE4A had no effect on α-SMA protein expression. Data are expressed as percent of TGF-β control (mean ± SD, n = 5), $^{**}p < 0.01$, $^{***}p < 0.001$.

In contrast, silencing of subtype PDE4B and PDE4D provoked a strong and significant decrease of TGF-β induced α-SMA protein expression by 66% ($p \leq 0.001$) and 34 % ($p \leq 0.01$), respectively. As a control the panPDE4 inhibitor piclamilast reduced the TGF-β induced α-SMA expression to the same extent as the individual knockdowns of PDE4B and D (-42 %, $p \leq 0.001$), which might also indicate that both PDE4 subtypes belong to the same TGF-β induced signaling pathway leading to myofibroblast differentiation.

4. Discussion

4.1 Cytokine-dependent effects in primary human lung fibroblasts related to cyclic AMP signaling and phosphodiesterase 4 inhibition

Human lung fibroblasts are major structural cells orchestrating repair and remodeling in ailments such as IPF, asthma or COPD. Persistent activation of these cells may foster their inappropriate proliferation, migration, production of extracellular matrix proteins, contractile properties, amongst others, and together will support fibrotic remodeling. (Dempsey et al., 2006; Chung, 2001; Larson et al., 2004; Gross et al., 2001; Bjornsdottir et al., 1999).
Previous data indicate the spatial heterogeneity of fibroblasts within the healthy lung and the phenotypic differences of lung fibroblasts between normal and disease state (Kotaru et al., 2006). For example, Kotaru and coworkers demonstrated that there are differences in morphology, proliferation, α-SMA and procollagen expression in primary lung fibroblast obtained from proximal airways compared to those derived from distal lung parenchyma of asthmatic patients.
The question still persists, whether these different phenotypes are derived from distinct subpopulations with unique progenitors or represent different stages of differentiation from a common progenitor (Phan, 2008). For these studies normal human lung fibroblasts, were derived from several donors, from different parts of healthy human lungs and therefore reflect the naturally occuring heterogeneity of fibroblasts in healthy tissues.

Proliferation is controlled by divergent (Huang et al., 2008) and sometimes opposing signals (Dumaz et al., 2005). To understand the mechanistic basis of fibrotic hyperproliferation in respiratory diseases, the complex network of numerous cytokines, growth factors and other mediators must be considered. Since IL-1β and bFGF are found to be increased in lungs of patients with asthma, COPD and IPF (Barnes, 2003; Jeffery, 2001; Gross et al., 2001), their interaction may be of interest in the pathogenesis of respiratory diseases with fibrotic components.

Previous studies investigated the effects of IL-1β–induced PGE_2 and bFGF on proliferation of various cell types. Overall these studies show that their effects on proliferation is dependent on the concentrations of these factors and/or the investigated cell types (White et al., 2008; Bourcier et al., 1995; Cozzolino et al., 1990).

In this study, the interaction of IL-1β and bFGF on lung fibroblast proliferation and related mechanisms such as COX-2 induction, PGE_2 release and cAMP synthesis were analyzed. That high levels of cAMP reduce proliferation of human lung fibroblasts has been repeatedly described in the past and more recently the cAMP-GEF (GTP exchange factor) Epac, yet not protein kinase A, was disclosed to mediate this antimitogenic effect (Liu et al., 2004; Sanchez et al., 2002; Schmitt et al., 2001).

The present data show that IL-1β treatment alone is able to increase proliferation significantly at a concentration of 10 pg/ml (2.2 fold, p-value: < 0.01) to an extent, which however, is by far less than that reached by incubation with bFGF. This is in agreement with the results of White and coworkers (White et al., 2008).

White et al. concluded that IL-1β induces proliferation by triggering low concentrations of PGE_2, thereby activating G_i-coupled EP_3-receptor, reducing cAMP and promoting proliferation. In contrast, the present data show that low IL-1β concentrations trigger only a very small amount of PGE_2, which does not reduce intracellular cAMP. Instead, these low concentrations of PGE_2 already seem to increase cAMP. In line, under the present used experimental conditions, PGE_2 in a concentration range from 1 pM to 1 µM concentration-dependently diminished bFGF-induced (^{3}H)thymidine incorporation to a maximum efficacy of approximately 70% and with a half-maximum inhibition at approximately 2 nM (data not shown). In contrast, White and colleagues described a biphasic effect of PGE_2 on the proliferation of human lung fibroblasts under their experimental conditions with a maximum mitogenic effect attained at about 3 nM. Differences in cell types, their expression pattern of PGE_2 receptors (EP_1-EP_4) and their coupling to intracellular signalling cascades as well as cell culture conditions may explain the discrepany between the results of this investigation and that of White et al. Therefore, it can be assumed that in the present experimental system the mitogenic effects of IL-1β are unrelated to PGE_2 and cAMP. An explanation for the mitogenic effect of IL-1β may be an influence on MAPK pathway as published by several other groups (Kida et al., 2005; Scherle et al., 1997).

The current report demonstrates that in normal human lung fibroblasts the mitogenic potential of bFGF is potentiated by low concentrations of IL-1β (≤ 10 pg/ml). Such a synergism has previously been described in different cell types, for example in rat aortic smooth muscle cells (Bourcier et al., 1995), in human endothelial cells (Norioka et al., 1994) or in primary rabbit and human dermal fibroblasts (Bond et al., 1998). One may hypothesize that converging downstream signalling shared by bFGF and IL-1ß accounts for this observation, yet the precise molecular mechanisms are not well understood.

The observation that IL-1β potentiates bFGF-induced DNA synthesis in NHLF was limited to low concentrations of the cytokine (10 pg/ml) while higher concentrations of IL-1β progressively reduced proliferation. At these higher concentrations of IL-1β intracellular cAMP strongly increased, which may explain the anti-proliferative effect of IL-1β. Since the higher IL-1β concentrations up-regulated COX-2 resulting in an increased accumulation of PGE_2 one may assume that the prostanoid binds to EP_2 and EP_4 receptor coupled to heterotrimeric Gs protein, and that finally adenylyl cyclase (tmACs) activity accounts for the rise in cAMP. Indeed, human lung fibroblasts express EP_2 and EP_4 receptors with EP_2 being the predominant subtype (Haag et al., 2008; Huang et al., 2007).

A major finding of the current study was that in NHLF bFGF strongly potentiated the induction of COX-2 by IL-1β, and consequently, the increase in PGE_2 and cAMP secondary to the cytokine. This crosstalk between FGF and IL-1β has been described earlier in human osteosarcoma cells, yet its mechanistic origin remains to be explored (Laulederkind et al., 2000).

Overall, there is a high level of complexity in the interactions between IL-1β and bFGF to control proliferation of lung fibroblasts. Whereas bFGF-induced proliferation is potentiated by lower concentrations of IL-1β, by a separate mechanism bFGF amplifies the potential of higher concentrations of the cytokine to diminish proliferation, thus limiting its own mitogenic effects. As mentioned before bFGF and IL-1β have been described up regulated in various respiratory diseases where excessive proliferation of lung fibroblasts occurs. Strategies to increase or stabilize intracellular cAMP levels may represent a therapeutic perspective in fibrotic conditions, a view shared by others (Haag et al., 2008; Dunkern et al., 2007; Liu et al., 2004).

Cyclic AMP is degraded by several phosphodiesterase isoenzymes, as a corollary inhibition of PDEs augments cAMP. PDE isoenzymes activities were analysed in primary human lung fibroblasts and the presence of PDE1, PDE3 and PDE4 hydrolysing cAMP as well as PDE1 and PDE5 hydrolysing cGMP was revealed.

Based on this analysis, the effects of a PDE4 and a PDE3 inhibitor on proliferation of human lung fibroblasts were investigated. The possible role of PDE1 cannot be further assessed due to the lack of specific inhibitors for this isoenzyme. Complete and selective inhibition of PDE4 by piclamilast at 1 µM reduced proliferation of these cells, as it has been described on various other cell types (Hatzelmann et al., 2001), however to a modest extent. The inhibitory efficacy of this compound on proliferation strongly increased by simultaneous treatment with IL-1β, which somehow could be expected due to the enhancement of cAMP. Therefore, PDE4 inhibition strengthens the IL-1β-induced PGE_2-driven biological response, namely the decrease in proliferation. This is further supported by data from our group, showing that treatment with a cyclooxygenase inhibitor (inhibiting PGE_2 formation) abolishes the synergistic effect between IL-1β and PDE4-inhibition on reducing proliferation.

Since besides PDE4, also cAMP-hydrolyzing PDE3 was detected in human lung fibroblasts, the effect of PDE3 inhibition on proliferation was also analyzed. PDE3 inhibition via motapizone by itself did not affect proliferation, however, it potentiated the anti-proliferative effect of PDE4 inhibition. This finding confirms the hypothesis of the role of different PDEs in generating subcellular signaling compartments and nucleotide pools (Conti et al., 2007). Therefore it can be as well hypothesized that under conditions of PDE4 inhibition the cAMP pool generated by adenylyl cyclase activity increases and looses confinement, consequently diffusing into compartments of the cell, where PDE3 gets access to cAMP and will hydrolyze it. In this case a PDE3 inhibitor becomes effective in blocking proliferation of these cells, since it even more increases the cAMP pool originally controlled by PDE4 only (Zaccolo et al., 2006).

In order to elucidate the mechanism of proliferation inhibition in more detail, cell cycle analysis were performed and the question, whether the inhibition of proliferation by PDE4 inhibitors under concomitant incubation with IL-1β induces changes in cell cycle distribution was considered. Overall, the cell cycle analysis reflected findings in the proliferation assays. In comparison to starved cells bFGF increased the proportion of S-phase cells, which was potentiated by lower concentrations of IL-1β. At higher concentrations of IL-1β the percentage of S-phase cells decreased again. A PDE4 inhibitor on its own reduced the number of S-phase cells following bFGF by inducing a partial G1-arrest. By analogy to results from measurements of (^{3}H)thymidine incorporation, co-incubation with IL-1β potentiated the efficacy of a PDE4 inhibitor in inducing partial G1 arrest. The G1 arrest was accompanied by a decrease in Cyclin E1, D1 and cyclin-dependent kinase 4 and 6 mRNA expression, which gives some mechanistical insight about the influence of PDE4 inhibitors/cAMP on cell cycle control. These results are in line with investigations by other groups using various cell types (Lee et al., 2003; Stuart et al., 2000; Musa et al., 1999; L'Allemain et al., 1997).

4.2 Functional impact of PDE4 subtypes in primary human lung fibroblasts

Another aim of the present study was to identify the role of the four PDE4 subtypes in human lung fibroblasts in specific functions as proliferation and myofibroblast conversion. These functions are of pathophysiological relevance in progression of fibrosis in the lung in diseases such as COPD, IPF and asthma. By increasing cyclic AMP, PDE4 inhibitors act anti-inflammatory but are also capable of preventing and reducing fibrotic and vascular remodeling in the lung. Former effects are affirmed in various clinical trials, whereas the latter are the matter of various investigations in vitro and in vivo (Cortijo et al., 2009; Togo et al., 2009; Shepherd, 2006; Rabe et al., 2005). In order to mimic the pathophysiological conditions relevant to humans, we examined primary human lung fibroblasts under defined cytokine stimulatory conditions. Primary cells have potential disadvantages (e.g. hard to transfect siRNAs, limited passage number (Thiel et al., 2006). Nevertheless under our conditions the use of primary NHFL resulted in very reproducible results and a donor dependent variability was not observed. Several investigations by our group already proved the presence of PDE4 in lung fibroblasts of various species by gene and protein expression analysis as well as isoenzyme activity determination. The used primer/probe sets to measure the expression of PDE4 subtypes quantitatively were tested for similar efficiencies in a standardized qPCR (Peter et al., 2007) and this study corrobarated these findings by measuring similar amplifications rates of defined amounts of plasmid DNA containing unique PDE4 subtype inserts with those primer/probe sets. That followed the quantification of the PDE4 mRNAs expression in human lung fibroblasts under non-stimulated conditions. It turned out that the subtype PDE4A is the most predominantly expressed one, followed by PDE4B and PDE4D. This is in accordance with findings of another group (Martin-Chouly et al., 2004; Kohyama et al., 2002a). In contrast PDE4C was expressed in NHLF at the absolute limit of detection and therefore can be considered as not to be present in these cells under the given conditions, as also described by Spina (Spina, 2008).

Since the intention of this study is to examine the effects of PDE4 subtype specific knockdowns on cytokine-induced proliferation, the PDE4 subtype expression pattern under the corresponding conditions was also analyzed. As described before, the mitogenic effects of various bFGF/IL-1β co-stimulation conditions were characterized in-depth and related to cyclic AMP. IL-1β showed biphasic effects; at concentrations of ≤ 10 pg/ml, IL-1β potentiated the bFGF-induced proliferation of NHFL, whereas concentrations of IL-1β at ≥ 50 pg/ml increased COX-2 expression, subsequently PGE_2 synthesis and cAMP generation to an extent that proliferation is not potentiated but commenced to inhibit proliferation (as seen in figure 7B).

Accordingly under conditions where NHLF get induced to proliferate (bFGF and co-treatment with IL-1β at 10 pg/ml) no changes in the PDE4 subtype expression pattern in comparison to non-stimulated cells was observed.

In contrast co-treatments using IL-1β at a concentration of 50 pg/ml (plus/minus bFGF), at which also cAMP is increased (as described in chapter 3.1.1), resulted in increased PDE4B and PDE4D mRNA expression. Since it has been described that both genes (PDE4B and PDE4D) have a cAMP-regulated intronic promotor (D'Sa et al., 2002; Vicini et al., 1997), IL-1β can be account for the effect of increased transcription and the related changes in cAMP as measured in figure 8 of chapter 3.1.1. No changes in PDE4A and PDE4C gene expression were observed.

These results demonstrate that the basal low expressed subtype PDE4D but not PDE4C can be upregulated by cAMP and therefore it was crucial for our further investigations to elaborate a method to knockdown all three expressed PDE4 subtypes A, B and D.

Since no PDE4 subtype specific inhibitors exist, a transfection method for subtype specific siRNAs was elaborated that operates gently and efficiently in terms of knockdown in NHLF but without affecting subtstantially the fibroblast functions to be investigated. An electroporation method was compared to a liposome-mediated tranfection and turned out to be inferior. Thus electroporation with PDE4 subtype specific siRNA mediated a considerable decrease of mRNA expression, however only compared to control electroporated cells since electroporation by itself induced PDE4 gene expression (significant for PDE4 A and B). This might be interpreted as a cellular stress response induced by the electroporation (Vernier et al., 2009; Beebe et al., 2003).

Since there was no significant downregulation of PDE4 subtype mRNAs by siRNA electroporation in comparison to the non-electroporated cells, the electroporation method was not considered to be suitable for further investigations.

Furthermore, the electroporation method induced a mortality of approximately 30% within minutes and siRNA concentrations for mRNA knockdown exceeded 1µM, which increases the probability of off-target effects affecting our functional readouts (Jackson et al., 2010; Baum et al., 2009). In contrast a cationic liposome-mediated siRNA transfection method for NHLF with fewer unwanted effects was established.

siRNA concentrations in the range from 0.015 nM to 150 nM were tested and a concentration of 5 nM identified as the convenient concentration for maximal and selective knockdown after 24h of all PDE4 subtypes in NHFL. On mRNA level a knockdown of about 80% for PDE4A and D and about 55% for PDE4B was achieved. The lipofection of NHLF with individual siRNAs versus PDE4A, PDE4B and PDE4D showed a very stable knockdown of mRNA over time, tested in a range from 24h to 96h.

A decrease in PDE4A and B protein was already observed 24h after transfection and was maximal between 72 and 96h, which indicates that the total turnover of these proteins in NHFL is done within this period. This has not been investigated before. However PDE4D protein was not detectable by Western blot analysis even using different antibodies, targeting different epitopes of PDE4D, and different Western blot protocols. This might be explained by a low expression level of PDE4D in these cells as also suggested by the results of the gene expression analysis.

Additionally, the PDE4 subtype specificity of the siRNAs was tested in these experiments. Indeed individual siRNAs for one subtype did not downregulate the other PDE4 subtypes. This shows that it is possible despite very high sequence homology between the PDE4 subtypes of about 80 to 84% within the catalytic region (Torphy, 1998), to identify siRNA target sequences, which guarantee subtype specificity.

However it should be mentioned that several commercially available siRNA´s, which were proposed to be subtype specific, have been tested in this investigations and turned out to be either inefficient with respect to knockdown or unspecific. Since the identified siRNAs were shown to be subtype specific, it can be assumed that each siRNA addressing a distinct subtype of PDE4 can also be used as high homology negative control for the other subtypes, as also described by Peter et al., 2007.

It is interesting to note that siRNA mediated knockdown of PDE4B conversely, significantly increased the mRNA expression of PDE4D. There was also a tendency of increasing mRNA levels of PDE4B and D by knockdown of PDE4A. This might be considered as a counterregulation of NHFL as a consequence of increased cAMP levels induced by the knockdown (due to reduced cAMP hydrolysis activity). However, in this study cAMP levels after siRNA transfection were not measured but the pattern of PDE4 subtype upregulation observed by specific knockdowns is similar to those after the treatment of NHLF with IL-1β at different concentrations, which also demonstrated to increase cAMP (as discussed before). Also under those circumstances only PDE4B and PDE4D but not PDE4A were upregulated. In contrast siRNA mediated knockdown of PDE4D did not increase PDE4B (and also not PDE4A) mRNA. This might be explained by the low expression level of this enzyme, as shown by qPCR, which suggests that a knockdown of this protein might increase cAMP only marginally and would thus not induces PDE4B expression.

The successful siRNA-mediated knockdown was additionally validated by measurements of overall PDE4 activity in NHLF and illustrates therewith several interesting aspects. First, the mRNA knockdown resulted in a time-dependent decrease of PDE4 activity with a maximal reduction 72h to 96h after tranfection. This is in accordance with the densitometric quantification of PDE4A and B Western blot analysis after siRNA-induced knockdown. Furthermore, the knockdown of PDE4B caused the most prominent reduction in overall PDE4 enzyme activity under the investigated conditions, followed by PDE4A and PDE4D. This interestingly does not reflect the mRNA expression pattern of the subtypes, which indicates that these enzymes are further regulated either on the level of protein translation or by post-translational modification as e.g. phosphorylation as described by Conti et al., 2002 or Houslay and Adams, 2003.

Noteworthy the sum of reduction in PDE4 activity by knockdown with PDE4A, B and D specific siRNAs resulted in nearly 100% of total PDE4 activity. Besides the already described gene expression data this provides further evidence, that PDE4C is not expressed under the used cell culture conditions in NHLF.

This is in discrepancy to a recent study of Martin-Chouly and coworkers (Martin-Chouly et al., 2004), who detected substantial amounts of subtype PDE4C in human lung fibroblasts. Apart from that they did not account PDE4C to a distinct cellular function. This difference might be explained by the usage of foetal lung fibroblast cell lines and different cell culture conditions. It is surprising that knowledge about PDE4C in humans is limited to its expression pattern and the enzymatic characterization but no cellular functions have been related to its expression up to now.

The optimized, effective and specific siRNA-mediated knockdown of the different PDE4 subtypes for the first time offers the opportunity to investigate their function in pathophysiological processes of normal human lung fibroblasts, such as excessive proliferation and conversion into myofibroblasts.
48h after transfection with the various PDE4 subtype specific siRNAs, proliferation was induced by either bFGF treatment (10 ng/ml) or in combination with IL-1β at a concentration of 10 pg/ml. As mentioned in the previous part of the discussion, expression of both cytokines has shown to be increased under pathophysiological fibrotic conditions (Kranenburg et al., 2005a; Zhang et al., 1993). Under co-stimulatory conditions proliferation of NHLF was shown to be maximal and a panPDE4 inhibitor to be effective, however not to a maximum. It turned out that the siRNA-mediated knockdown of the subtypes PDE4A and PDE4B reduced the bFGF/IL-1β induced proliferation significantly, whereas a scrambled control siRNA did not. The efficacy of the PDE4A knockdown on bFGF/IL-1β induced proliferation inhibition was comparable to the efficacy of the PDE4 inhibitor piclamilast, administered under the same experimental conditions. Knockdown of PDE4B was slightly less effective. Interestingly, the PDE4D siRNA transfection did not inhibit bFGF/IL-1β induced proliferation and could be therefore also considered as a high homology siRNA negative control in these experiments. The same pattern of inhibited proliferation by PDE4 subtype-specific mRNA knockdown was also observed under bFGF-treatment alone. This indicates that also under this condition a continous cAMP production is ongoing, which provides the basis for anti-proliferative efficacy of PDE4 inhibition as seen in figure 12 of chapter 3.1.4.

Besides proliferation, the differentiation to myofibroblast is an important pathophysiological feature and plays a key role in lung fibrosis. Several studies have demonstrated that PDE4 inhibitors reduce TGF-β-induced conversion of fibroblasts to myofibroblasts by analyzing alpha-smooth muscle actin expression, which is a key marker for myofibroblast differentiation (Dunkern et al., 2007). However, the interrelation of PDE4 subtypes in this process is unknown. This investigation now demonstrates, that the knockdown of the PDE4 subtype B and D, but not PDE4A reduces the expression of α–SMA induced by TGF-β and thus inhibits myofibroblast differentiation. Inhibition by PDE4B knockdown was most effective and comparable to the treatment with a pan PDE4 inhibitor piclamilast.

Overall we should be aware that this study provides first evidences for the involvement of PDE4A and B in controlling fibroproliferation and 4B and 4D in regulating differentiation to myofibroblasts. However in order to explain the detailed mode of action and to exclude potential off-target effects completely, further studies regarding signaling would be required.

4.3 Conclusions

In summary, the interaction of bFGF and IL-1β on proliferation of human lung fibroblasts has been described. Both cytokines are assumed to be involved in pathophysiological processes leading to fibrosis in various respiratory disorders. In particular, the presence of IL-1β may be considered in view of ongoing inflammatory processes such as those described in IPF. In the experimental system of in-vitro cultured human primary lung fibroblasts, it was shown that IL-1β may either drive the fibrotic process by its ability to stimulate proliferation on its own but also by potentiating the proliferative action of bFGF, or that IL-1β may be anti-proliferative by inducing COX-2 and subsequently enhancing PGE_2. It is most likely that the expression balance of these two cytokines will determine, at least in part, whether fibrotic processes are ongoing or tissue homeostasis is maintained.

Up to now there is no therapy available targeting the fibrotic component of e.g. IPF, COPD or asthma. PDE4 inhibitors as e.g. roflumilast, which succeeded recently in phase III trials in COPD, are well known anti-inflammatory agents (Hatzelmann et al., 2001) by their ability to increase intracellular cAMP. The actual in-vitro investigations now also suggest that these drugs might offer additional therapeutic benefit by inhibiting

proliferation of lung fibroblasts especially under pathological conditions of enhanced IL-1β and PGE_2. This might be of particular importance since different groups (Vancheri et al., 2000; Wilborn et al., 1995) have shown, that the capability of lung fibroblasts to produce anti-proliferative PGE_2 levels is diminished in patients with pulmonary fibrosis.
It might therefore be important to boost the anti-proliferative signal transduction initiated by PGE_2 via inhibition of cAMP hydrolysis by PDE4 inhibitors.
Roflumilast N-oxide has already been shown to be therapeutically effective in bleomycin-induced lung fibrosis in mice, already after an established fibrosis (Cortijo et al., 2009).
This is of special interest since corticosteroids, which are standard anti-inflammatory drugs, failed in therapeutic protocols in this animal model and also did not show efficacy in clinical trials with IPF patients as also meta-analysis have revealed. Whether PDE4 inhibitors might be effective in fibrotic lung diseases in man remains to be ascertained.
One of the key findings of this study is about the dominant role of PDE4B in controling both, lung fibroblast proliferation and the transition to myofibroblasts. In contrast PDE4D, whose inhibition is also proposed to be responsible for side effects provoked by PDE4 inhibitors in humans, seems not to control proliferation. Thus it is logical to focus further drug discovery efforts on developing subtype-specific inhibitors exclusively targeting PDE4B, which should then provide a broader therapeutic window, allowing to be dosed higher and thus to be more efficacious.

5. Summary

Lung fibroblast proliferation and differentiation into myofibroblast are pathological key events during fibrotic alterations occuring in pulmonary diseases such as asthma, idiopathic pulmonary fibrosis or chronic obstructive pulmonary disease. Cyclic nucleotide signaling is described as a negative modulator of these cellular processes, and cyclic AMP degrading type 4 phosphodiesterases (PDE4) are important regulators of these pathways. Together with various cAMP-generating isoforms of adenylyl cyclases and effectors, PDE4 subtypes constitute a network that regulates the signaling via numerous mediators, e.g. growth factors or cytokines. Several studies using selective PDE4 inhibitors under clinical development have shown that the induced increase of cAMP can inhibit lung fibroblast functions and might be able to mitigate lung tissue remodeling. The role of PDE4 subtypes in these functions remains unknown.

This thesis aims to analyze mechanisms of cytokine-induced functions of human lung fibroblasts, such as proliferation and differentiation, and to determine the role of PDE4 subtypes within these processes. This study demonstrates, that bFGF-induced proliferation of human lung fibroblasts is either potentiated by the presence of the inflammatory cytokine IL-1β or inhibited depending on the IL-1β concentration. The antiproliferative activity of PDE4 inhibitors (but not of PDE3 inhibitors) is due to the increase of PGE_2 by IL-1β via the COX-2/PGE_2-synthase pathway. Moreover, this IL-1β triggered signaling pathway is further potentiated by bFGF by increasing IL-1β induced COX-2 expression.

In order to assess the role of PDE4 subtypes, their expression in human lung fibroblasts was down regulated by using an optimized liposome mediated transfection method and specific siRNA´s. With this technology, different PDE4 subtypes were assigned to distinct functions of human lung fibroblast. The knockdown of PDE4A and PDE4B inhibited cytokine-induced proliferation, whereas knockdown of PDE4D did not. In contrast, TGF-β induced differentiation of lung fibroblasts to myofibroblasts was only prevented by knockdown of PDE4B and PDE4D, but not of PDE4A. The identification of the predominant role of PDE4B in controlling pathophysiological relevant functions of human lung fibroblasts provides now a rationale for pharmaceutical development of subtype specific PDE4 inhibitors with higher efficacy and a broader therapeutic window.

6. Zusammenfassung

Proliferation von Lungenfibroblasten und ihre Differenzierung zu Myofibroblasten sind pathologische Schlüsselereignisse bei fibrotischen Veränderungen, die in Atemwegserkrankungen wie Asthma, idiopathische Lungenfibrose oder chronisch obstruktiven Atemwegserkrankungen vorkommen. Bei diesen zellulären Vorgängen gelten die Signalwirkungen von zyklischen Nukleotiden als negative Regulatoren. Die cAMP degradierenden Phosphodiesterasen vom Typ 4 (PDE4) sind wesentliche Regler dieser Signalwege. Im Zusammenspiel mit verschiedenen cAMP-generierenden Isoformen der Adenylatzyklasen und Effektoren, bilden die Subtypen der PDE4 ein Netzwerk der Regulation von Signalen, die von Mediatoren wie Wachstumsfaktoren oder Zytokinen ausgelöst werden. Studien mit PDE4 Inhibitoren, die sich in der klinischen Entwicklung befinden, haben gezeigt, das der induzierte Anstieg von cAMP die Funktionen von Lungenfibroblasten unterbindet und damit in der Lage ist Lungengewebsveränderungen zu unterdrücken. Welche Rolle bei diesen Funktionen die Subtypen der PDE4 spielen, ist nach wie vor unbekannt.

Diese Dissertation hat zum Ziel, die Mechanismen der Zytokin-induzierten Funktionen, wie die Proliferation und Differenzierung von humanen Lungenfibroblasten zu analysieren, sowie die Aufgabe der PDE4 Subtypen bei diesen Prozessen zu untersuchen. Die Studie zeigt, daß die bFGF-induzierte Proliferation von humanen Lungenfibroblasten, abhängig von der gegenwärtigen Konzentration des inflammatorischen Zytokins IL-1β, verstärkt oder inhibiert wird. Die antiproliferierende Wirkung der PDE4 Inhibitoren (jedoch nicht der PDE3 Inhibitoren) beruht auf der Erhöhung der Bildung von PGE_2 durch IL-1β über den COX-2/PGE_2-Syntheseweg. Zusätzlich wird dieser durch IL-1β ausgelöste Signalweg durch bFGF noch weiter verstärkt, indem dieses die IL-1β-induzierte COX-2 Expression potenziert.

Um die Rolle der in humanen Lungenfibroblasten exprimierten Subtypen der PDE4 zu charakterisieren, wurden diese individuell mittels einer optimierten Liposomen vermittelten Transfektionsmethode und spezifischen siRNAs herunterreguliert. Damit war es möglich, den verschiedenen Subtypen der PDE4 diskrete Funktionen in humanen Lungenfibroblasten zuzuordnen. So inhibierte der Knockdown der PDE4A und PDE4B die Zytokin-induzierte Proliferation, wohingegen der Knockdown von PDE4D keine Wirkung zeigte. Im Gegensatz dazu wurde die TGF-β-induzierte Differenzierung von Lungenfibroblasten zu Myofibroblasten durch den Knockdown der PDE4B und PDE4D verhindert, jedoch nicht durch den Knockdown der PDE4A.

Die Identifizierung der dominierenden Rolle der PDE4B, in der Kontrolle patho-physiologisch relevanter Funktionen in humanen Lungenfibroblasten, liefert damit einen klar definierten, molekularen Ansatzpunkt für die pharmazeutische Entwicklung besserer subtypspezifischer PDE4 Inhibitoren.

7. References

American Thoracic Society. 2000. Idiopathic pulmonary fibrosis: diagnosis and treatment. International consensus statement. American Thoracic Society (ATS), and the European Respiratory Society (ERS). Am J Respir Crit Care Med 161:646-664.

Adams JA, McGlone ML, Gibson R, Taylor SS. 1995. Phosphorylation modulates catalytic function and regulation in the cAMP-dependent protein kinase. Biochemistry 34:2447-2454.

Agostini C, Gurrieri C. 2006. Chemokine/cytokine cocktail in idiopathic pulmonary fibrosis. Proc Am Thorac Soc 3:357-363.

Amin AR, Ichigotani Y, Oo ML, Biswas MH, Yuan H, Huang P, Mon NN, Hamaguchi M. 2003. The PLC-PKC cascade is required for IL-1beta-dependent Erk and Akt activation: their role in proliferation. Int J Oncol 23:1727-1731.

Andersson-Sjoland A, de Alba CG, Nihlberg K, Becerril C, Ramirez R, Pardo A, Westergren-Thorsson G, Selman M. 2008. Fibrocytes are a potential source of lung fibroblasts in idiopathic pulmonary fibrosis. Int J Biochem Cell Biol 40:2129-2140.

Ariga M, Neitzert B, Nakae S, Mottin G, Bertrand C, Pruniaux MP, Jin SL, Conti M. 2004. Nonredundant function of phosphodiesterases 4D and 4B in neutrophil recruitment to the site of inflammation. J Immunol 173:7531-7538.

Baillie GS, Houslay MD. 2005. Arrestin times for compartmentalised cAMP signalling and phosphodiesterase-4 enzymes. Curr Opin Cell Biol 17:129-134.

Baillie GS, Huston E, Scotland G, Hodgkin M, Gall I, Peden AH, MacKenzie C, Houslay ES, Currie R, Pettitt TR, Walmsley AR, Wakelam MJ, Warwicker J, Houslay MD. 2002. TAPAS-1, a novel microdomain within the unique N-terminal region of the PDE4A1 cAMP-specific phosphodiesterase that allows rapid, Ca2+-triggered membrane association with selectivity for interaction with phosphatidic acid. J Biol Chem 277:28298-28309.

Baillie GS, MacKenzie SJ, McPhee I, Houslay MD. 2000. Sub-family selective actions in the ability of Erk2 MAP kinase to phosphorylate and regulate the activity of PDE4 cyclic AMP-specific phosphodiesterases. Br J Pharmacol 131:811-819.

Baillie GS, Sood A, McPhee I, Gall I, Perry SJ, Lefkowitz RJ, Houslay MD. 2003. beta-Arrestin-mediated PDE4 cAMP phosphodiesterase recruitment regulates beta-adrenoceptor switching from Gs to Gi. Proc Natl Acad Sci U S A 100:940-945.

Barnes PJ. 2003. New concepts in chronic obstructive pulmonary disease. Annu Rev Med 54:113-129.

Bauer AC, Schwabe U. 1980. An improved assay of cyclic 3',5'-nucleotide phosphodiesterases with QAE-Sephadex columns. Naunyn Schmiedebergs Arch Pharmacol 311:193-198.

Baum P, Fundel-Clemens K, Kreuz S, Kontermann RE, Weith A, Mennerich D, Rippmann JF. 2009. Off-Target Analysis of Control siRNA Molecules Reveals Important Differences in the Cytokine Profile and Inflammation Response of Human Fibroblasts. Oligonucleotides. Online ahead of print.

Beard MB, Olsen AE, Jones RE, Erdogan S, Houslay MD, Bolger GB. 2000. UCR1 and UCR2 domains unique to the cAMP-specific phosphodiesterase family form a discrete module via electrostatic interactions. J Biol Chem 275:10349-10358.

Beavo JA, Brunton LL. 2002. Cyclic nucleotide research -- still expanding after half a century. Nat Rev Mol Cell Biol 3:710-718.

Beebe SJ, Fox PM, Rec LJ, Willis EL, Schoenbach KH. 2003. Nanosecond, high-intensity pulsed electric fields induce apoptosis in human cells. FASEB J 17:1493-1495.

Bergeron C, Al-Ramli W, Hamid Q. 2009. Remodeling in Asthma. Am Thorac Soc 6:301-305.

Berthet J, Rall TW, Sutherland EW. 1957. The relationship of epinephrine and glucagon to liver phosphorylase. IV. Effect of epinephrine and glucagon on the reactivation of phosphorylase in liver homogenates. J Biol Chem 224:463-475.

Bjornsdottir US, Cypcar DM. 1999. Asthma: an inflammatory mediator soup. Allergy 54 Suppl 49:55-61.

Bolger G, Michaeli T, Martins T, St John T, Steiner B, Rodgers L, Riggs M, Wigler M, Ferguson K. 1993. A family of human phosphodiesterases homologous to the dunce learning and memory gene product of Drosophila melanogaster are potential targets for antidepressant drugs. Mol Cell Biol 13:6558-6571.

Bond M, Fabunmi RP, Baker AH, Newby AC. 1998. Synergistic upregulation of metalloproteinase-9 by growth factors and inflammatory cytokines: an absolute requirement for transcription factor NF-kappa B. FEBS Lett 435:29-34.

Borbe HO, Hilboll G, Prop G. 1986. Inhibition of human platelet aggregation by motapizone via an increase in intracellular cAMP. Agents Actions Suppl 20:249-257.

Bosse Y, Rola-Pleszczynski M. 2008. FGF2 in asthmatic airway-smooth-muscle-cell hyperplasia. Trends Mol Med 14:3-11.

Bourcier T, Dockter M, Hassid A. 1995. Synergistic interaction of interleukin-1 beta and growth factors in primary cultures of rat aortic smooth muscle cells. J Cell Physiol 164:644-657.

Bourne HR. 1997. How receptors talk to trimeric G proteins. Curr Opin Cell Biol 9:134-142.

Bourtchouladze R, Lidge R, Catapano R, Stanley J, Gossweiler S, Romashko D, Scott R, Tully T. 2003. A mouse model of Rubinstein-Taybi syndrome: defective long-term memory is ameliorated by inhibitors of phosphodiesterase 4. Proc Natl Acad Sci U S A 100:10518-10522.

Bruno O, Romussi A, Spallarossa A, Brullo C, Schenone S, Bondavalli F, Vanthuyne N, Roussel C. 2009. New Selective Phosphodiesterase 4D Inhibitors Differently Acting on Long, Short, and Supershort Isoforms. J Med Chem .

Bruss MD, Richter W, Horner K, Jin SL, Conti M. 2008. Critical role of PDE4D in beta2-adrenoceptor-dependent cAMP signaling in mouse embryonic fibroblasts. J Biol Chem 283:22430-22442.

Butcher RW, Sutherland EW. 1962. Adenosine 3',5'-phosphate in biological materials. I. Purification and properties of cyclic 3',5'-nucleotide phosphodiesterase and use of this enzyme to characterize adenosine 3',5'-phosphate in human urine. J Biol Chem 237:1244-1250.

Calverley PM, Rabe KF, Goehring UM, Kristiansen S, Fabbri LM, Martinez FJ. 2009. Roflumilast in symptomatic chronic obstructive pulmonary disease: two randomised clinical trials. Lancet 374:685-694.

Chapman HA. 2004. Disorders of lung matrix remodeling. J Clin Invest 113:148-157.

Cheng X, Ji Z, Tsalkova T, Mei F. 2008. Epac and PKA: a tale of two intracellular cAMP receptors. Acta Biochim Biophys Sin (Shanghai) 40:651-662.

Chung KF. 2001. Cytokines in chronic obstructive pulmonary disease. Eur Respir J Suppl 34:50s-59s.

Chung KF. 2006. Cytokines as targets in chronic obstructive pulmonary disease. Curr Drug Targets 7:675-681.

Conti M, Beavo J. 2007. Biochemistry and physiology of cyclic nucleotide phosphodiesterases: essential components in cyclic nucleotide signaling. Annu Rev Biochem 76:481-511.

Conti M, Jin SL. 1999. The molecular biology of cyclic nucleotide phosphodiesterases. Prog Nucleic Acid Res Mol Biol 63:1-38.

Conti M, Richter W, Mehats C, Livera G, Park JY, Jin C. 2003. Cyclic AMP-specific PDE4 phosphodiesterases as critical components of cyclic AMP signaling. J Biol Chem 278:5493-5496.

Cortijo J, Iranzo A, Milara X, Mata M, Cerda-Nicolas M, Ruiz-Sauri A, Tenor H, Hatzelmann A, Morcillo EJ. 2009. Roflumilast, a phosphodiesterase 4 inhibitor, alleviates bleomycin-induced lung injury. Br J Pharmacol 156:534-544.

Cozzolino F, Torcia M, Aldinucci D, Ziche M, Almerigogna F, Bani D, Stern DM. 1990. Interleukin 1 is an autocrine regulator of human endothelial cell growth. Proc Natl Acad Sci U S A 87:6487-6491.

D'Sa C, Tolbert LM, Conti M, Duman RS. 2002. Regulation of cAMP-specific phosphodiesterases type 4B and 4D (PDE4) splice variants by cAMP signaling in primary cortical neurons. J Neurochem 81:745-757.

Dastidar SG, Rajagopal D, Ray A. 2007. Therapeutic benefit of PDE4 inhibitors in inflammatory diseases. Curr Opin Investig Drugs 8:364-372.

Davis RL, Takayasu H, Eberwine M, Myres J. 1989. Cloning and characterization of mammalian homologs of the Drosophila dunce+ gene. Proc Natl Acad Sci U S A 86:3604-3608.

de Boer WI, van Schadewijk A, Sont JK, Sharma HS, Stolk J, Hiemstra PS, Van Krieken JH. 1998. Transforming growth factor beta1 and recruitment of macrophages and mast cells in airways in chronic obstructive pulmonary disease. Am J Respir Crit Care Med 158:1951-1957.

Dempsey OJ, Kerr KM, Gomersall L, Remmen H, Currie GP. 2006. Idiopathic pulmonary fibrosis: an update. QJM 99:643-654.

Diaz A, Chepenik KP, Korn JH, Reginato AM, Jimenez SA. 1998. Differential regulation of cyclooxygenases 1 and 2 by interleukin-1 beta, tumor necrosis factor-alpha, and transforming growth factor-beta 1 in human lung fibroblasts. Exp Cell Res 241:222-229.

DiPilato LM, Cheng X, Zhang J. 2004. Fluorescent indicators of cAMP and Epac activation reveal differential dynamics of cAMP signaling within discrete subcellular compartments. Proc Natl Acad Sci U S A 101:16513-16518.

Dodge KL, Khouangsathiene S, Kapiloff MS, Mouton R, Hill EV, Houslay MD, Langeberg LK, Scott JD. 2001. mAKAP assembles a protein kinase A/PDE4 phosphodiesterase cAMP signaling module. EMBO J 20:1921-1930.

Dohlman HG, Thorner J, Caron MG, Lefkowitz RJ. 1991. Model systems for the study of seven-transmembrane-segment receptors. Annu Rev Biochem 60:653-688.

Dumaz N, Marais R. 2005. Integrating signals between cAMP and the RAS/RAF/MEK/ERK signalling pathways. Based on the anniversary prize of the Gesellschaft fur Biochemie und Molekularbiologie Lecture delivered on 5 July 2003 at the Special FEBS Meeting in Brussels. FEBS J 272:3491-3504.

Dunkern TR, Feurstein D, Rossi GA, Sabatini F, Hatzelmann A. 2007. Inhibition of TGF-beta induced lung fibroblast to myofibroblast conversion by phosphodiesterase inhibiting drugs and activators of soluble guanylyl cyclase. Eur J Pharmacol 572:12-22.

Essayan DM. 1999. Cyclic nucleotide phosphodiesterase (PDE) inhibitors and immunomodulation. Biochem Pharmacol 57:965-973.

Felgner PL, Gadek TR, Holm M, Roman R, Chan HW, Wenz M, Northrop JP, Ringold GM, Danielsen M. 1987. Lipofection: a highly efficient, lipid-mediated DNA-transfection procedure. Proc Natl Acad Sci U S A 84:7413-7417.

Fine A, Goldstein RH. 1987. The effect of PGE2 on the activation of quiescent lung fibroblasts. Prostaglandins 33:903-913.

Foord SM, Bonner TI, Neubig RR, Rosser EM, Pin JP, Davenport AP, Spedding M, Harmar AJ. 2005. International Union of Pharmacology. XLVI. G protein-coupled receptor list. Pharmacol Rev 57:279-288.

Gamble E, Grootendorst DC, Brightling CE, Troy S, Qiu Y, Zhu J, Parker D, Matin D, Majumdar S, Vignola AM, Kroegel C, Morell F, Hansel TT, Rennard SI, Compton C, Amit O, Tat T, Edelson J, Pavord ID, Rabe KF, Barnes NC, Jeffery PK. 2003. Antiinflammatory effects of the phosphodiesterase-4 inhibitor cilomilast (Ariflo) in chronic obstructive pulmonary disease. Am J Respir Crit Care Med 168:976-982.

Gantner F, Gotz C, Gekeler V, Schudt C, Wendel A, Hatzelmann A. 1998. Phosphodiesterase profile of human B lymphocytes from normal and atopic donors and the effects of PDE inhibition on B cell proliferation. Br J Pharmacol 123:1031-1038.

Gautam N, Downes GB, Yan K, Kisselev O. 1998. The G-protein betagamma complex. Cell Signal 10:447-455.

Geng W, Wang Z, Zhang J, Reed BY, Pak CY, Moe OW. 2005. Cloning and characterization of the human soluble adenylyl cyclase. Am J Physiol Cell Physiol 288:C1305-C1316.

Goldring MB, Birkhead J, Sandell LJ, Kimura T, Krane SM. 1988. Interleukin 1 suppresses expression of cartilage-specific types II and IX collagens and increases types I and III collagens in human chondrocytes. J Clin Invest 82:2026-2037.

Gong B, Vitolo OV, Trinchese F, Liu S, Shelanski M, Arancio O. 2004. Persistent improvement in synaptic and cognitive functions in an Alzheimer mouse model after rolipram treatment. J Clin Invest 114:1624-1634.

Gresch O, Engel FB, Nesic D, Tran TT, England HM, Hickman ES, Korner I, Gan L, Chen S, Castro-Obregon S, Hammermann R, Wolf J, Muller-Hartmann H, Nix M, Siebenkotten G, Kraus G, Lun K. 2004. New non-viral method for gene transfer into primary cells. Methods 33:151-163.

Gross TJ, Hunninghake GW. 2001. Idiopathic pulmonary fibrosis. N Engl J Med 345:517-525.

Haag S, Warnken M, Juergens UR, Racke K. 2008. Role of Epac1 in mediating anti-proliferative effects of prostanoid EP(2) receptors and cAMP in human lung fibroblasts. Naunyn Schmiedebergs Arch Pharmacol 378:617-630.

Hanoune J, Defer N. 2001. Regulation and role of adenylyl cyclase isoforms. Annu Rev Pharmacol Toxicol 41:145-174.

Hansen G, Jin S, Umetsu DT, Conti M. 2000. Absence of muscarinic cholinergic airway responses in mice deficient in the cyclic nucleotide phosphodiesterase PDE4D. Proc Natl Acad Sci U S A 97:6751-6756.

Hatzelmann A, Schudt C. 2001. Anti-inflammatory and immunomodulatory potential of the novel PDE4 inhibitor roflumilast in vitro. J Pharmacol Exp Ther 297:267-279.

Hermans E. 2003. Biochemical and pharmacological control of the multiplicity of coupling at G-protein-coupled receptors. Pharmacol Ther 99:25-44.

Herrmann M, **Selige** J, Raffael S, Sachs G, Brambilla A, Klein T. 2007. Systematic expression profiling of the gastric H+/K+ ATPase in human tissue. Scand J Gastroenterol 42:1275-1288.

Hogg JC, Timens W. 2008. The Pathology of Chronic Obstructive Pulmonary Disease. Annu Rev Pathol Mech Dis 4:435-459.

Houslay MD, Adams DR. 2003. PDE4 cAMP phosphodiesterases: modular enzymes that orchestrate signalling cross-talk, desensitization and compartmentalization. Biochem J 370:1-18.

Houslay MD, Kolch W. 2000. Cell-type specific integration of cross-talk between extracellular signal-regulated kinase and cAMP signaling. Mol Pharmacol 58:659-668.

Houslay MD, Milligan G. 1997. Tailoring cAMP-signalling responses through isoform multiplicity. Trends Biochem Sci 22:217-224.

Houslay MD, Schafer P, Zhang KY. 2005. Keynote review: phosphodiesterase-4 as a therapeutic target. Drug Discov Today 10:1503-1519.

Huai Q, Liu Y, Francis SH, Corbin JD, Ke H. 2004. Crystal structures of phosphodiesterases 4 and 5 in complex with inhibitor 3-isobutyl-1-methylxanthine suggest a conformation determinant of inhibitor selectivity. J Biol Chem 279:13095-13101.

Huang S, Wettlaufer SH, Hogaboam C, Aronoff DM, Peters-Golden M. 2007. Prostaglandin E(2) inhibits collagen expression and proliferation in patient-derived normal lung fibroblasts via E prostanoid 2 receptor and cAMP signaling. Am J Physiol Lung Cell Mol Physiol 292:L405-L413.

Huang SK, Wettlaufer SH, Chung J, Peters-Golden M. 2008. Prostaglandin E2 inhibits specific lung fibroblast functions via selective actions of PKA and Epac-1. Am J Respir Cell Mol Biol 39:482-489.

Huang SK, White ES, Wettlaufer SH, Grifka H, Hogaboam CM, Thannickal VJ, Horowitz JC, Peters-Golden M. 2009. Prostaglandin E(2) induces fibroblast apoptosis by modulating multiple survival pathways. FASEB J 23:4317-4326.

Inoue Y, King TE, Jr., Barker E, Daniloff E, Newman LS. 2002. Basic fibroblast growth factor and its receptors in idiopathic pulmonary fibrosis and lymphangioleiomyomatosis. Am J Respir Crit Care Med 166:765-773.

Ito K, Lim S, Caramori G, Cosio B, Chung KF, Adcock IM, Barnes PJ. 2002. A molecular mechanism of action of theophylline: Induction of histone deacetylase activity to decrease inflammatory gene expression. Proc Natl Acad Sci U S A 99:8921-8926.

Jackson AL, Linsley PS. 2010. Recognizing and avoiding siRNA off-target effects for target identification and therapeutic application. Nat Rev Drug Discov 9:57-67.

Jacobitz S, McLaughlin MM, Livi GP, Burman M, Torphy TJ. 1996. Mapping the functional domains of human recombinant phosphodiesterase 4A: structural requirements for catalytic activity and rolipram binding. Mol Pharmacol 50:891-899.

Jaiswal BS, Conti M. 2001. Identification and functional analysis of splice variants of the germ cell soluble adenylyl cyclase. J Biol Chem 276:31698-31708.

Jeffery PK. 2001. Remodeling in asthma and chronic obstructive lung disease. Am J Respir Crit Care Med 164:S28-S38.

Jin SL, Conti M. 2002. Induction of the cyclic nucleotide phosphodiesterase PDE4B is essential for LPS-activated TNF-alpha responses. Proc Natl Acad Sci U S A 99:7628-7633.

Jin SL, Lan L, Zoudilova M, Conti M. 2005. Specific role of phosphodiesterase 4B in lipopolysaccharide-induced signaling in mouse macrophages. J Immunol 175:1523-1531.

Jin SL, Richard FJ, Kuo WP, D'Ercole AJ, Conti M. 1999. Impaired growth and fertility of cAMP-specific phosphodiesterase PDE4D-deficient mice. Proc Natl Acad Sci U S A 96:11998-12003.

Kamenetsky M, Middelhaufe S, Bank EM, Levin LR, Buck J, Steegborn C. 2006. Molecular details of cAMP generation in mammalian cells: a tale of two systems. J Mol Biol 362:623-639.

Kanes SJ, Tokarczyk J, Siegel SJ, Bilker W, Abel T, Kelly MP. 2007. Rolipram: a specific phosphodiesterase 4 inhibitor with potential antipsychotic activity. Neuroscience 144:239-246.

Kaupp UB, Seifert R. 2002. Cyclic nucleotide-gated ion channels. Physiol Rev 82:769-824.

Khalil N, O'Connor RN, Unruh HW, Warren PW, Flanders KC, Kemp A, Bereznay OH, Greenberg AH. 1991. Increased production and immunohistochemical localization of transforming growth factor-beta in idiopathic pulmonary fibrosis. Am J Respir Cell Mol Biol 5:155-162.

Khalil N, Xu YD, O'Connor R, Duronio V. 2005. Proliferation of pulmonary interstitial fibroblasts is mediated by transforming growth factor-beta1-induced release of extracellular fibroblast growth factor-2 and phosphorylation of p38 MAPK and JNK. J Biol Chem 280:43000-43009.

Kida Y, Kobayashi M, Suzuki T, Takeshita A, Okamatsu Y, Hanazawa S, Yasui T, Hasegawa K. 2005. Interleukin-1 stimulates cytokines, prostaglandin E2 and matrix metalloproteinase-1 production via activation of MAPK/AP-1 and NF-kappaB in human gingival fibroblasts. Cytokine 29:159-168.

Kohyama T, Ertl RF, Valenti V, Spurzem J, Kawamoto M, Nakamura Y, Veys T, Allegra L, Romberger D, Rennard SI. 2001. Prostaglandin E(2) inhibits fibroblast chemotaxis. Am J Physiol Lung Cell Mol Physiol 281:L1257-L1263.

Kohyama T, Liu X, Wen FQ, Kobayashi T, Fang Q, Abe S, Cieslinski L, Barnette MS, Rennard SI. 2004. Cytokines modulate cilomilast response in lung fibroblasts. Clin Immunol 111:297-302.

Kohyama T, Liu X, Wen FQ, Zhu YK, Wang H, Kim HJ, Takizawa H, Cieslinski LB, Barnette MS, Rennard SI. 2002a. PDE4 inhibitors attenuate fibroblast chemotaxis and contraction of native collagen gels. Am J Respir Cell Mol Biol 26:694-701.

Kohyama T, Liu X, Zhu YK, Wen FQ, Wang HJ, Fang Q, Kobayashi T, Rennard SI. 2002b. Phosphodiesterase 4 inhibitor cilomilast inhibits fibroblast-mediated collagen gel degradation induced by tumor necrosis factor-alpha and neutrophil elastase. Am J Respir Cell Mol Biol 27:487-494.

Kolb M, Margetts PJ, Anthony DC, Pitossi F, Gauldie J. 2001. Transient expression of IL-1beta induces acute lung injury and chronic repair leading to pulmonary fibrosis. J Clin Invest 107:1529-1536.

Kossel A. 1888. Über eine neue Base aus dem Pflanzenreich. Ber Dtsch Chem Ges 21:2164-2167.

Kossel A. 1889. Über das Theophyllin, einen neuen Bestandtheil des Thees. Hoppe Seylers Z Physiol Chem 13:298-308.

Kotaru C, Schoonover KJ, Trudeau JB, Huynh ML, Zhou X, Hu H, Wenzel SE. 2006. Regional fibroblast heterogeneity in the lung: implications for remodeling. Am J Respir Crit Care Med 173:1208-1215.

Kranenburg AR, de Boer WI, Alagappan VK, Sterk PJ, Sharma HS. 2005a. Enhanced bronchial expression of vascular endothelial growth factor and receptors (Flk-1 and Flt-1) in patients with chronic obstructive pulmonary disease. Thorax 60:106-113.

Kranenburg AR, Willems-Widyastuti A, Mooi WJ, Saxena PR, Sterk PJ, de Boer WI, Sharma HS. 2005b. Chronic obstructive pulmonary disease is associated with enhanced bronchial expression of FGF-1, FGF-2, and FGFR-1. J Pathol 206:28-38.

L'Allemain G, Lavoie JN, Rivard N, Baldin V, Pouyssegur J. 1997. Cyclin D1 expression is a major target of the cAMP-induced inhibition of cell cycle entry in fibroblasts. Oncogene 14:1981-1990.

Lappalainen U, Whitsett JA, Wert SE, Tichelaar JW, Bry K. 2005. Interleukin-1beta causes pulmonary inflammation, emphysema, and airway remodeling in the adult murine lung. Am J Respir Cell Mol Biol 32:311-318.

Larsen K, Tufvesson E, Malmstrom J, Morgelin M, Wildt M, Andersson A, Lindstrom A, Malmstrom A, Lofdahl CG, Marko-Varga G, Bjermer L, Westergren-Thorsson G. 2004. Presence of activated mobile fibroblasts in bronchoalveolar lavage from patients with mild asthma. Am J Respir Crit Care Med 170:1049-1056.

Laulederkind SJ, Kirtikara K, Raghow R, Ballou LR. 2000. The regulation of PGE(2) biosynthesis in MG-63 osteosarcoma cells by IL-1 and FGF is cell density-dependent. Exp Cell Res 258:409-416.

Lee HT, Kay EP. 2003. Regulatory role of cAMP on expression of Cdk4 and p27(Kip1) by inhibiting phosphatidylinositol 3-kinase in corneal endothelial cells. Invest Ophthalmol Vis Sci 44:3816-3825.

Lehnart SE, Wehrens XH, Reiken S, Warrier S, Belevych AE, Harvey RD, Richter W, Jin SL, Conti M, Marks AR. 2005. Phosphodiesterase 4D deficiency in the ryanodine-receptor complex promotes heart failure and arrhythmias. Cell 123:25-35.

Liu S, Laliberte F, Bobechko B, Bartlett A, Lario P, Gorseth E, Van Hamme J, Gresser MJ, Huang Z. 2001. Dissecting the cofactor-dependent and independent bindings of PDE4 inhibitors. Biochemistry 40:10179-10186.

Liu X, Ostrom RS, Insel PA. 2004. cAMP-elevating agents and adenylyl cyclase overexpression promote an antifibrotic phenotype in pulmonary fibroblasts. Am J Physiol Cell Physiol 286:C1089-C1099.

Lu S, Liu N, Dass SB, Reiss TF, Knorr BA. 2009. Randomized, placebo-controlled study of a selective PDE4 inhibitor in the treatment of asthma. Respir Med 103:342-347.

Lugnier C. 2006. Cyclic nucleotide phosphodiesterase (PDE) superfamily: a new target for the development of specific therapeutic agents. Pharmacol Ther 109:366-398.

Marchmont RJ, Houslay MD. 1980. A peripheral and an intrinsic enzyme constitute the cyclic AMP phosphodiesterase activity of rat liver plasma membranes. Biochem J 187:381-392.

Marienfeld U, Walter U, Simm A. 2001. Inhibition of rat cardiac fibroblast growth by cAMP--but not by cGMP-dependent protein kinase. Basic Res Cardiol 96:184-191.

Martin-Chouly CA, Astier A, Jacob C, Pruniaux MP, Bertrand C, Lagente V. 2004. Modulation of matrix metalloproteinase production from human lung fibroblasts by type 4 phosphodiesterase inhibitors. Life Sci 75:823-840.

Maxwell CR, Kanes SJ, Abel T, Siegel SJ. 2004. Phosphodiesterase inhibitors: a novel mechanism for receptor-independent antipsychotic medications. Neuroscience 129:101-107.

Mehats C, Jin SL, Wahlstrom J, Law E, Umetsu DT, Conti M. 2003. PDE4D plays a critical role in the control of airway smooth muscle contraction. FASEB J 17:1831-1841.

Mei FC, Qiao J, Tsygankova OM, Meinkoth JL, Quilliam LA, Cheng X. 2002. Differential signaling of cyclic AMP: opposing effects of exchange protein directly activated by cyclic AMP and cAMP-dependent protein kinase on protein kinase B activation. J Biol Chem 277:11497-11504.

Moeller A, Gilpin SE, Ask K, Cox G, Cook D, Gauldie J, Margetts PJ, Farkas L, Dobranowski J, Boylan C, O'Byrne PM, Strieter RM, Kolb M. 2009. Circulating fibrocytes are an indicator of poor prognosis in idiopathic pulmonary fibrosis. Am J Respir Crit Care Med 179:588-594.

Musa NL, Ramakrishnan M, Li J, Kartha S, Liu P, Pestell RG, Hershenson MB. 1999. Forskolin inhibits cyclin D1 expression in cultured airway smooth-muscle cells. Am J Respir Cell Mol Biol 20:352-358.

Nakamura Y, Tate L, Ertl RF, Kawamoto M, Mio T, Adachi Y, Romberger DJ, Koizumi S, Gossman G, Robbins RA, . 1995. Bronchial epithelial cells regulate fibroblast proliferation. Am J Physiol 269:L377-L387.

Nazarian R, Weinberg JM. 2009. AN-2728, a PDE4 inhibitor for the potential topical treatment of psoriasis and atopic dermatitis. Curr Opin Investig Drugs 10:1236-1242.

Neer EJ. 1995. Heterotrimeric G proteins: organizers of transmembrane signals. Cell 80:249-257.

Nikulina E, Tidwell JL, Dai HN, Bregman BS, Filbin MT. 2004. The phosphodiesterase inhibitor rolipram delivered after a spinal cord lesion promotes axonal regeneration and functional recovery. Proc Natl Acad Sci U S A 101:8786-8790.

Norioka K, Mitaka T, Mochizuki Y, Hara M, Kawagoe M, Nakamura H. 1994. Interaction of interleukin-1 and interferon-gamma on fibroblast growth factor-induced angiogenesis. Jpn J Cancer Res 85:522-529.

Pages L, Gavalda A, Lehner MD. 2009. PDE4 inhibitors: a review of current developments (2005-2009). Expert Opin Ther Pat. 19: 1501-1519.

Palmer JN, Hartogensis WE, Patten M, Fortuin FD, Long CS. 1995. Interleukin-1 beta induces cardiac myocyte growth but inhibits cardiac fibroblast proliferation in culture. J Clin Invest 95:2555-2564.

Peter D, Jin SL, Conti M, Hatzelmann A, Zitt C. 2007. Differential expression and function of phosphodiesterase 4 (PDE4) subtypes in human primary CD4+ T cells: predominant role of PDE4D. J Immunol 178:4820-4831.

Phan SH. 2008. Biology of fibroblasts and myofibroblasts. Proc Am Thorac Soc 5:334-337.

Pierce KL, Premont RT, Lefkowitz RJ. 2002. Seven-transmembrane receptors. Nat Rev Mol Cell Biol 3:639-650.

Piguet PF, Vesin C, Grau GE, Thompson RC. 1993. Interleukin 1 receptor antagonist (IL-1ra) prevents or cures pulmonary fibrosis elicited in mice by bleomycin or silica. Cytokine 5:57-61.

Qiu YH, Chen CN, Malone T, Richter L, Beckendorf SK, Davis RL. 1991. Characterization of the memory gene dunce of Drosophila melanogaster. J Mol Biol 222:553-565.

Rabe KF, Bateman ED, O'Donnell D, Witte S, Bredenbroker D, Bethke TD. 2005. Roflumilast--an oral anti-inflammatory treatment for chronic obstructive pulmonary disease: a randomised controlled trial. Lancet 366:563-571.

Rabe KF, Dent G. 1998. Theophylline and airway inflammation. Clin Exp Allergy 28 Suppl 3:35-41.

Rabe KF, Tenor H, Dent G, Schudt C, Liebig S, Magnussen H. 1993. Phosphodiesterase isozymes modulating inherent tone in human airways: identification and characterization. Am J Physiol 264:L458-L464.

Raeburn D, Underwood SL, Lewis SA, Woodman VR, Battram CH, Tomkinson A, Sharma S, Jordan R, Souness JE, Webber SE, . 1994. Anti-inflammatory and bronchodilator properties of RP 73401, a novel and selective phosphodiesterase type IV inhibitor. Br J Pharmacol 113:1423-1431.

Raines EW, Dower SK, Ross R. 1989. Interleukin-1 mitogenic activity for fibroblasts and smooth muscle cells is due to PDGF-AA. Science 243:393-396.

Reeves ML, Leigh BK, England PJ. 1987. The identification of a new cyclic nucleotide phosphodiesterase activity in human and guinea-pig cardiac ventricle. Implications for the mechanism of action of selective phosphodiesterase inhibitors. Biochem J 241:535-541.

Richter W, Conti M. 2002. Dimerization of the type 4 cAMP-specific phosphodiesterases is mediated by the upstream conserved regions (UCRs). J Biol Chem 277:40212-40221.

Robichaud A, Stamatiou PB, Jin SL, Lachance N, MacDonald D, Laliberte F, Liu S, Huang Z, Conti M, Chan CC. 2002. Deletion of phosphodiesterase 4D in mice shortens alpha(2)-adrenoceptor-mediated anesthesia, a behavioral correlate of emesis. J Clin Invest 110:1045-1052.

Rodriguez-Barbero A, Dorado F, Velasco S, Pandiella A, Banas B, Lopez-Novoa JM. 2006. TGF-beta1 induces COX-2 expression and PGE2 synthesis through MAPK and PI3K pathways in human mesangial cells. Kidney Int 70:901-909.

Salter H. 1859. On some points in the treatment and clinical history of asthma. Edinburgh Med J 4:1109-1115.

Sanchez T, Moreno JJ. 2002. Role of EP(1) and EP(4) PGE(2) subtype receptors in serum-induced 3T6 fibroblast cycle progression and proliferation. Am J Physiol Cell Physiol 282:C280-C288.

Scherle PA, Pratta MA, Feeser WS, Tancula EJ, Arner EC. 1997. The effects of IL-1 on mitogen-activated protein kinases in rabbit articular chondrocytes. Biochem Biophys Res Commun 230:573-577.

Schmitt JM, Stork PJ. 2001. Cyclic AMP-mediated inhibition of cell growth requires the small G protein Rap1. Mol Cell Biol 21:3671-3683.

Schwabe U, Miyake M, Ohga Y, Daly JW. 1976. 4-(3-Cyclopentyloxy-4-methoxyphenyl)-2-pyrrolidone (ZK 62711): a potent inhibitor of adenosine cyclic 3',5'-monophosphate phosphodiesterases in homogenates and tissue slices from rat brain. Mol Pharmacol 12:900-910.

Scott JD, McCartney S. 1994. Localization of A-kinase through anchoring proteins. Mol Endocrinol 8:5-11.

Selige J, Tenor H, Hatzelmann A, Dunkern T. 2010. Cytokine-dependent balance of mitogenic effects in primary human lung fibroblasts related to cyclic AMP signaling and phosphodiesterase 4 inhibition. J Cell Physiol: 15. January (Epub ahead of print)

Sette C, Conti M. 1996. Phosphorylation and activation of a cAMP-specific phosphodiesterase by the cAMP-dependent protein kinase. Involvement of serine 54 in the enzyme activation. J Biol Chem 271:16526-16534.

Shakur Y, Pryde JG, Houslay MD. 1993. Engineered deletion of the unique N-terminal domain of the cyclic AMP-specific phosphodiesterase RD1 prevents plasma membrane association and the attainment of enhanced thermostability without altering its sensitivity to inhibition by rolipram. Biochem J 292 (Pt 3):677-686.

Shepherd MC. 2006. Phosphodiesterase 4 regulation of cyclic AMP in pulmonary remodelling: potential roles for isoform selective inhibitors. Pulm Pharmacol Ther 19:24-31.

Sinclair ML, Wang XY, Mattia M, Conti M, Buck J, Wolgemuth DJ, Levin LR. 2000. Specific expression of soluble adenylyl cyclase in male germ cells. Mol Reprod Dev 56:6-11.

Spina D. 2008. PDE4 inhibitors: current status. Br J Pharmacol 155:308-315.

Spurzem JR, Rennard SI. 2005. Pathogenesis of COPD. Semin Respir Crit Care Med 26:142-153.

Strieter RM. 2005. Pathogenesis and natural history of usual interstitial pneumonia: the whole story or the last chapter of a long novel. Chest 128:526S-532S.

Stuart WD, Maeda S, Khera P, Fagin JA, Clemens TL. 2000. Parathyroid hormone-related protein induces G1 phase growth arrest of vascular smooth muscle cells. Am J Physiol Endocrinol Metab 279:E60-E67.

Sugimoto Y, Narumiya S. 2007. Prostaglandin E receptors. J Biol Chem 282:11613-11617.

Sugiura H, Liu X, Togo S, Kobayashi T, Shen L, Kawasaki S, Kamio K, Wang XQ, Mao LJ, Rennard SI. 2007. Prostaglandin E(2) protects human lung fibroblasts from cigarette smoke extract-induced apoptosis via EP(2) receptor activation. J Cell Physiol 210:99-110.

Sutherland EW, Rall TW. 1958. Fractionation and characterization of a cyclic adenine ribonucleotide formed by tissue particles. J Biol Chem 232:1077-1091.

Swinnen JV, Joseph DR, Conti M. 1989. Molecular cloning of rat homologues of the Drosophila melanogaster dunce cAMP phosphodiesterase: evidence for a family of genes. Proc Natl Acad Sci U S A 86:5325-5329.

Takami M, Cho ES, Lee SY, Kamijo R, Yim M. 2005. Phosphodiesterase inhibitors stimulate osteoclast formation via TRANCE/RANKL expression in osteoblasts: possible involvement of ERK and p38 MAPK pathways. FEBS Lett 579:832-838.

Taylor SS, Buechler JA, Yonemoto W. 1990. cAMP-dependent protein kinase: framework for a diverse family of regulatory enzymes. Annu Rev Biochem 59:971-1005.

Tenor H, Hedbom E, Hauselmann HJ, Schudt C, Hatzelmann A. 2002. Phosphodiesterase isoenzyme families in human osteoarthritis chondrocytes--functional importance of phosphodiesterase 4. Br J Pharmacol 135:609-618.

Thiel C, Nix M. 2006. Efficient transfection of primary cells relevant for cardiovascular research by nucleofection. Methods Mol Med 129:255-266.

Thompson WJ, Terasaki WL, Epstein PM, Strada SJ. 1979. Assay of cyclic nucleotide phosphodiesterase and resolution of multiple molecular forms of the enzyme. Adv Cyclic Nucleotide Res 10:69-92.

Togo S, Holz O, Liu X, Sugiura H, Kamio K, Wang X, Kawasaki S, Ahn Y, Fredriksson K, Skold CM, Mueller KC, Branscheid D, Welker L, Watz H, Magnussen H, Rennard SI. 2008. Lung fibroblast repair functions in patients with chronic obstructive pulmonary disease are altered by multiple mechanisms. Am J Respir Crit Care Med 178:248-260.

Togo S, Liu X, Wang X, Sugiura H, Kamio K, Kawasaki S, Kobayashi T, Ertl RF, Ahn Y, Holz O, Magnussen H, Fredriksson K, Skold CM, Rennard SI. 2009. PDE4 inhibitors roflumilast and rolipram augment PGE2 inhibition of TGF-{beta}1-stimulated fibroblasts. Am J Physiol Lung Cell Mol Physiol 296:L959-L969.

Torphy TJ. 1998. Phosphodiesterase isozymes: molecular targets for novel antiasthma agents. Am J Respir Crit Care Med 157:351-370.

Vancheri C, Mastruzzo C, Sortino MA, Crimi N. 2004. The lung as a privileged site for the beneficial actions of PGE2. Trends Immunol 25:40-46.

Vancheri C, Sortino MA, Tomaselli V, Mastruzzo C, Condorelli F, Bellistri G, Pistorio MP, Canonico PL, Crimi N. 2000. Different expression of TNF-alpha receptors and prostaglandin E(2)Production in normal and fibrotic lung fibroblasts: potential implications for the evolution of the inflammatory process. Am J Respir Cell Mol Biol 22:628-634.

Vanderbeld B, Kelly GM. 2000. New thoughts on the role of the beta-gamma subunit in G-protein signal transduction. Biochem Cell Biol 78:537-550.

Verde I, Pahlke G, Salanova M, Zhang G, Wang S, Coletti D, Onuffer J, Jin SL, Conti M. 2001. Myomegalin is a novel protein of the golgi/centrosome that interacts with a cyclic nucleotide phosphodiesterase. J Biol Chem 276:11189-11198.

Vernier PT, Levine ZA, Wu YH, Joubert V, Ziegler MJ, Mir LM, Tieleman DP. 2009. Electroporating fields target oxidatively damaged areas in the cell membrane. PLoS One 4:e7966.

Vicini E, Conti M. 1997. Characterization of an intronic promoter of a cyclic adenosine 3',5'-monophosphate (cAMP)-specific phosphodiesterase gene that confers hormone and cAMP inducibility. Mol Endocrinol 11:839-850.

Wachtel H. 1982. Characteristic behavioural alterations in rats induced by rolipram and other selective adenosine cyclic 3', 5'-monophosphate phosphodiesterase inhibitors. Psychopharmacology (Berl) 77:309-316.

Wachtel H. 1983. Potential antidepressant activity of rolipram and other selective cyclic adenosine 3',5'-monophosphate phosphodiesterase inhibitors. Neuropharmacology 22:267-272.

Waddleton D, Wu W, Feng Y, Thompson C, Wu M, Zhou YP, Howard A, Thornberry N, Li J, Mancini JA. 2008. Phosphodiesterase 3 and 4 comprise the major cAMP metabolizing enzymes responsible for insulin secretion in INS-1 (832/13) cells and rat islets. Biochem Pharmacol 76:884-893.

Walsh DA, Perkins JP, Krebs EG. 1968. An adenosine 3',5'-monophosphate-dependant protein kinase from rabbit skeletal muscle. J Biol Chem 243:3763-3765.

Wang P, Wu P, Ohleth KM, Egan RW, Billah MM. 1999. Phosphodiesterase 4B2 is the predominant phosphodiesterase species and undergoes differential regulation of gene expression in human monocytes and neutrophils. Mol Pharmacol 56:170-174.

Wess J. 1998. Molecular basis of receptor/G-protein-coupling selectivity. Pharmacol Ther 80:231-264.

White KE, Ding Q, Moore BB, Peters-Golden M, Ware LB, Matthay MA, Olman MA. 2008. Prostaglandin E2 mediates IL-1beta-related fibroblast mitogenic effects in acute lung injury through differential utilization of prostanoid receptors. J Immunol 180:637-646.

Wilborn J, Crofford LJ, Burdick MD, Kunkel SL, Strieter RM, Peters-Golden M. 1995. Cultured lung fibroblasts isolated from patients with idiopathic pulmonary fibrosis have a diminished capacity to synthesize prostaglandin E2 and to express cyclooxygenase-2. J Clin Invest 95:1861-1868.

Xu RX, Hassell AM, Vanderwall D, Lambert MH, Holmes WD, Luther MA, Rocque WJ, Milburn MV, Zhao Y, Ke H, Nolte RT. 2000. Atomic structure of PDE4: insights into phosphodiesterase mechanism and specificity. Science 288:1822-1825.

Yarwood SJ, Steele MR, Scotland G, Houslay MD, Bolger GB. 1999. The RACK1 signaling scaffold protein selectively interacts with the cAMP-specific phosphodiesterase PDE4D5 isoform. J Biol Chem 274:14909-14917.

Zaccolo M, Di Benedetto G, Lissandron V, Mancuso L, Terrin A, Zamparo I. 2006. Restricted diffusion of a freely diffusible second messenger: mechanisms underlying compartmentalized cAMP signalling. Biochem Soc Trans 34:495-497.

Zaccolo M, Pozzan T. 2002. Discrete microdomains with high concentration of cAMP in stimulated rat neonatal cardiac myocytes. Science 295:1711-1715.

Zhang J, Bui TN, Xiang J, Lin A. 2006. Cyclic AMP inhibits p38 activation via CREB-induced dynein light chain. Mol Cell Biol 26:1223-1234.

Zhang J, Ma Y, Taylor SS, Tsien RY. 2001. Genetically encoded reporters of protein kinase A activity reveal impact of substrate tethering. Proc Natl Acad Sci U S A 98:14997-15002.

Zhang Y, Lee TC, Guillemin B, Yu MC, Rom WN. 1993. Enhanced IL-1 beta and tumor necrosis factor-alpha release and messenger RNA expression in macrophages from idiopathic pulmonary fibrosis or after asbestos exposure. J Immunol 150:4188-4196.

Zhao Y, Zhang HT, O'Donnell JM. 2003. Antidepressant-induced increase in high-affinity rolipram binding sites in rat brain: dependence on noradrenergic and serotonergic function. J Pharmacol Exp Ther 307:246-253.

Zufall F, Shepherd GM, Barnstable CJ. 1997. Cyclic nucleotide gated channels as regulators of CNS development and plasticity. Curr Opin Neurobiol 7:404-412.